Wetting Behaviour of Silicon and Dielectric Materials Attributed to Texturing and Self Assembled Monolayer

THESIS

Submitted in the partial fulfillment of the requirements for the degree of

DOCTOR OF PHILOSOPHY

by

VIJAY KUMAR

Under the supervision of

PROF. NITI NIPUN SHARMA

BITS Pilani
Pilani | Dubai | Goa | Hyderabad

BIRLA INSTITUTE OF TECHNOLOGY & SCIENCE
PILANI – 333 031 (RAJASTHAN) INDIA

2015

Wetting Behaviour of Silicon and Dielectric Materials Attributed to Texturing and Self Assembled Monolayer

THESIS

Submitted in the partial fulfillment of the requirements for the degree of

DOCTOR OF PHILOSOPHY

by

VIJAY KUMAR
(ID. No. 2010PHXF418P)

Under the supervision of

PROF. NITI NIPUN SHARMA

BITS Pilani
Pilani | Dubai | Goa | Hyderabad

BIRLA INSTITUTE OF TECHNOLOGY & SCIENCE
PILANI – 333 031 (RAJASTHAN) INDIA

2015

BIRLA INSTITUTE OF TECHNOLOGY & SCIENCE
PILANI – 333 031 (RAJASTHAN) INDIA

CERTIFICATE

This is to certify that the thesis entitled **"Wetting Behaviour of Silicon and Dielectric Materials Attributed to Texturing and Self Assembled Monolayer"** submitted by **VIJAY KUMAR**, ID.No. **2010PHXF418P** for award of Ph.D. Degree of the institute embodies original work done by him under my supervision.

Signature

Prof. NITI NIPUN SHARMA
Professor, Mechanical Engineering Department
BITS-Pilani, Pilani Campus

Date: 23/02/2015

Dedicated

to

my parents

ACKNOWLEDGEMENT

I am extremely grateful to my Ph.D. supervisor Prof. Niti Nipun Sharma. He is an immensely kind and patient person and goes out of his way to help the people. In addition, he is terrific researcher, great advisor, and wonderful teacher. He has a logical, rational, and holistic way of approaching any scientific issue and goes to the depth of every research problem. He was available at any time for discussing any research query and any other problem that I had. He has an expertise in presenting the scientific work, which helped me in my presentation. I am fortunate to work under such supervisor.

I am immensely grateful to Prof. K.N. Bhat, Visiting Professor, Indian Institute of Science, Bangalore. He guided me for my PhD work as Co-supervisor. I cannot find enough words to thank him for his help and support during my research work at IISc, Bangalore. With the help of Prof. Bhat, I am able to finish my all experimental work. I would like to thanks Prof. M.M.Nayak, Visiting Professor, Indian Institute of Science, Bangalore for his guidance and support. He helped me to make a setup for my PhD experimental work. I express my gratitude to Prof. V. Ramgopal Rao, Indian Institute of Technology, Bombay, his help and support during my research work at IIT, Bombay.

I am thankful to Dr. B. D. Pant for their support and guidance. I express my gratitude to Dr. V. K. Khanna, Dr. Ram Gopal and Dr. Ravindar Mukhiya all from CEERI, Pilani for their support, motivation and guidance.

I am immensely thankful to Professor B.N. Jain, Vice-Chancellor, BITS - Pilani; Prof. G. Raghurama, Director, BITS-Pilani, Pilani Campus; Prof. R. K. Mittal, Director (Special Projects) BITS, Pilani for providing me the opportunity to teach in the Mechanical Engineering Department of BITS-Pilani, Pilani Campus and allowing me to pursue my doctoral thesis by providing necessary facilities and financial support. I express my gratitude to Prof. S. K. Verma (Dean, Academic Research Division); Prof. Hemant R Jadhao (Professor-in-Charge, Academic Research Division) BITS-Pilani, Pilani Campus for their constant official support and encouragement. I feel obliged to Prof. Ravi Prakash (former Dean, Research and Consultancy Division); Prof. K.S. Sangwan (former Head of the Department, Mechanical Engineering); Prof. Ajit Pratap Singh (Dean, Admission and Instruction

Division) and Prof. Srikanta Routroy (Associate Dean, Instruction Division) for their support.

My sincere thanks to Prof. Sai Jagan Mohan (Head of the Department, Mechanical Engineering) for his support during completion of the research work. I am grateful to the entire faculty and staff of Mechanical Engineering Department and central workshop unit BITS - Pilani for their kind support and assistance.

I thank Prof. M.S. Dasgupta (Chief, Placement Unit); Prof. B.K. Rout (Associate Dean, Academic Registration & Counselling Division) and Prof. P Srinivasan (Associate Dean, Practice School) Doctoral Research Committee (DRC) and Doctoral Advisory Committee (DAC) members, Mechanical Engineering Department, who spared their precious time to provide valuable suggestions that immensely helped in improving the quality of my Ph.D. thesis. I also express my gratitude to Prof. Anshuman Dalvi, for their continuous support, motivation and guidance.

I have been gifted with friends like, Dr. Sachin U. Belgamber, Dr. Jitendra Singh Rathore, Ms. Neha Arora, Ms. Paridhi Puri, Ms. Shivani Nain and Ms. Tamalika Bhakat, and Amar singh who have not only supported me in times thick and thin but have also made the journey of life extremely interesting, meaningful and fun.

I would like to thanks Mr. Santosh Kumar Saini (ARC Division) for his help in compilation of thesis. I also express my thanks to all other faculty and staff of ARC Division and CAHU, BITS-Pilani, Pilani Campus for their kind support and cooperation towards the completion of my thesis.

VIJAY KUMAR

ABSTRACT

Since last decade, people have been attracted by the self-cleaning properties of the lotus leaf, and dream to develop superhydrophobic surfaces. Many methods have been developed to produce a surface with water contact angle higher than 150°. In general, the hydrophobic surfaces are prepared by combining high surface roughness and modify the surface with hydrophobic coating. The challenge here is to develop a robust hydrophobic surface with a simple process, so that it can be manufactured at industrial scale. The aim of this PhD research is to develop a simple method to prepare hydrophobic surfaces with common method to all semiconductor materials. We have studied the semiconductor materials like silicon, low-k and high-k dielectric and polymers materials for betterment of wetting properties of these materials.

In Chapter 3, we have studied the wetting behaviour of silicon surface. In this chapter, we used the chemical etchant and plasma etching system to make the silicon surface rough. After texturing, the surface were modified using the Octadecyltrichlorosilane (OTS) Self assembled monolayers (SAM). In addition, we also investigated the modification of back side silicon wafer surfaces, piranha treated silicon surfaces and piranha with HF treated silicon surfaces for wetting behaviour of Silicon.

In Chapter 4, we investigated the wetting behaviour of many a dielectric materials using the simple method developed for silicon surface given in Chapter 3. The low-k (SiO_2) and high-k dielectric (HfO_2, Al_2O_3, TiO_2 and Ta_2O_5) materials were used for the investigations. As for silicon surfaces, texturing with plasma followed with OTS SAM modification was used for different dielectric materials for the study. The fluorine (SF_6) plasma was used to texture the dielectric surfaces.

In Chapter 5, we have studied the wetting behaviour of SU8 surface. The SU8 is most widely used materials for the microfluidics applications. The SU8 surfaces were textured using the fluorine and oxygen plasma chemistry. After texturing the OTS SAM modification was carried out to change the wetting behaviour of SU8. A time study over five months was also carried out to study the stability of developed superhydrophobic SU8 surfaces.

In Chapter 6, we discuss and present the overall conclusions and future scope of the present study.

CONTENTS	Page No.

Acknowledgement i-ii

Abstract iii

Table of Contents iv-vii

List of Figures viii-x

List of Tables xi

CHAPTER 1 Introduction 1-19

1.1 General Introduction 1

1.2 Classical Model of Wetting on Solid Surface 5

1.2.1 Wetting on flat surface 5

1.2.2 Wetting on rough surface 7

1.3 Fabrication Methods of Superhydrophobic Surfaces 11

1.3.1 Making a rough surface on hydrophobic materials 11

1.3.2 Modification of rough surface with hydrophobic coating 12

1.4 Deposition of Octadecyltrichlorosilane self Assembled Monolayer 12

1.5 Motivation 14

References 16

CHAPTER 2 Literature Review 20-59

2.1 Overview 20

2.2 Wetting behaviour of Silicon Surface 20

2.3 Wetting behaviour of Dielectric Materials 26

2.3.1 Low-*k* dielectric materials 27

2.3.2 High-*k* dielectric materials 31

2.3.2.1 Hafnium oxide (HfO_2) 31

2.3.2.2 Aluminum oxide (Al_2O_3) 33

2.3.2.3 Tantalum oxide (Ta_2O_5) 35

2.3.2.4 Titanium oxide (TiO_2) 36

CONTENTS	Page No.

		Page No.
2.4	Polymer Material	37
2.5	Gap in existing Research and Investigations	39
2.6	Organization of Thesis	41
	References	43
CHAPTER 3	**Wetting behaviour of Silicon**	**60-86**
3.1	Overview	60
3.2	Experimental Details	61
3.2.1	Cleaning and sample preparation	61
3.2.2	Silicon surface without any texturing	62
3.2.3	Chemical texturing of silicon surface	62
3.2.4	Plasma texturing of silicon surface	64
3.2.5	Deposition of OTS SAM on textured silicon	65
3.2.6	Characterization tool	65
3.3	Results and Discussion	66
3.3.1	Surface topography by AFM/SEM	66
3.3.1.1	*Silicon surface treated with cleanser (untextured)*	66
3.3.1.2	*Chemically textured silicon surface*	69
3.3.1.3	*Plasma textured silicon surface*	72
3.3.2	Contact angle measurements	74
3.3.2.1	*Silicon surfaces treated with cleanser (untextured)*	75
3.3.2.2	*Chemical textured surface*	75
3.3.2.3	*Plasma textured surface*	76
3.3.3	Raman spectra	77
3.3.4	X-Ray photoelectron spectra	79
3.4	Conclusion	82
	References	84

CONTENTS	Page No.

CHAPTER 4 Wetting behaviour of Dielectric materials **87-107**

4.1 Overview 87

4.2 Experimental Details 88

4.2.1 Sample preparation 88

4.2.2 Dielectric materials 89

4.2.2.1 Low-k dielectric materials 89

4.2.2.2 High-k dielectric materials 89

4.2.2.3 Plasma texturing of dielectric materials 91

4.2.2.4 Deposition of OTS SAM on textured dielectrics 91

4.2.2.5 Characterization tool 91

4.3 Result and Discussion 92

4.3.1 Surface topography by AFM/SEM 92

4.3.1.1 Untextured OTS modified oxide surface 92

4.3.1.2 Plasma textured OTS modified oxide surface 94

4.3.2 Contact angle measurement 98

4.3.2.1 Untextured OTS modified oxide surface 98

4.3.2.2 Plasma textured OTS modified oxide surface 99

4.3.3 Raman spectra 100

4.3.4 X-ray photoelectron spectra 102

4.4 Conclusion 104

References 105

CHAPTER 5 Wetting behaviour of SU8 **108-137**

5.1 Overview 108

5.2 Experimental Details 109

5.2.1 Cleaning and sample preparation 109

5.2.2 SU8 coating 110

CONTENTS	Page No.

5.2.3 Plasma treatment	110
5.2.4 Deposition of OTS SAM	110
5.2.5 Characterization tool	111
5.3 Results and Discussion	111
5.3.1 Surface topography by AFM/SEM	111
5.3.1.1 SU8 surface	112
5.3.1.2 Oxygen plasma treatment	113
5.3.1.3 Fluorine plasma treatment	115
5.3.1.4 Fluorine and Oxygen plasma treatment	118
5.3.2 Contact angle measurements	121
5.3.2.1 SU8 surface	121
5.3.2.2 Oxygen plasma with OTS SAM	122
5.3.2.3 Fluorine plasma with OTS SAM	123
5.3.2.4 Fluorine and Oxygen plasma with OTS SAM	123
5.3.3 Chemical behaviour of SU8 surface	125
5.3.3.1 Raman spectra	125
5.3.3.2 XPS spectra	128
5.3.4 Stability study of plasma treated OTS SAM deposited SU8 surface	130
5.4 Conclusion	132
References	135
CHAPTER 6 Overall Conclusions and Future Scope	**138-142**
6.1 Overall Conclusion	138
6.2 Future Scope of the work	141
Appendix-A	A-1 – A-5
List of Publications	C-1
Brief biography of the Candidate	C-2
Brief biography of the Supervisor	C-3

Figure No	Title	Page No.
1.1	Young model of a liquid droplet on solid surface	3
1.2	Schematic of hydrophilic surface and hydrophobic surface	7
1.3	Wetted contact between the liquid and the rough substrate (Wenzel Model) (b) Non-wetted contact between the liquid and the rough substrate (Cassie Model) (c) Intermediate state between Cassie-Wenzel state	8
1.4	Schematic of droplet on a tilted substrate showing advancing (θ_a) and receding angle (θ_r) contact angle	10
1.5	Schematic of formation mechanism of OTS SAM	13
2.1	Schematic diagram of dielectric materials distribution	26
3.1	Atomic force morphology values (a) untreated silicon surface without OTS SAM (b) untreated silicon surface with OTS SAM	67
3.2	Atomic force morphology values (a) untreated silicon surface without OTS SAM (b) untreated silicon surface with OTS SAM	68
3.3	Atomic force morphology (a) Untextured silicon surface (a1) BS (a2) PR (a3) HF; Scanning electron microscope images (b) Untextured silicon surface with contact angle inset (b1) BS (b2) PR (b3) HF	69
3.4	AFM RMS Roughness (a) chemical textured silicon surface without OTS modification (b) chemical textured silicon surface with OTS modified	70
3.5	Atomic force morphology (a) chemical textured silicon surface (a1) K (a2) T (a3) KT. Scanning electron microscope images (b) chemical textured silicon surfaces with contact angle inset (b1) K (b2) T (b3) KT	71
3.6	Atomic force morophology (a) chemical textured OTS modified silicon surface (a1) K (a2) T (a3) KT; Scanning electron microscope images (b) chemical textured OTS modified silicon surfaces with contact angle inset (b1) K (b2) T (b3) KT	71
3.7	Atomic force morphology values (a) plasma textured without OTS SAM (b) plasma textured with OTS SAM	73
3.8	Atomic force morphology (a) plasma textured silicon surface (a1) S (a2) O (a3) SO; Scanning electron microscope images (b) plasma textured silicon surfaces with contact angle inset (b1) S (b2) O (b3) SO	73

Figure No	Title	Page No.
3.9	Atomic force morphology (a) plasma textured OTS modified silicon surface (a1) S (a2) O (a3) SO; Scanning electron microscope images (b) plasma textured OTS modified surfaces with contact angle inset (b1) S (b2) O (b3) SO	74
3.10	Water contact angle (a) untextured, chemical and plasma textured silicon (b) OTS modify untextured, chemical and plasma textured silicon surface	77
3.11	Raman spectra information (a) Untextured silicon with piranha cleaned surface (b) Chemical textured silicon surface (c) Plasma textured silicon surface	79
3.12	XPS spectra information (a) Untreated silicon with piranha cleaned surface (b) Chemical textured silicon surface (c) Plasma textured surface	81
4.1	Surface roughness by AFM (a) Plasma untextured dielectric surface with and without OTS SAM (b) Plasma textured dielectric surface with and without OTS SAM	95
4.2	Atomic force morphology (a) for untextured oxide surface (b) for OTS modify untextured oxide surface (c) Scanning electron microscope images for untextured OTS modify oxide surface with contact angle inset (1) HfO_2 (2) Al_2O_3 (3) TiO_2 (4) Ta_2O_5 (5) SiO_2	96
4.3	Atomic force morphology (a) for plasma textured oxide surface (b) for OTS modify plasma textured oxide surface (c) Scanning electron microscope images for plasma textured OTS modify oxide surface with contact angle inset (1) HfO_2 (2) Al_2O_3 (3) TiO_2 (4) Ta_2O_5 (5) SiO_2	97
4.4	Water contact angle for untextured oxide surface with and without OTS SAM	99
4.5	Water contact angle for plasma textured oxide surface with and without OTS SAM	100
4.6	Typical Raman spectra of OTS modify (a) untextured surface (b) textured surface	101
4.7	XPS spectra of OTS modify (a) untextured surface (b) textured surface	103
5.1	Atomic force morphology (a) Untreated SU8 surface (b) SEM of untreated SU8	112
5.2	Atomic force morphology (a) Untreated SU8 surface (b) SEM of untreated SU8	112
5.3	Atomic force morphology OTS modified (a) untreated silicon surface (b) OTS modify untreated surface	113

Figure No	Title	Page No.
5.4	Oxygen plasma treated SU8 surface (a) Atomic force morophology (a1) O10 (a2) O30 (a3) O60. (b) Scanning electron microscope images (b1) O10 (b2) O30 (b3) O60	114
5.5	Oxygen plasma treated OTS modify SU8 surface (a) Atomic force morphology (a1) O10 (a2) O30 (a3) O60. (b) Scanning electron microscope images (b1) O10 (b2) O30 (b3) O60	115
5.6	Atomic force morphology OTS Modified (a) untreated silicon surface (b) OTS modify untreated surface	117
5.7	Atomic force morphology (a) Untextured SU8 surface (a1) S10 (a2) S30 (a3) S60. Scanning electron microscope images (b) Untextured silicon surface with contact angle inset (b1) S10 (b2) S30 (b3) S60	117
5.8	Atomic force morphology after OTS SAM modification (a) Untreated SU8 surface (a1) S10 (a2) S30 (a3) S60. Scanning electron microscope images (b) Untreated SU8 surface with contact angle inset (b1) S10 (b2) S30 (b3) S60.	118
5.9	Atomic force morphology SF_6+ O_2 plasma treated surface (a) without OTS SAM (b) with OTS SAM	119
5.10	Atomic force morphology (a) Untreated SU8 surface (a1) SO10 (a2) SO30 (a3) SO60. Scanning electron microscope images (b) Untreated SU8 surface with contact angle inset (b1) SO10 (b2) SO30 (b3) SO60	120
5.11	Atomic force morphology (a) Untreated SU8 surface (a1) SO10 (a2) SO30 (a3) SO60. Scanning electron microscope images (b) Untreated SU8 surface with contact angle inset (b1) SO10 (b2) SO30 (b3) SO60	120
5.12	WCA of O_2 plasma treated SU8 surface (a) without OTS modification (b) with OTS modification	122
5.13	WCA of SF_6 plasma treated SU8 surface (a) without OTS modification (b) with OTS modification	123
5.14	WCA of plasma treated SU8 surface SF_6+O_2 plasma (a) without OTS modification (b) with OTS modification	124
5.15	(a) Raman spectra of plasma treated without OTS SU8 surface (b) Raman spectra of plasma activated with OTS SU8 surface (1) bare SU8 (2) O60 (3) SO60 (4) S60	127
5.16	(a) XPS spectra of plasma treated without OTS SU8 surface (b) XPS spectra of plasma activated with OTS SU8 surface (1) bare SU8 (2) O60 (3) SO60 (4) S60	129
5.17	Stability behavior of OTS modified plasma treated SU8 surface with time (a) bare SU8 (b) O_2 plasma (c) SF_6 plasma (d) SF_6+O_2 plasma	131

List of Tables

Table No	Title	Page No.
3.1	Parameter details for PR, HF and BS samples.	62
3.2	Parameter details of used chemical textured methods	64
3.3	Parameter details of used plasma textured methods	65
4.1	Deposition parameter details for High-k dielectric materials	90
5.1	Raman spectra information of plasma treated SU8 without and with OTS SAM	127

Chapter 1

Introduction

1.1 General Introduction

Nature around us exemplifies itself with constitution of problem of extremities and in providing their amazing simple solution. For example, had water droplet stuck to the leaves wetting and covering them, it would have blocked transpiration to a great extent. It would have thereby caused a probable death of plants, leading to no photosynthesis, no solar energy conversion, suffocation and an end to life. Difficulty to this extreme have a simple solution i.e. evaporation of water which helps remove water on leaves. Additionally leaves are devised with fibrous nanostructure which makes their surface hydrophobic. The hydrophobicity of the leaves helps them to let water not stick to them and rolls off the surface. The rolling off water not only helps remove water but also clean the dirt and sand accumulated over the leaf surface. Imagine if, evaporation of water was not coupled with rolling off phenomenon; the cleaning of leaves would have been an unresolved problem in nature. The analogous situation is that of clothes soaked in water which is not able to remove dust from clothes. In both situations, this will eventually lead to damage of leaves and clothes respectively. Therefore, cleaning effect associated with rolling off water is as important as evaporation. The effect is very pronounced in Lotus leaves and the observations led to studies and making of artificially surfaces hydrophobic to harness benefits out of such surface engineering. Hydrophobic surfaces have many applications, we have focused one fabricating hydrophobic surfaces for microfluidics applications in this thesis. In fact, the interaction of water with matter have been the subject of fascination since time immemorial and gained momentum in 1940's [1]. The manner with which water droplet interacts with the matter surfaces is termed as the *Wettability* of surfaces and is characterized by the measurement of contact angle. The contact angle also known as water contact angle (WCA) denoted as θ_c is the angle between the surface and droplet. The droplet interaction with solid surface or for that matter indexed by WCA is related to the energy of surface and we have range of surface energy which renders surface superhydrophilic in which water can fully wet the surface to form a flat puddle due to strong water-surface interaction, through to

superhydrophobic in which water is effectively repelled from the surface to form a near spherical shape and in which there are very weak water-surface interactions.

The interaction between the liquid and solid has been research topic where in the early studies, Thomas young published the qualitative theory on surface tension [2]. The intermolecular attraction between like molecules in the liquid, such as the water-water attraction force is called cohesion. The attractive interaction between a liquid and a solid phase, such as between water and the solid surfaces, is called an adhesion. When the liquid drop comes in contact with solid surfaces, cohesive interaction are lost to large extent and attractive intermolecular interaction with the substrate are gained, thus forming the surface energy $\gamma_{sl}$of the solid-liquid interface. According to Young-Dupre [2] the work of adhesion per unit area W_{sl} can then be written as equation (1):

$$W_{sl} = \gamma_{sg} + \gamma_{gl} + \gamma_{sl} \quad (1)$$

whereas γ_{sg} and γ_{gl} denote the solid-gas and liquid-gas surface tensions. The chemical nature of the solid and liquid strongly influence the surface energy.

In the water-solid surface interactions, wetting is the term used to describe the study of how a drop of liquid spreads out on a solid. The wettability is usually determined by measuring the contact angle (CA) of the water droplet on the solid surface which is referred to in the literature as the water contact angle (WCA). The WCA (θ_c) on a surface is classified in four categories, namely (a) superhydrophilic θ_c<10°; (b) 90°>θ_c>10°, the surface is called hydrophilic; (c) for 90°< θ_c< 150°, the surface is called hydrophobic and (d) for θ_c>150° the surface is superhydrophobic. The behaviour of liquid drops on solid surfaces depends mainly on two properties of solid surfaces: the surface energy and surface roughness.

The surface energy of a material, for liquid often called as surface tension, depends on the intermolecular forces within materials. A strong interaction between the molecules gives materials with high surface energy and vice-versa as discussed in section 1.2.1. According to the Young's law, the degree of wetting and thus the contact angle (θ_c) is controlled by the surface tension of the liquid (γ_{gl}) the surface free energy of the solid (γ_{sg}) and the interfacial tension between two medium $(\gamma_{sl})$and is shown schematically in

Figure 1.1. In order to obtain high water contact angle, materials must have a low surface energy.

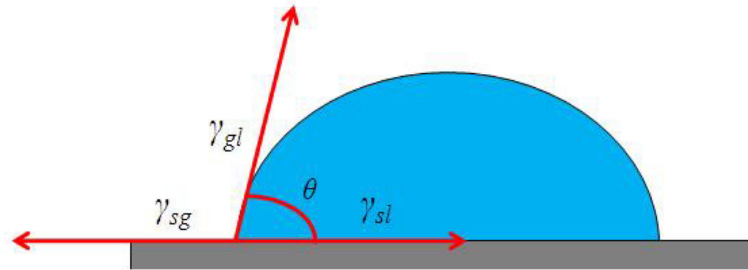

Figure 1.1: Young model of a liquid droplet on solid surface

The roughness of the surface area can be defined by index of surface area, including peaks and valleys of the surface morphology and the planner or geometric area. The later is the area of contact the water droplet makes with the surface assuming a totally smooth surface, whereas the actual surfaces area takes in account the protrusions as well. The change in water contact angle depends upon the surface roughness and the surface energy. The lower surface energy makes the surface more hydrophobic. The surface energy of the materials controls the hydrophobicity of the flat surface and, as a general rule the hydrophobicity increase when the surface energy is lowered and decrease when the surface energy is increased [3].

Lotus leaves are well-known naturally occurring superhydrophobic surfaces inspiring research, and consequently exciting engineering applications of artificial superhydrophobic surfaces. The superhydrophobic effect is exhibited by solid surfaces and concerns the wettability of a solid surface. The investigation on superhydrophobicity has been attempted from both a fundamental and practical perspectives by tailoring surface topography and surface chemical compositions. Hydrophobic surfaces have attracted significant attention with in the scientific community as well as the industrial world over the last couple of decades. These surfaces promises a wide range of usage like self-cleaning [4-6], non-wetting [7-9] low adhesion [10-12], drag reduction [13-14], oil-water separation and anti-befouling [15-16]. Basically, there are two possible physical modes of fluid motion on a solid surface: either the liquid follows the solid surface, or it moves on air trapped inside the texture present on the surface. These modes of the motion of fluid over a solid surface are referred to as Wenzel or Cassie state motion after the scientists who proposed these models [17-19]. In the Wenzel model, the wetting is attributed to the minimization of the surface energy by the increased surface

roughness, while in the Cassie-Baxter model the hydrophobic properties of the micro/nano structured surface are attributed to the solid-gas contact area that carries or supports a droplet on the surface. Conventionally, the preparation of a superhydrophobic surface can be divided into two main categories: (i) Surface roughing of hydrophobic materials, (ii) Surface roughening followed by chemical modification of the surfaces.

Due to low surface energy, fluorinated polymers intrinsically exhibit strong hydrophobicity. For example, the water contact angle on flat PDMS surface is typically 110°-115°. Roughing these surfaces using the laser ablation methods leads to superhydrophobicity with contact angle 160° which is further discussed in section 1.3.1.The most widely used roughness methods are plasma and chemical roughening of the surfaces. There are many chemicals and a mixture that roughens silicon anisotropically and includes the chemicals likes alkali metal hydroxides and ammonium hydroxides. Many of these are still the subject of research and in practice only Potassium hydroxide (KOH), Tetramethylammonium hydroxide (TMAH) are regularly used in MEMS manufacturing. Texturing by RIE plasma can be performed with or without patterning the surface. Plasma texturing is most preferable method because of reduced silicon loss attributed to pyramid formation via a chemical etch which requires only tens of microns of silicon consumption. Another method of interest is combining effect of roughening and chemical treatments. The organosilane modification is used to further modify the rougher surface. For example, the silicon texturing makes the surface rougher with contact angle <90°and the chemical modification of the textured silicon surface makes the surface superhydrophobic with water contact angle > 150°.

The chemical modification of the surface by the self-assembly of organosilane is one of the efficient strategies to make the surface superhydrophobic by lowering the surface energy of the surface [20-22]. In the last few decades, large variety of self-assembled monolayer (SAM) have been deposited on substrates and studied to prepare superhydrophobic surfaces. For example, alkylnthiol on gold and other metallic surfaces [23] and alkylsilane on silicon [24] are reported in the literature. The other class of SAMs deposited on an oxide surface include n-alkanoic acid (e.g. Carboxylic end) and phosphonic acid [25-28]. These classes of molecules have gained attention due to their ability to bind a wide range of metal oxide surfaces to form robust SAM of similar quality to those of thiol on Au.

The other most extensively investigated SAM is alkyltrichlorosilane (ATS) which requires a hydrolyte substrate e.g. metal oxide and amorphous surfaces. The SAM of alkyltrichlorosilane has become important as a functional coating for micro/nano and organic electronics applications [29]. The derivative of alkyltrichlorosilane e.g. Octadecyltrichlorosilane (OTS, $Cl_3Si\ (CH_3)_{17}$), is commonly used for the modification of inorganic materials. The modification with organic silane on silicon surface has been widely investigated because of its application in molecular electronic devices and microfluidics applications [30-32]. It serves as an alternative to SiO_2 as a gate insulator in organic thin film transistors. Substrates like polymeric dielectric materials like SU-8, PDMS, Parlyene, inorganic materials for example SiO_2, Si_3N_4, HfO_2 and Al_2O_3 are also widely investigated for making superhydrophobic surfaces which find extensive applications in microfluidics and microelectronics applications [33-38].

1.2 Classical Model of Wetting on Solid Surface

In this section, we introduce the basic concept of wettability, which describes the behaviour of a liquid on a solid surface. The wetting phenomenon of surface materials is not only dependent upon their chemical compositions, but also closely related to the micro/nano texturing on their surface.

1.2.1 Wetting on flat surface

It is observed in day to day life that the smaller size droplets have a spherical shape on horizontal surface and larger size droplets flatten on a surface. For a small drop where the gravitational effects are negligible, the interior pressure of the drop is uniform thus the interface must have a uniform curvature. The pressure jump across the interface is given by the product of the surface tension coefficient and the curvature. The length scale l_0 at which the hydrostatic pressure $\rho g l_0$ is balanced by the capillary pressure $\frac{\gamma_{gl}}{l_0}$ is referred to as the capillary length (L_c)

$$L_c = \sqrt{\frac{\gamma_{gl}}{\rho g}} \tag{2}$$

For pure water, the capillary length L_c is approximately equal to 2.5 mm at room temperature, where ρ and γ_{gl} are the density and the surface tension of the liquid-gas

respectively, and g is the gravitational acceleration. However, if the drop dimension is smaller than L_c, droplet has a shape resembling that of a sphere. Therefore, a small drop whose characteristics length is much smaller than L_c can be approximately by a truncated sphere, allowing us to determine the drop shape only with the contact angle and drop volume. However, as the drop size becomes comparable to or exceeds the capillary length, the gravitational effect is no longer negligible thus the shape deviates from the truncated sphere. The drops larger in size than the L_c are flattened by the gravitational force. The ratio between the gravitational force and surface tension is called as Bond number and is expressed as:

$$B_0 = \frac{\rho g d^2}{\gamma_{gl}} \quad (3)$$

This dimensionless number characterizes the type of drop. For $B_0 < 1$, drop formation is dominated by surface tension, in which case the drop assumes nearly spherical shape; else drop formation is significantly dominated by gravitational force which tends to flatten the drops on the solid surface. When a liquid is brought into contact with a flat homogenous solid surface, the degree of the spreading depends on the energy of the surface in contact. Young and Laplace in 1805 first established the connection between the drop shape and the interfacial energy between the solid, liquid and gas. Young and Laplace found that when there is an interface between two materials, there is specific energy termed as interfacial energy which is proportional to the surface area of the interface and the constant of proportionality is called the surface tension. Since, in the wetting phenomenon we typically have a liquid, solid and a surrounding gas, there are three type of surface tension: the liquid gas γ_{gl} the gas solid γ_{sg} the liquid solid γ_{sl} surface tensions which are schematically shown in Figure1.1.

When a liquid droplet is in the air, it is spherical in shape in order to minimize the surface energy. When it is in contact with a solid, the liquid-gas interfacing surface maintains a spherical shape profile. The angle between the line tangent to the liquid drop and solid surface is called the contact angle (θ_c) and is shown in Figure 1.1. The relation between the interfacial tension and contact angle in the system is based on the Young equations [4] and is given by:

$$\cos\theta c = \frac{\gamma_{sg} - \gamma_{sl}}{\gamma_{gl}} \qquad (4)$$

In equation (4), the measure of surface hydrophobicity i.e. WCA (θ_c) is related to the surface tension between a solid-liquid (γ_{sl}), solid-gas (γ_{sg}) and liquid-gas (γ_{gl}). When θ_c is smaller than 90°, the solid surface is considered intrinsically hydrophilic, and when θ_c is greater than 90°, the solid surface is considered intrinsically hydrophobic, as illustrated schematically in Figure 1.2.

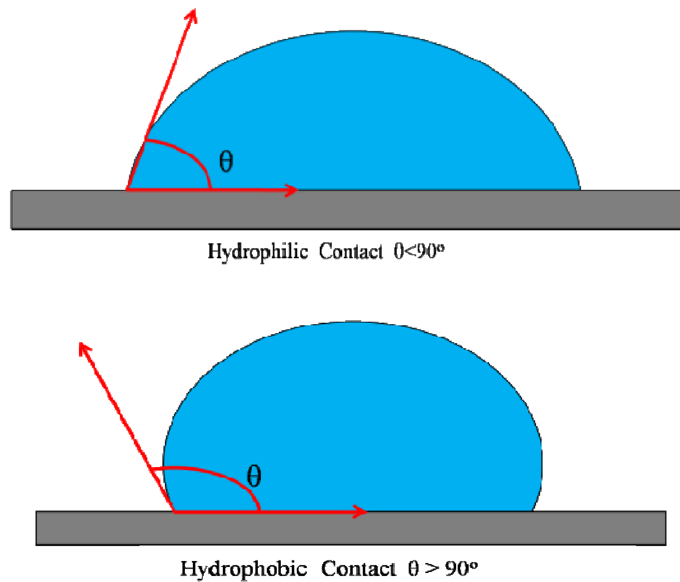

Figure 1.2: Schematic of hydrophilic surface and hydrophobic surface

1.2.2 Wetting on rough surface

Young's equation is a very simplistic approximation that is used in the case of ideally flat surfaces. The effect of wettability on surface roughness was first discovered by Wenzel in 1936 and then by Cassie-Baxter in 1944. Wenzel suggested that the effective surface area increases as the surface becomes rough and, hence water will tend to spread more on a rough hydrophilic substrate to develop more solid-liquid contact, while it will spread less on a rough hydrophobic substrate to decrease the contact area with the solid. A key assumption of this conclusion is that water is in complete contact with the solid surface, which is called the Wenzel state and is shown in Figure 1.3(a). The liquid contact angle θ_r formed from a drop in contact with rough surface to the contact angle θ_f shown by the

same liquid deposited on a flat surface with the same chemical compositions. The Wenzel contact angle is determined by the equation given as:

$$\cos\theta_r = r\cos\theta_f \tag{5}$$

Equation (4) relates the parameter in the Wenzel effect state, where *r* is the roughness factor, defined as the ratio of the actual surface area to its planner area. Since *r* is always greater than 1 for a rough surface, this equations predicts that if $\theta_f > 90^\circ$. $\theta_r > \theta_f$ and if $\theta_f > 90^\circ$, $\theta_r < \theta_f$. Therefore, in the Wenzel state, the surface roughness will make intrinsically hydrophobic surface more hydrophobic and intrinsically hydrophilic surface more hydrophilic.

The Cassie-Baxter state, also known as the composite or heterogeneous state, considers that the water droplet sits on top of the surface protrusions and air is trapped underneath the droplet resides in the surface porosity as shown schematically in Figure 1.3(b). In this case, the liquid-surface interface is actually an interface consisting of two phases, namely a liquid-solid interface (Phase 1) and a liquid-air interface (Phase 2).

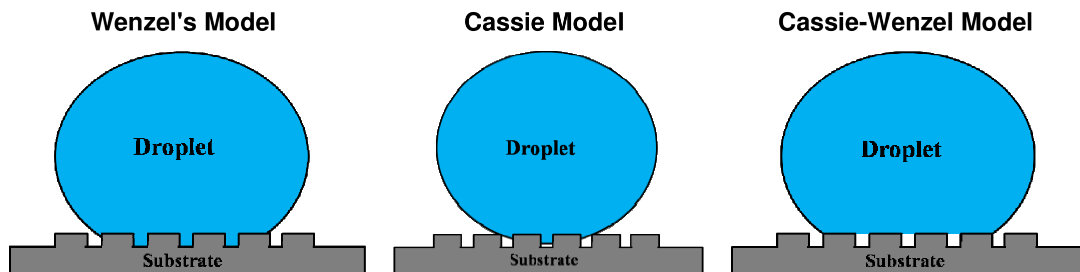

Figure 1.3: Wetted contact between the liquid and the rough substrate (Wenzel Model) (b) Non-wetted contact between the liquid and the rough substrate (Cassie Model)(c) Intermediate state between Cassie-Wenzel state

The apparent contact angle is the sum of the contribution of all the phases as defined below [2]

$$\cos\theta_c = f_1\cos\theta_1 + f_2\cos\theta_2 \tag{6}$$

where θ_c the apparent contact angle, f_1 and f_2 are the surface fractions of phase 1 and phase 2, respectively; θ_1 and θ_2 are the contact angles in phase 1 and phase 2 respectively. This equation (5) is the general form, which also applies when there is no roughness. For

an air-liquid interface, considering f as the fraction defined as the fraction of the solid surface that is wet by the liquid, the fraction corresponding to an air-liquid interface is $(1-f)$. The water droplet has a 180° contact angle with air, so equation (6) becomes

$$\cos\theta_c = f\cos\theta_f + (1-f)\cos180^\circ = f(1+\cos\theta_f) - 1 \tag{7}$$

The parameter f ranges from 0 to 1, where at $f = 0$ the droplet does not touch the surface at all and at $f = 1$ the surface is completely wetted, which makes the surface hydrophilic. When the droplet in the Cassie state, the small contact area between the droplet and solid surface allows the droplet to roll easily over the surface. A Wenzel type wetting mechanism means that there is complete contact between the surface and the water droplet at any point of coverage, with no air trapped underneath. The greater area of contact between the water and the surface renders water movement across the surface relatively hard.

The surface often exhibits wetting behaviour intermediate to those of the Wenzel and Cassie-Baxter models with partial liquid penetration of the rough surface called Cassie-Wenzel transition as shown in Figure 1.3(c). The surface Cassie-Baxter allow the water to roll-off if tilted slightly, but water droplet from height fill the roughness and may become hydrophilic. The transition from Cassie-Baxter state to Wenzel state depends upon the hydrophobicity of the surface and shape of texture features. These two states are usually separated by energy barrier between them. Thus for wetting transition the energy barrier must be overcome. Such transition from one state to another state induces under certain external stimuli, such as pressure or force on the droplet or may be by applying electric field. Recently, it is understood from experimental observations that the transition from Cassie-Baxter to Wenzel region can be irreversible event [40-41]. From literature, it has been also suggested that the transition take place, when the net surface energy of Wenzel state become equal to Cassie-Baxter state. The mechanism of transition from Cassie to Wenzel state is still widely debated in literature.

Besides high static contact angles, the easy sliding-off behaviour of liquid droplet is another phenomenon of interest related to superhydrophobicity. The sliding behaviour of the droplet is again governed by the balance between the surface tension and gravity. On the tilted surface, the liquid drop becomes asymmetric and the contact angle of the lower side becomes larger and that of the upper side gets reduced. The difference between these two contact angles known as hysteresis reaches the maximum when the liquid drop

begins to slide down the tilted surface. The contact angle of the forefront and the trailing edges of the liquid drop just prior to the movement of its contact lines are called the advancing (θ_a) and receding (θ_r) contact angles, respectively. When the gravity acting on the liquid drop becomes larger than the surface tension forces (*F*) caused by the contact angle which is holding the liquid droplet from sliding as in Figure 1.4, the liquid droplet starts sliding. So, the critical angle (θ_a) for the water droplet to slide off the surface can be calculated by balancing the gravitational forces and surface tension forces [3-6]. The force balance is given in equation (8).

$$\frac{mg \sin \alpha}{w} = \gamma_{gl} (\cos \theta_r + \cos \theta_a) \quad (8)$$

$$F = \gamma_{gl} (\cos\theta_r - \cos\theta_a) \quad (9)$$

where α denotes the sliding (tilt) angle, *m* is the mass of the droplet, *g* is the gravitational acceleration and *w* is the droplet width. This equation predicts that for a given mass of water droplet, a smaller contact angle hysteresis will result in a smaller sliding angle and easier roll-off. When the water drops roll over the surface, it can easily trap and remove dust particles from the surface. Due to this reason, a superhydrophobic surface is often called "self-cleaning" since the rolling-off of water droplets keeps the surface clean.

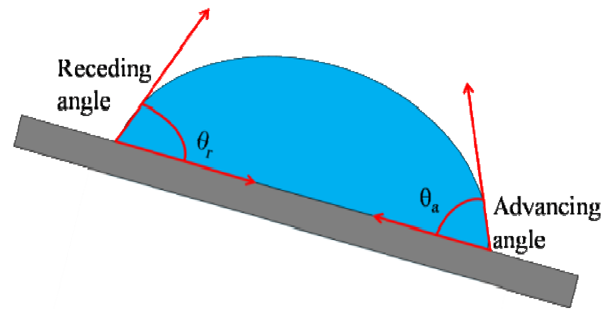

Figure 1.4: Schematic of droplet on a tilted substrate showing advancing (θ_a) and receding angle (θ_r) contact angle

The Wenzel state tends to give a larger contact angle hysteresis than the Cassie-Baxter state. As the contact line recedes, some liquid can be trapped in the surface texture and liquid is conformal filled in the texture initially. This can decrease the receding contact angle significantly, resulting in a large contact angle hysteresis and thus in a large critical sliding angle. This liquid trapping in the surface texture is not

expected for the Cassie-Baxter state; so, the contact angle hysteresis and critical sliding contact angle are much smaller than in the Wenzel state. In other words, the total wetting Wenzel regime is ‘‘sticky’’ in that drops of water tend to adhere to them more than to a flat surface of the same type; those following the regime of Cassie and Baxter are ‘‘slippy’’ and allow drops of water to roll off more easily than an equivalent flat surface.

1.3 Fabrication Methods of Superhydrophobic Surface

A wide variety of physical and chemical methods have been explored to fabricate superhydrophobic surfaces through one of the following two approaches (1) Creating a rough surface on a hydrophobic material (2) Modifying a rough surface by functionalization with a hydrophobic material coating.

1.3.1 Making a rough surface on hydrophobic materials

It is a relatively simple and one-step process to make superhydrophobic surfaces by using intrinsically hydrophobic materials and increasing the surface roughness further. In this approach, hydrophobic materials are used to obtain superhydrophobicity. One group of materials that is of great interest are fluorinated polymers which have extremely low surface energy. For example, the water contact angle of a tetrafluoroethylene (Teflon) surface is typically 115-120°. Further roughening these polymer surfaces leads to a superhydrophobic surface. One of the most widely used methods for roughening fluorinated polymer is plasma etching. The high-energy oxygen species generated by O_2 plasma can randomly etch fluorinated polymer materials and create the surface roughness needed to increase the water contact angle to >160° [41]. The mechanical stretching of the Teflon surface can also increase the roughness of the Teflon surface. The stretched Teflon film consists of a sub micrometer diameter fibrous crystal with a large fraction of void space on the surface.

Another hydrophobic polymer with low surface energy is Poly-dimethylsiloxane (PDMS) that can easily be processed to make a rough textured hydrophobic surface. A high power laser source can make PDMS rough. The contact angle obtained is in excess of 175°. The superhydrophobicity achieved is attributed to the high porosity and chain ordering on the PDMS surface [41-42].

1.3.2 Modification of rough surface with hydrophobic coating

In order to make superhydrophobic surfaces on the intrinsically hydrophilic materials is a two-step process i.e. making a rough surface first and then modifying it with coating of chemicals, such as organosilane which can offer low surface energy after linking to the rough surface. Because of the well-established micro/nano fabrication technologies on silicon it has been widely used for making superhydrophobic surfaces through the fabrication of a wide variety of surface structures. There are several ways to obtain a texture on a silicon substrate either by chemical texturing by an alkaline solution or plasma texturing using fluorine based plasma. Texturing can be performed on silicon with or without patterning. A study on increase in the hydrophobicity of silicon by the use of various chemicals for texturing to increasing roughness has been reported in literature. Eric Mazur et al. had shown the silicon texturing using laser followed by silane monolayer to obtain the WCA for 160° [41]. C. Wong et al. and Jie Hu established the chemical texturing of silicon using alkaline solution and metal assisted etching to obtain superhydrophobic silicon surface [44-45]. Beng Tay et al. reported the WCA of 162° by metal assisted silicon etching followed by SAM [46].

1.4 Deposition of Octadecyltrichlorosilane self Assembled Monolayer

The formation of SAM on silica and other dielectrics had been studied for a few decades now and a clear picture of the chemistry and structure of these SAM is available. The structure, formation and properties of SAM have attracted the large interest in the scientific community in recent years due to their potential in organic electronics applications [38]. In order to form a SAM it is necessary to find the self-assembly capable molecules which can covalently bond to a specific surface. The SAM molecule consists of three groups', namely an anchor group, a spacer group, and a terminal group. The anchor or head group namely $-SiCl_3$ is responsible for the absorption of the molecule by forming a chemical bond with the adsorbing surface. The terminal group namely $-CH_2$ determines the properties of SAM surface. This non-polar methyl group gives a hydrophobic surface. The spacer group between the anchor and terminal group consists of a long alkyl chain of the methylene group $(-CH_2)_n$. The spacer group determines intermolecular interaction and promotes the ordering and orientation of SAM molecules within the monolayer. The rate of formation of the Self-assembled monolayer is

influenced by many factors, some of which can be controlled relatively easily, such as temperature, solvent, and concentration of the absorbate and cleanness of substrate. In order to form high quality monolayers it is very important to ensure a high level of cleanliness on the surface to keep the error by contamination as low as possible. There has been considerable research on the formation mechanism of SAM on dielectric material surfaces.

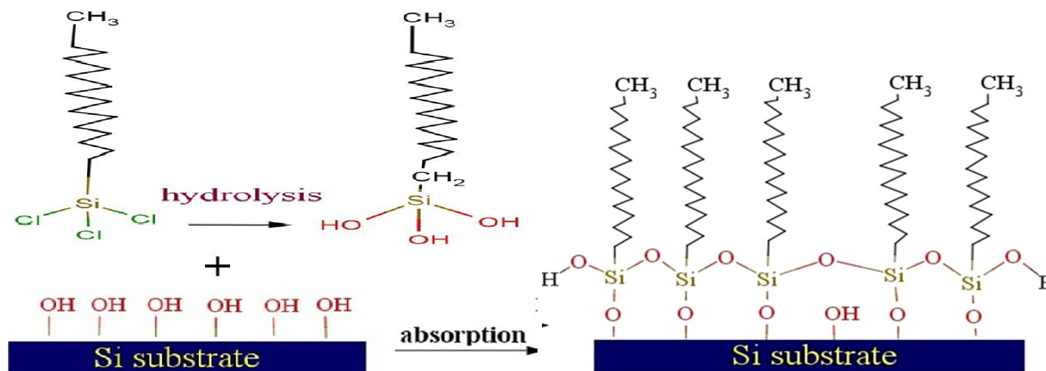

Figure 1.5: Schematic of formation mechanism of OTS SAM

The most common way of a SAM formation in the scientific community is silanization for which a schematic shown in Figure 1.5. The silanization includes a multi process, where absorption is followed by hydrolysis of the chlorosilane (Si-Cl) groups to form a siloxy (Si-OH) group as shown schematically in Figure 1.5. The strong bonding of the head group to the substrate is normally essential for a stable monolayer. After hydrolysis, the OH groups in organosilane also interact with the OH group on the substrate forming Si-O-Si bonds to the substrate as shown in Figure 1.5 after absorption. High quality SAM of organosilane are not simple to deposit, because it is processed in number of steps and strongly depends upon the various parameter including amount of water in solution, deposition time and temperature. The water trace is essential for formation of high quality monolayer but excess amount of water can make polycondensed silane in solution. Cleaning of the surface usually with chemicals or by oxygen plasma increases the possibility of formation of number of silanol group on the surface. However, by controlling the amount of water and deposition time also, good quality of monolayer can be formed on the surfaces.

Making a hydrophilic and hydrophobic surface into a superhydrophobic surface is an interesting challenge to the scientific community and has been attempted and published

in the literature. From the basic principles, there are two key requirements to obtain superhydrophobicity. One is appropriate surface chemistry and the other is appropriate surface roughness. On a flat surface, the highest water contact angle that can be obtained is about 110°-115° on materials like Poly-dimethylsiloxane (PDMS) and Poly-Tetraflouro Ethylene (PTFE). By preparing a surface with appropriate roughness and hydrophobic treatment, water contact angles higher than 150° and easy water run-off can be attained.

1.5 Motivation

As discussed in pervious sections, form last few decades the superhydrophobic surfaces have been investigated with various methods and are reported in literature. The fabrication of superhydrophobic surface required a solid surface with a low surface energy with water contact angle (WCA) > 90° which need to be further enhanced by tailoring the surface roughness. The prime reasons for advancing the attempts in the fields of superhydrophobicity are the application in self-cleaning, low adhesion, non-wetting, and electrowetting. A wide variety of organic and inorganic materials has already been studied to produce superhydrophobic surfaces. There is growing literature on the subject but interestingly there had been few attempts made towards making high-k dielectric materials superhydrophobic and comparing the methodology and results of achieving superhydrophobicity in low-k and high-k dielectrics. Moreover, there are no studies available on whether similar approaches for making silicon superhydrophobic are appropriate for low-k and high-k dielectric materials.

The most popular dielectric materials SiO_2 is used for semiconductor device fabrication and microelectronics applications. In the past few decades, the reduction of thickness in SiO_2 dielectric has enabled enhanced device functionality and performance at low cost. Small thickness makes SiO_2 device prone to breakdown and degrades the quality of material. Instead, for the downward scaling, the dielectrics with high dielectric constant are better choices and therefore a lack of literature on such dielectric surfaces superhydrophobicity, comparing them with low-k dielectric superhydrophobic surfaces opens up research area which needs to be explored. This quest had been the guiding factor for the present work.

Interestingly, all dielectric materials low-k (SiO_2) and high-k (HfO_2, Al_2O_3, TiO_2, and Ta_2O_5) are intrinsically hydrophilic in nature. Among many facet in the fabrication of superhydrophobic surfaces of dielectric materials challenge is for obtaining the low surface energy to enhance the hydrophobicity. Further, process for obtaining the low surface energy process involves the modification of the surfaces with hydrophobic coating. Teflon is most commonly used hydrophobic materials. The Teflon though has lowest dielectric constant ≈1.93 among available dielectric materials and due to poor dielectric constant breakdown can occur in electro wetting applications. To avoid such breakdown another dielectric materials films is combined with Teflon, but it well known that the use of additional dielectric material increases the cost and the process steps. Other polymeric materials such as PDMS, polyimide are intrinsically hydrophobic but requires a high voltage for actuation of the droplet in electrowetting system. Another alternate hydrophobic material i.e. self-assembled monolayer (SAM) can be used for improving the hydrophobicity of the materials. In literature, a wide variety of monolayer has been studied to modify the surface properties of dielectric materials. The quality and density of SAM is a challenging issue to produce superhydrophobic surface.

The available literature through contain volumes on use of dielectric materials with alternate surface properties, concerted efforts towards lowering the surface energy, optimized and economicuse of materials for reduction in process steps and comparative investigation on different dielectric materials generates a significant interest for further investigation. Towards this intent, we present a comprehensive review in Chapter 2 and frame specific problem statements. In Chapter 3 we present investigation on wetting behaviour of silicon. In Chapter 4, we have given the wetting behaviour of dielectric materials included low-k and high-k dielectric. In Chapter 5, we have presented the surface modification for SU8 polymer. Finally in Chapter 6 we give conclusions and scope for future work.

References:

1] G. Fogg (1947) Quantitative studies on the wetting of Leaves by water, proceeding of the Royal Society, 134: 523-522.

2] M. Schrader (1995) Young-Dupre Revisited, Langmuir, 11:3585-3589.

3] A. Nakajima (2011) Design of hydrophobic surfaces for liquid droplet control, NPG Asia Materials, 3: 49-56.

4] R. Furstner, W. Barthlott, C. Neinhuis (2005) Wetting and Self-Cleaning properties of artificial Superhydrophobic Surfaces, Langmuir, 21: 956-961.

5] B. Bhushan, Y. Jung, and K. Koch (2009) Self-Cleaning efficiency of artificial superhydrophobic surfaces, Langmuir, 25: 3240-3248.

6] L. Sas, R. Gorga, J. Joiness et al (2012) Literature review on superhydrophobic self-cleaning surface produced by electrospinning. J. of polymer science B, 50: 824-845.

7] L. Gao, T. McCarthy, X. Zhang (2009) Wetting and superhydrophobicity. Langmuir. 25 (24): 14100-14104.

8] J. Drelich, J. Milles, A. Kumar et al (1994) Wetting characteristics of liquid drops at heterogeneous surface. J. Colloids and Interface, 93: 1-13.

9] Z. Yang, C. Chiu, J. Yang (2009) Investigation and application of an ultra hydrophobic hybrid-structured surface with anti-sticking character. J. Micromachining and Micro engineering, 19: 085022-085033.

10] B. Bhushan, K. Koch and Y. Jung (2008) Nanostructures for superhydrophobicity and low adhesion. Soft matter, 4: 1799-1804.

11] Y. Su, B. Ji, Y. Huang (2010) Nature's Design of Hierarchical Superhydrophobic Surfaces of a water strider for low adhesion and low-energy dissipation. Langmuir, 26(24): 18926-18937.

12] K. Koch, B. Bhushan, Y. Jung (2009) Fabrication of artificial Lotus leaves and significance of hierarchical structure for superhydrophobicity and low adhesion. Soft matter, 5: 1386-1393.

13] J. Ou, B. Perot, and J. Rothstein (2004) Laminar drag reduction in microchannels using ultrahydrophobic surfaces. Physics of fluids, 16(12): 4635-4643.

14] M. Samaha, H. Tafreshi et al (2012) Superhydrophobic surfaces: From the lotus leaf to the submarine. Comptes Rendus Mecanique, 340: 18-34.

15] L. Wu, J. Zhang, B. Li et al (2013) Mimic nature, beyond nature: facile synthesis of durable superhydrophobic textiles using organosilane. J. Materials Chemistry, B, 1: 4756-4763.

16] X. Zhang, F. Shi, J. Niu et al (2008) Superhydrophobic surfaces: from structural control to functional application. J. Materials chemistry, 18:621-633.

17] J. Liu, X. Feng, G. Wang et al (2007) Mechanisms of superhydrophobicity on hydrophilic substrates., J. Physics: Condensed Matter, 19: 356002

18] B. Wang, Y. Zhang, L. Shi et al (2012) Advances in the theory of superhydrophobic surfaces. J. Materials Chemistry, 22: 20112-20117.

19] Y. Yan, N. Gao, W. Barthlott (2011) Mimicking natural superhydrophobic surfaces and grasping the wetting process: A review on recent progress in preparing superhydrophobic surfaces. Advances in Colloid and Interface Science, 169: 80-105.

20] George M. Whiteside's and Paul E. Laibinis (1990) Wet Chemical Approaches to the Characterization of Organic Surfaces: Self- Assembled Monolayers, Wetting, and the Physical-Organic Chemistry of the Solid-Liquid Interface. Langmuir, .6: 1.

21] J. Gooding, F. Mearns, W. Yang et al (2003) Self-Assembled Monolayers into the 21st Century: Recent advances and applications. Electroanalysis, 15 (2): 81-96.

22] R. Otero, J. Gallego, A. Parga et al (2011) Molecular Self-Assembly at Solid Surfaces. J. Advance in Materials, 23: 5148-5176.

23] Lauren Newton, Thomas Slater, Nick Clark et al (2013) Self assembled monolayers (SAM) on metallic surfaces (gold and grapheme) for electronic applications. J. Mater. Chem. C, 1: 376-393.

24] M. Wang, K. Liechti, Q. Wang (2005) Self-Assembled Silane Monolayers: Fabrication with Nanoscale Uniformity. Langmuir, 21: 1848-1857.

25] S. Jadhav (2011) Self-assembled monolayer (SAMs) of carboxylic acids: an overview. Central European Journal of Chemistry, 9(3): 369-378.

26] S. Pawsey, K. Yach, and L. Reven (2002) Self-Assembly of Carboxyalkyl phosphonic Acids on metal-oxide powders. Langmuir, 18: 5205-5212.

27] N. McIntyre, H. Nie, A. Grosvenor (2005) XPS studies of octadecylphosphonic acid (OPA) monolayer interactions with some metal and mineral surfaces. Surface and Interface Analysis; 37: 749-754.

28] O. Yildirim, M. Yilmaz, D. Reinhoudt (2011) Electrochemical Stability of Self-Assembled Alkyl phosphate Monolayers on Conducting Metal Oxides. Langmuir, 27: 9890-9894.

29] S.Wasserman, Y.Tao, and G.Whitesides (1989) Structure and Reactivity of Alkylsiloxane Monolayers Formed by Reaction of Alkyltrichlorosilane on Silicon Substrates. Langmuir, 5(4): 1074-1087.

30] D. Aswal, S. Lenfant, D. Guerin et al (2006) Self assembled monolayer on silicon for molecular electronics. Analytica Chimica Acta 568: 84-108.

31] N. Glass, R.Tjeung, Peggy Chan l (2011) Organosilane deposition for microfluidics applications. Biomicrofluidics, 5: 036501-036501-7.

32] J. Takeya, T. Nishikawa, T. Takenobu (2004) Effects of polarized organosilane self-assembled monolayers on organic single-crystal field-effect transistors. Applied physics letters, 85(21): 5078-5080.

33] V. Kumar, N.N. Sharma (2012) SU-8 as Hydrophobic and Dielectric Thin Film in Electrowetting-on-Dielectric based microfluidics device. J. of Nanotechnology, Article ID 312784 (6), doi: 10.1155/2012/312784.

34] Wei Dai and Ya-Pu Zhao (2007) The Nonlinear Phenomena of Thin Polydimethylsiloxane (PDMS) Films in Electrowetting. Int. J. of Nonlinear Sciences and Numerical Simulation, 8(4): 519-526.

35] E. L. Papadopoulos , V. Zorba , Emmanuel Stratakis et al (2012) Properties of Silicon and Metal Oxide Electrowetting Systems.J. of Adhesion Science and Technology 26: 2143-2163.

36] H. Liu, S. Dharmatilleke, D. K. Maurya et al (2010) Dielectric materials for electrowetting-on-dielectric actuation. Microsystems Technology, 16:449-460.

37] R. Ortiz, A. Facchetti, and Tobin J. Marks (2010) High-k Organic, Inorganic, and Hybrid Dielectrics for Low-voltage Organic Field-Effect Transistors. Chem. Rev., 110: 205-239.

38] X. Sun, C. Di and Y. Liu (2010) Engineering of the dielectric-semiconductor interface in organic field-effect transistors. J. Mater. Chem., 20: 2599-2611.

39] E. Martines, K. Seunarine, H. Morgan et al (2005) Superhydrophobicity and Superhydrophobicity of regular Nanopatterns. ACS NANO LETTERS, 5(10): 2097-2103.

40] Y. Song, R. Nair, M. Zou (2009) Superhydrophobic Surfaces Produced by applying a Self- Assembled Monolayer to Silicon Micro/Nano-Textured Surfaces. Nano Res., 2: 143-150.

41] B. Bhushan, Y. Jung (2008) Wetting, adhesion and friction of superhydrophobic and hydrophilic leaves and fabricated micro/nanopatterened surfaces. J. of Physics condensed Matter, 20; 225010-225034, doi:10.1088/0953-8984/20/225010.

42] E. Bormashenko (2010) Wetting transitions on biomimetric surfaces. Philosophical transactions of the Royal Society A, 368:4695-4711, doi:10.1098/rsta.2010.0121.

43] T. Baldacchini, J. Carey, M. Zhou, Eric Mazur et al (2006) Superhydrophobic surfaces prepared by Microstructuring of Silicon using a Femtosecond Laser, Langmuir, 22, 4917-4919.

44] Y. Xiu, L. Zhu, D. Hess, C. Wonget al (2007) Hierarchical silicon etched structures for controlled hydrophobicity/Superhydrophobicity, Nano Letters, 7, pp.3388-3393.

45] W. Zhang, X. Fan, S. Sang, P. Li, G. Li, Y. Sun, and J. Hu, et al (2014), Fabrication and characterization of silicon nanostructures based on metal-assisted chemical etching. Korean Jl. Chemical Engineering, 31(10), 62-67.

46] X. Li, B. Tay, P. Miele, A. Brioude, D. Cornu et al. (2009) Fabrication of silicon pyramid/nanowires binary structure with superhydrophobicity", Applied Surface Science, 255, 7147-7152.

Chapter 2

Literature Review

2.1 Overview

The potential and importance of the wetting phenomenon has been discussed in pervious chapter. The earliest direct observation of wetting phenomenon was given by Galileo. After Galileo, Thomas young developed the concept of wetting and contact angle. In 1805, Thomas published an article [1] on essay on cohesion of fluids in which he described the balance of various forces acting on sessile liquid drop on solid surface which is known as Young's Equation (equation 1.3). The wettability behaviour can be quantitatively analyzed based on the sessile drop contact angle on the surface. Motivated by behaviour of Lotus leave from nature, there is intense interest to modifying the solid surfaces to alter their wetting behaviour to render them to hydrophilic, hydrophobic and superhydrophobic. The superhydrophobic properties of surfaces such as water repellency and self-cleaning give rise to wide range of applications. Numerous organic and inorganic materials have been studied for altering the wetting behaviour. Among many others, silicon (semiconductor), oxide and polymers are materials of great interest in MEMS and microfluidics application [2, 3]. This chapter aims to provide a clear and concise understanding and highlighting the aspects relevant to the current study related to these materials based on the extensive literature review presented in next section.

2.2 Wetting behaviour of Silicon Surface

Silicon is widely used material for the semiconductor industries because of a large variety of mature, easily accessible processing techniques and well characterized materials readily available. The numerous devices such as MOS transistors and Schottky barriers and solar cell rely on quite complex surface phenomenon; much remains to be learned about the properties of silicon surfaces. Numerous methods are used to produce the silicon superhydrophobic surfaces.

In 1990, Plamskog et al. [4] introduced the wetting properties of silicon surface by chemical etching of silicon using standard etchant KOH, EDP (EthylenDiamine: Pyro

cathecol :water)and mixture of Nitric acid and HF dip. The surface after the etching chemically modified using silane made the surface hydrophobic.

In 2000, McCarthy et al. [5] reported the superhydrophobic surface using the silicon patterning with photolithography and followed by organosilane coating.

In 2002, K. Hashimoto et al. [6] studied the effect of surface structures like pillar formation and groove structured prepared on the silicon wafer by dicing. The structured silicon surface subsequently coated with alkylsilane achieved the superhydrophobic surface.

In 2003, Lei Jiang et al. [7] investigated the novel way for controlling the surface wettability by adjusting the anisotropic structure of surface. The primary objective of this work was to determine wettability behaviour with aligned carbon nanotube depositions by CVD on silicon template with well-defined structure. The study [7] revealed that anisotropic microstructures could bring about better controllability over the surface wettability.

In 2004, L. Jiang [8] had shown the wettability behaviour by applying the poly N-isopropylacrylamideon flat and a rough silicon surface. The rough silicon surface exhibited a regular array of square silicon micro convexes by laser cutter. L. Jiang showed the superhydrophobicity by roughing the silicon by laser etching and chemical modification using silane monolayer to achieve the superhydrophobic surfaces.

In 2005, R. Furstner et al. [9] studied the Wetting and self-cleaning properties of Silicon and artificial surfaces. In their work, the silicon wafer with regular patterns of spikes was manufactured by X-ray lithography and made hydrophobic by Au-thiol. M. Lejeune et al. [10] studied the way of producing superhydrophobic surfaces by tailoring their surface topography and chemical properties. The key steps of this process were the modification of surface topography of the silicon surface to create high roughness before deposition of fluorocarbon coating to improve the hydrophobicity. M. Callies et al. [11] investigated the superhydrophobic behaviour of silicon by conventional lithography patterned silicon surface followed by the hydrophobic coating. O. Riehle et al. [12] studied theoretically and experimentally wetting behaviour of nanopatterned silicon surfaces. Riehle fabricated the regular pattern of nanopits and nanopillars and investigated their wettability before and after chemical modification with Octadecyltrichlorosilane (OTS) monolayer.

In 2006, C. Wong et al. [13] reported an optimized design to achieve the superhydrophobic surfaces for MEMS applications. The silicon surface was patterned by standard lithography and followed by fluorocarbon deposition. Y. Feng et al. [14] described a method to control the surface wettability from the contact angle on the flat surface to superhydrophobic apparent contact angles through tuning surface roughness using silicon micromachining and self-assembled monolayer modification. E. Mazur et al. [15], presented the structuring process that use intense femtosecond laser pulses to create microstructure on silicon and followed by organosilane monolayer to achieve the superhydrophobicity.

In 2007, Bhushan et al. [16] studied the wetting behaviour on silicon surface patterned with standard lithography with pillars of different values and heights with varying the pitch values and modified with PF_3 (tetrahydroperfluorodecyltrichlorosilane). B. Ziaie et al. [17] demonstrated the superhydrophobicity of silicon by incorporating electrochemical surface modification. D. Gao et al. [18] who reported the design and fabrication of micro-textures for inducing a superhydrophobic behaviour on hydrogen terminated silicon surfaces. W. Hess et al. [19] demonstrated the effect of two scale roughness on superhydrophobicity. Micron scale pyramid structures were generated by anisotropic KOH etching and the nanostructures were prepared by metal-assisted etching. The micro/nano textured surface was chemically modified with different organosilane monolayer to achieve the superhydrophobicity.

In 2008, Bhushan et al. [20] employed superhydrophobic surfaces by micro and nano structuring in silicon surface. The micro structuring were fabricated by replication of micro patterned silicon surface using an epoxy resin and nanostructuring was carried out using the alkane self-assembly monolayers on microstructure surface. Again, B. Bhushan with Y.C. Jung [21] investigated the dynamic effect of bouncing water droplet on patterned silicon with silane modification. S. Franssila et al. [22] demonstrated the wetting behaviour of silicon by chemical modification the silicon nanograss. D. Gao et al. [23] reported the water and oil repellent surfaces on porous silicon films. Gao investigated the porous silicon films fabrication by convenient gold-assisted electroless etching process which possess a porous structure consisting of micrometer sized asperities and it was shown that they were able to produce superhydrophobic surface and a superoleophobic phenomenon on an intrinsically oleophillic trichlorosilane coated silicon surface. C. Wong et al. [24] performed metal (Au) assisted etching to form

nanoscale roughness on form micron-sized textured surfaces. After fabrication of the surface structures, surface fluorination was performed by treatment with perfluorooctyl trichlorosilane (PFOS). R. Boukherroub et al. [25] reported the use of patterned superhydrophobic silicon nanowire surfaces for selective transfer of biological molecules and nanoparticles. The silicon nanowires investigated in this study were prepared by chemical etching using $AgNO_3$ and HF aqueous solution. After formation of nanowire, a chemical modification of surface with Octadecyltrichlorosilane (OTS) led to formation of a superhydrophobic surface.

In 2009, Nan Lu et al. [26] studied the simple approach to fabricate the superhydrophobic surface by employing the KOH etching and silver catalytic etching. Pyramidal hierarchical structures were generated on the silicon surface which exhibited superhydrophobic behaviour after fluorination treatment. J. Wang et al. [27] reported the superhydrophobic behaviour by patterning silicon surface to create T-shape micropillar surface coated with diamond-like carbon. E. Stratakis et al. [28] developed the superhydrophobic surface by irradiating silicon wafers with femtosecond laser pulse and subsequently coating them with alkylsilane monolayers. H. Fenget al. [29] reported the various superhydrophobic surfaces with pillars fabrication using standard photolithography and hydrophobic with Octadecyltrichlorosilane (OTS). B. Tay et al. [30] had shown the superhydrophobic surface via formation of pyramid/nanowire binary structure using NaOH anisotropic etching technique followed by a silver-catalyzed chemical etching process followed by the hydrophobic coating of OTS.

In 2010, M. Zou et al. [31] presented the novel way to fabrication of superhydrophobicity surfaces by applying a self-assembled monolayer (SAM) to micro/nano textured silicon surface. The textured surfaces on silicon substrates were generated by the aluminum-induced crystallization of amorphous silicon. C. Wong et al. [32] used the same procedure to study the wetting behaviour of silicon. Their work was focused on the liquid-based metal assisted etching and various silane treatments to create the superhydrophobic and oleophobic surfaces. Boggild et al. [33] demonstrated the fabrication of silicon nanograss with overhanging nanostructures at the apexes of silicon nanograss by controlling the etching parameter of the Si wafer and showed the significant improvement in the water and oil repellence by employing the hydrophobic coating. Lee et al. [34] fabricated the superhydrophobic surface using MEMS technology and microwave plasma-enhanced chemical vapor depositions (MPCVD) of Carbon-nanotubes on silicon micro-post arrays

surfaces. The micro-post surfaces also characterized after the silane hydrophobic coating on the surfaces. D. Sarkar et al. [35]had shown the wetting characteristics of micro/nano rough substrates of aluminum and smooth silicon substrates and compared them with depositing hydrocarbon and fluorinated-hydrocarbon coating via plasma enhanced chemical vapor deposition (PECVD) techniques.

In 2011, G. Lim et al. [36] demonstrated the nanostructure silicon surfaces with study of reflectance using the simple mask-less deep reactive ion etching (DRIE) technique. The superhydrophobicity was shown by applying the fluorocarbon by DRIE on nanostructure silicon surface. W. Yuan et al. [37] studied the wetting behaviour of silicon by dual scale pillar formation. The method for achieving the superhydrophobic surface formation of micropillars by reactive ion etching and nanopillars by catalyzed Ag etching. T. Lee et al. [38] presented the hydrophilicity in patterned superhydrophobic silicon nanowires. The organosilane coating was used to produce the superhydrophobic silicon nanowire. K. Jardi et al. [39] demonstrated simple method for generating microstructure surface on silicon substrate. The surface was cleaned using the piranha solution and the functionalized using the aminosilyalted.

In 2012, Choi et al. [40] described the surface wettability of silicon by fabricating the Si nanowire array. The metal (Au) assisted chemical etching of silicon was used to form Si nanowire arrays. The glancing angle method was used for deposition of gold nanoparticles. These silicon nanowires chemically modified and made hydrophobic by fluorosilane deposition. Jiang et al. [41] also presented the superhydrophobic surface by fabrication of nanowire arrays assisted by superhydrophobic pillar-structured surface with high adhesion. After modification by a monolayer of heptadecafluorodecyltri-methoxysilane (FAS), the microstructure exhibited the superhydrophobic behaviour. Chen et al. [42] demonstrated the pattern dependent superhydrophobic surface which was prepared by femtosecond laser. These surfaces were composed of spikes induced by laser and patterned array of triangular, rhombus and circle. After patterning by laser the sample was deposited with the fluoroalkylsilane monolayer to achieve the superhydrophobic surfaces.

In 2013, Ma et al. [43] demonstrated the high aspect ratio (HAR) micro/nano hierarchical structures using conventional micro technologies. The silicon nanopillars array was fabricated by DRIE. Ruhe et al.[44] studied the mechanical stability of superhydrophobic surface by nano, micro texturing and combination of both texturing. The surfaces were

generated by silicon etching and subsequent coating with a monolayer of fluoropolymer (PFA). In similar manner Wiedemann et al. [45] studied the silicon superhydrophobicity with hexagonal arranged nanopillars followed by coating of the hydrophobic Teflon like materials. Huang et al. [46] developed the nonporous silicon nanopillars array through standard fabrication technique to study the superhydrophobic behaviour.

In 2014, Coffinier et al. [47] studied the methods for the preparation of superhydrophobic and highly oleophobic nanostructure silicon surfaces. The technique relied on metal-assisted electroless etching of silicon in sodium tetrafluroborate ($NaBF_4$) aqueous solution. The resulting structured surface was chemically modified with PFTS to achieve the superhydrophobic surfaces. Ruhe et al. [48] also studied the mechanically stable superhydrophobic surfaces, which had a hierarchical roughness that was composed of silicon microcones and silicon nanograss. Both micro and nanostructures were made using standard micro fabrication techniques. All structures on surfaces were covered with a layer of a fluorinated film to achieve the superhydrophobic surface. Hu et al. [49] presented the superhydrophobic behaviour of silicon by nano-structuring based on Ag induced selective etching of silicon wafers and followed by the chemical treatment. In 2014, R. Moboudin et al. [50] investigated the wetting behaviour of hydrophobic silicon nanowire. The silicon nanowires were produced by a combination of colloidal patterning and metal-catalyzed etching. After the silicon nanowire fabrication, the silicon surface was chemically modified by either hydrocarbon or fluorinated monolayers. The combination of silicon nanowire and monolayers provided the water contact angle of $\approx 170^o$. Z. Zhong et al. [51] reported the wettability behaviour of silicon wafers cleaned with piranha followed by HF dip and different plasma (Ar and O_2) treatment. G. Vereecke et al. [52] investigated the wetting behaviour of silicon nanopillars. The silicon nanopillars were formed using the plasma etching system. After plasma etching surface was modified using self-assembled monolayer and a maximum of 132° contact angle was obtained. Y. Coffinier et al. [53] reported the superhydrophobic nanostructure silicon surfaces. The nanostructuring of silicon was carried out using metal assisted etching. The textured surfaces were coated with silanization or C_4F_8 plasma deposition and a contact angle of 160° was achieved in this process.

All the techniques outlined above, it is observed that the superhydrophobic silicon surface can be achieved by tailoring the surface roughness using chemical and plasma etching and by modification the surfaces with hydrophobic coating such as Teflon and organosilane

monolayer. The literature though lacks a comparative investigation on various texturing methods with and without permutation with SAMs. In order to produce a hydrophobic surface we have used various possible combinations to texture the silicon surface rough and used the organosilane monolayer to improve the hydrophobicity of silicon surface. The interest was to see if all the texturing and a combination with SAM deposition lead to a water contact angle in the limits of superhydrophobic surfaces. Further the investigation was also to develop a method which could be applied on other material of importance in MEMS other than silicon, to achieve water contact angle >150° in superhydrophobic range. The silicon roughing was carried out without any patterning to make the roughing process simple, easy and less time consuming [54, 55]. Conditions for wetting and non-wetting were analyzed and are discussed in Chapter 3.

2.3 Wetting behaviour of Dielectric Materials

Next to silicon (semiconductor material), a dielectric materials is an electrically insulating material that can be polarized by an applied electric field and therefore has the ability to store charge when an external electrical field is applied. Dielectrics are critical component of various technologies, including microelectronics transistor developed in the early 1960's [56-58], organic electronics [59-60] and microfluidics applications [61].The dielectric material can be largely grouped into two categories: organic and inorganic dielectric schematically shown in Figure 2.1. A literature review on making different dielectric superhydrophobic is given in following sections.

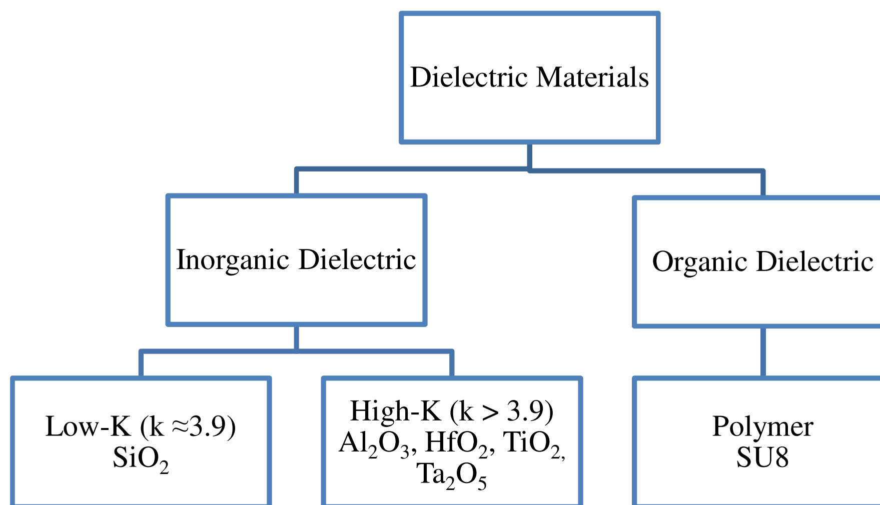

Figure 2.1: Schematic diagram of dielectric materials distribution

2.3.1 Low-*k* dielectric materials

The inorganic dielectric materials can be further classified as: Low-k dielectric materials and High-k dielectric materials. In semiconductor technology, Silicon dioxide (SiO_2) is the most commonly used low-*k* dielectric. The utilization of this dielectric is very convenient due to the ready availability of the thermally grown dioxide. In fact, silicon reacts with oxygen or nitrogen in a controlled manner to form superb is insulating layers with excellent mechanical, electrical, and dielectric properties. SiO_2 is intrinsically hydrophilic. The various methods and materials are used for modification of SiO_2 surface for making it hydrophobic. The surface modification of SiO_2had been widely attempted in microfluidics applications. Various hydrophobic materials such as hexamethyldisilazane (HMDS), Teflon, and Self assembled monolayers are studied to change the surface properties of silicon dioxide.

In 1974, Frieser et al. [62] demonstrated first time the characterization of thermally grown SiO_2 surface. Their work investigated surface characteristics using water and an organic solvent to characterize thermally grown SiO_2surfaces. The surface modifications were found to be hydrophobic when the oxide surface was removed from the substrate after oxidation, hydrophilic when hydrophobic surface were boiled in deionized water and organophilic when the surface was modified by immersing the SiO_2 surface in trichloroethylene and drying the surface in stream of filtered nitrogen.

In 1996, Thomas et al. [63] investigated the wettability of polished thermally grown silicon dioxide surfaces. The purpose of their work was to distinguish between the chemical and mechanical interactions at an oxide surface during the chemical mechanical polishing.

In 1999, Fujii et al. [64] studied the wetting behaviour of SiO_2 by liquid silicon. The contact angle measurement by liquid silicon was carried out by sessile drop method at 1723K temperature.

In 2000, Huzumi at al [65] reported the surface modification of SiO_2 by self-assembled monolayer. Their work was a study of amino terminated monolayer through a chemical vapor deposition method using N-(6-aminohexyl)-3-aminopropyltrimethoxysilane(H_2N $(CH_2)_6NHCH_2CH_2CH_2Si$ $(OCH_3)_3$, AHAPS) as a precursor. Kim et al. [66] investigated the hydrophobic SiO_2 powder. The powder was prepared by surface modification of TEOS (tetrathylorthosilicate) wet gel.

In 2001, S. Yitzchaik et al. [67] studied the monolayer for surface modification of hydroxyl terminated surface. The Polyaniline (PAN) was assembled on hydroxyl - terminated native oxide silicon. Borguet et al. [68] investigated the surface modification of silicon dioxide with alkylsiloxane to study the photo reactivity of SAM.

In 2002, Salleo et al. [69] chemically modified the SiO_2 for polymer thin film transistor. Their work pertained to investigation of effect of modification of SiO_2 with organic trichlorosilane SAM on polymer transistor. H. Klauk et al. [70] also modified the $SiO_2$with pentacene for thin film transistor. The thermally grown oxide surface was modified with OTS monolayer to improve the device characterization.

In 2003, M. Lieberman et al. [71] reported SiO_2 surface modification with OTS self-assembled monolayer. The works focused on the effect of different growth environments on growth mechanism of monolayer at microscopic level. Y. Wu et al. [72] studied the wetting behaviour of SiO_2films prepared by microwave plasma-enhanced CVD. After preparation of the SiO_2 films, the film surfaces were treated with self-assembled monolayer of fluoroalkylsilane on the surface, in order to improve water repellency. A. Kawai et al. [73] demonstrated the wetting behaviour of SiO_2 surface by chemical and plasma treatment. The silane coupling treatment with hexamethyldisilazane (HMDS) was used to make surface hydrophobic and oxygen plasma treatment were carried out to make surface further hydrophilic.

In 2004, Yuan et al. [74] demonstrated the wetting behaviour on SiO_2 surface using the molten silicon at 1693K.J.Veinot [75] et al., introduced the superhydrophobicity of SiO_2 by fabricating the nanostructure and functionalization with siloxane. The Glancing angle deposition method was used for fabricating the nanostructure thin films and sample was further treated with oxygen plasma to maximize the reactivity between alkyltrichlorosilane reagents and SiO_2 pillar surface. Shiratori et al. [76] demonstrated the ultra-water repellent surface with SiO_2 nanoparticles. The film was prepared by absorption of poly-allylamine, SiO_2nanoparticles and Poly acrylic acid. The film was treated with dichlorodimethylsilane to achieve the superhydrophobic surface.

In 2005, Ekerdt et al. [77] reported the SiO_2 surface modification with fluorinated monolayers. The work was to study the effect of self-assembled monolayer

tridecafluoro-1, 1, 2, 2,-tetrahydrooctyltrichlorosilane (FOTS) deposition by vapor phase on oxide surface.

In 2006, Heremans et al. [78] studied the wetting behaviour with various self-assembled monolayers. Various organosilane and carboxyl monolayer were used for altering the wetting behaviour of silicon dioxide surface. H. Ji et al [79] investigated the formation of mechanics of the controller perfluorocarbon nanoneedle on SiO_2 surface for biomedical applications.

In 2007, C. Franco et al. [80] demonstrated the modification of Plasma enhanced CVD of Si/SiO_2 interface for organic electronics. The functionalization of silicon dioxide surface was performed with PECVD with plasma treatment of O_2 and CF_4. Rosenman et al. [81] studied the wettability of modified silicon dioxide surface using environmental scanning electron microscope. The thermally grown silicon dioxide surfaces were treated with electron irradiation to achieve the hydrophobic surface.

In 2008, H. Lu [82] used Cytop fluoropolymer as the hydrophobic material for silicon dioxide. The study was performed with electro wetting-on-dielectric (EWOD) driven droplet. The PECVD deposited silicon dioxide materials was used as dielectric materials for electrowetting applications. R. Cohen et al. [83] developed the superhydrophobic surface by fabrication of microhoods in silicon. Silicon dioxide was etched using a mask and was further modified with silane treatment by chemical vapor deposition of perfluorodecyltrichlorosilane. Yoon et al. [84] studied the droplet manipulation on an open surface. Electrowetting based open microchannels using SiO_2 as dielectric materials were modified with Teflon hydrophobic materials. C. Smits et. al. [85] developed the self-assembled monolayer field effect transistor (SAMFET). The silicon dioxide was used as gate dielectric and was activated using oxygen plasma treatment followed by acid hydrolysis.

In 2009, Y. Ito et al. [86] demonstrated the self-assembled monolayer of alkylsilanes for silicon dioxide which served as gate dielectric materials for organic FET. The OTS monolayer was spin coated on the surface of SiO_2. J.P. Simonato et al. [87] used the self-assembled monolayer to modify the SiO_2 surface. The thermally grown silicon dioxide were modified with 3-mercaptopropyltrimethoxysilane (MPTS) in vapor phase.

In 2010, Linfordet al. [88] studied the surface modification of $SiO_2$with three different variants of aminosilane which were deposited by chemical vapor deposition. H. Graaf et al. [89] studied the wettability behaviour of SiO_2 using self-assembled monolayer. The

monolayer deposition on oxide surface were carried out using solution based methods and characterized by contact angle measurement.

In 2011, Y.R. Liu et al. [90] studied the effect of OTS monolayer on electrical properties of thin film transistor. Their thermally grew SiO_2 surface, modified then with monolayer by spin coating methods and examined the I-V and C-V properties of transistor.

In 2012, R. Diebold et al. [91] investigated the smooth and aggregate free self-assembled monolayer for SiO_2 surface. The study involved the coupling agent employing a spin coated perfluoropolyether (PFPE) as diffusion barrier that reduced the surface roughness while maintaining the high contact angle. A. Mahajan et al. [92] reported the modification of oxide surface deposited by SiO_2 xerogel spin coating techniques. The hydrophobic SiO_2 thin films were obtained by surface modification using TMCS (trimethylchlorosilane) and hexane as surface modifying agent. Y. Do et al. [93] reported the superhydrophobic SiO_2 microrod arrays. The superhydrophobic structures were prepared by a combination of the two steps micro/nano sphere lithography and RIE processes. X. Ge et al. [94] reported the fabrication of raspberry SiO_2/Polystyrene particle. The nano-sized hydrophobic polystyrene particular on the surface of submicron silica particle were synthesized by radiation mini emulsion polymerization at room temperature with highest achieved contact angle of 151°. W. Li et al [95] reported superhydrophobic surfaces by dipping method using the Ammonium metavanadate (NH_4VO_3) solution and SiO_2. The maximum contact angle reported was 167° by dipping for long time.

In 2013, S. Arscott et al. [96] studied the wetting of soap bubbles on hydrophilic and hydrophobic SiO_2surfaces. R. Linford et al. [97] described the method of modification of SiO_2 surface using plasma treatment. The hydrogen and Argon plasma was used to enhance the silane deposition. After plasma treatment the SiO_2surface was chemically modified with chemical vapor deposition of silanes.

In 2014, W. Rui et al [98] prepared the superhydrophobic surface by introducing in situ functionalizing nano-SiO_2 into side-amino modified hydroxyl-terminated curing system and reported maximum contact angle of 154.8 ± 1°. W. Xu et al. [99] investigated the superhydrophobic behaviour of combined effect of chemistry and RAFT (Reversible addition-fragmentation chain transfer polymerization) technology. The SiO_2 surface was modified using the RAFT technology and achieved water contact angle of 157 ± 2°. J. Lin et al. [100] reported the fabrication of superhydrophobic surface on cotton fabric modified

SiO_2 nanoparticle and flouropolymer and achieved the contact angle >150°. L. Zhefeng et al. [101] investigated the phosphonic acid monolayer for surface modification of the SiO_2 for the organic field effect transistor. F. Meiners et al. [102] reported the surface modification of silicon dioxide using trichlorosilane and dichlorosilane monolayer.

All the techniques outlined above presents the chronological development of the investigation on SiO_2 surface with various chemical treatments. HMDS, Teflon and various variety of self-assembled monolayer were used for altering the chemical properties of SiO_2. A self-assembled monolayer is widely used hydrophobic materials for changing the SiO_2 wetting properties. The highest water contact angle was achieved by using silica nanoparticle and hydrophobic coating. We have shown the achievement of hydrophobic SiO_2 surface by combined effect of plasma and organosilane monolayers [55].

2.3.2 High-*k* dielectric materials

The interest in new dielectric materials has arisen primarily from the necessity for inexpensive device fabrication processes and the reduction of the operating voltage required for new devices fabrications. In fact, one of the major challenges in the development of organic and electrowetting devices are the need of high voltages for their operation when low-*k* dielectrics are used making these devices impractical for low-priced applications. It is thus mandatory to search for thin, high-*k* gate dielectrics to achieve the requirements needed for new technologies. In this sense, SiO_2 has reached its scaling limit, directing the study of many groups in the search for alternative high-k materials such as: Al_2O_3, HfO_2, Ta_2O_5, TiO_2, Si_3N_4 and a-poly [103]. A literature review on making of hydrophobic surfaces of that high-k dielectric is given in following sections.

2.2.2.1 *Hafnium oxide (HfO_2)*

High dielectric constant (k) metal oxides such as hafnium oxide have gained significant interest due to their applications in microelectronics. HfO_2 thin films have been widely investigated as potential high-k oxides to replace SiO_2. HfO_2 has a dielectric constant of 16-29 and a wide band gap of 5.8eV, which is suitable for dielectric with high capacitance and low leakage current even using films of only a few nanometer thickness.

In 2002, Fadeev et al. [104] investigated the preparation of the self-assembled monolayer of organosilane hydrides on the metal oxides. In 2003-2007 there is no published literature available on surface modification of Hafnium oxide.

In 2008, Jen et al. [105] studied the thin film transistor characteristics after monolayer modification for hafnium oxide. The hafnium oxide used as dielectric material was prepared by sol gel methods. After deposition the hafnium oxide, surface was modified with n-octadecylphosphonic acid with improved performance over bare HFO_2.

In 2009, C. Wei et al. [106] investigated the use of Hafnium oxide as dielectric for thin film transistor. The Hafnium oxide was prepared by mixing of hafnium dichloride oxide ocatahydrate with glycine and water. After preparation the surface was thermally evaporated to modify the Hafnium oxide surface. A. Jen et al. [107] studied the surface modification of Hafnium oxide using different self-assembled monolayer. The monolayers of phosphonic acid, carboxylic acid were used to improve the interface properties.

In 2010, C. Hsieh et al. [108] studied the fluorinated hafnium oxide use as inter poly dielectric. The fluorine incorporation process is effective to improve the insulating characteristics of Hafnium oxide. Y. Liu et al. [109] studied the Hafnium oxide as gate dielectric for thin film transistor. The Hafnium oxide surface was modified using the Octadecyltrichlorosilane (OTS) and performance characteristics were studied.

In 2011, Liu et al. [110] reported the passivation process by oxygen plasma treatment on non-stoichiometric HfO_2 films deposited by magnetron sputtering. They concluded after optimal oxygen plasma treatment on reduced leakage current and improved breakdown voltage. Guha et al. [111] demonstrated electrowetting on hydrophobic Hafnium oxide. The thin film of hafnium oxide dielectric was submersed in dodecane containing sorbitan trioleate and lipophilic surfactant. When a water drop was deposited onto Hafnium oxide, sorbitan trioleate adsorbed the oil-water and oil-hafnium oxide interfaces, forming a lipid bilayer which made the surface of Hafnium oxide hydrophobic. Durov et al. [112] studied the wetting behaviour of hafnium oxide by pure metals liquid. The metal liquid of tin, copper, silver, gold, iron, nickel, platinum, aluminum was used for in the work of Durov.

In 2012, Renaudot et al. [113] studied the performance of Hafnium oxide materials for liquid dielectrophoresis microfluidics devices. The silicone oxycarbide and

trichlorosilane monolayer were used for changing the wetting behaviour. M. Lee et al. [114] developed the biosensor based on Hafnium oxide. The Hafnium oxide was deposited by atomic layer deposition on silicon and modified with triethoxysily self-assembled monolayer to study the antibody detection. Ma et al. [115] studied the phosphonic acid self-assembled monolayer for organic field transistor and compared the performance with and without OTS modified dielectric. A. Jain et al. [116] reports the surface modification of HfO_2 using n-alkylphosphonic self-assembled monolayer for organic thin film transistors.

In 2013, Chandra et al. [117] studied the structural, optical and hydrophobic properties of sputtered hafnium oxide thin films. The objective of their work was to prepare hydrophobic hafnium oxide thin film to migrate contamination problem by altering the sputtering parameter. Chandra et al. [118] again studied the hydrophobic properties of hafnium oxide by angle sputter deposition methods. Bashir et al. [119] studied the hydrophobic behaviour by inducing the nanopores in HfO_2 for biosensing applications. The crystallization of the high-k dielectric suggested improved wettability in HfO_2 nanopores.

In 2014, A. Dattelbaum et al. [120] studied the stability of phosphate monolayer for the Hafnium oxide surfaces. The self-assembled monolayer was made from octadecylpholphonic acid (ODPA) or a perfluorinated phosphonic acid (PFPA).

2.2.2.2 Aluminum oxide (Al_2O_3)

The $Al_2O_3$is another important dielectric material ($k = 8$) material used in microelectronics applications. In 1997, Stratmann et al. [121] studied the self-assembled monolayer on oxidized aluminum surface. The phosphonic acids based monolayer was used to modify the aluminum oxide surface.

In 2004, Majewski et al. [122] investigated the effect of surface modification of Al_2O_3. The $Al_2O_3$was used as gate insulator which was prepared by means of anodization. The surface was covered by OTS self-assembled monolayer which gave the same effect as thermally grown silicon dioxide.

In 2005, Herrmann et al. [123] demonstrated the conformal hydrophobic coating on Al_2O_3surface prepared using Atomic layer deposition. The gas phase method was used

for the deposition of reliable and robust hydrophobic coatings on MEMS structures. The Al_2O_3 surface was modified using alykylsilane.

In 2006, White et al. [124] reported the deposition of report the octadecylsiloxane monolayer on Al_2O_3. The OTS derived adsorbate layers were compared on piranha treated and non-piranha treated Al_2O_3 substrate by controlled exposure to OTS.

In 2007, Timperman et al. [125] studied the adsorption and desorption mechanism of monolayer on Aluminum oxide. The amorphous alumina was used as substrate to study the effect of functionalized steric acid monolayer with different annealed temperature. Leggett et al. [126] demonstrated the modification of Aluminum with phosphonic acid monolayers. The work reported the photo patterning of monolayer used as a photo resist for etching of structure into aluminum substrates. S. Jon et al. [127] suggested a facile and effective method for water repellent coating of aluminum oxide surface. The aluminum membrane was prepared using the Anodic Aluminum Oxide (AAO). The oxidized substrate then was immersed in solution of fluoromonomer to form a superhydrophobic surface with contact angle of 163°.

In 2009, Valtiner et al. [128] reported the monolayer modification and stability of monolayer on Al_2O_3. The focus of the study was to improve the knowledge of the binding of organophosphonic acid molecules on aluminum oxide surface.

In 2013, J. Buijnsters [129] reported the wetting behaviour of anodized Aluminum oxide. The hydrophobic surfaces were prepared by pore opening by a wet chemical etching and surface modification by Lauric acid. The contact angle reported was 140°. N. Williams et al. [130] studied the adsorption of n-octadecylphosphonic acid on aluminum oxide and achieved contact angle of 116°. B. Durso et al [131] studied the aluminum oxide wetting behaviour using the texture and hydrophobic coating. The textured surfaces were prepared using anodized aluminum oxide and a fluoropolymer hydrophobic coating was used for improving the water contact angle. The organosilane monolayer may also be used to increase the contact angle. The contact angle was increased to 161° after surface modifications.

In 2014, M. Psarski et al. [132] obtained superhydrophobic structure by superposition of microstructure and chemically modification using 1H, 1H, 2H, 2H-perflurotetradecyltri-ethoxy silane (PETDTES). The microstructure was prepared using laser micromachining followed by fabrication of hexagonally spaced microcavities. H.

Klauk et al. [133] investigated the self-assembled monolayer to modified Al_2O_3 dielectric as gate dielectric.

2.2.2.3 Tantalum oxide (Ta_2O_5)

N. Yasuda et al. in 1999 [134] first time reported the structural properties of Ta_2O_5 ($k \approx 23$). The thin film $Ta_2O_5$was deposited on Si surface and they studied the properties of the surface after annealing at different temperatures. In 2000, N. Spencer et al. [135] studied the structural chemistry of phosphoric acid monolayer on tantalum oxide surfaces. In 2001-2006 there are no published literatures available on surface modification techniques of Ta_2O_5.

In 200, R. Palma et al. [136] studied modification of Ta_2O_5 with monolayers. The work was focused on the effect of cleaning, dehydration and deposition time on the formation of silane SAM on Ta_2O_5.

In 2008, Y. Li et al. [137] studied the Ta_2O_5 for low voltage electrowetting-on-dielectric application. The sputtered high-*k* material surface was modified using Teflon to improve hydrophobicity of Ta_2O_5.

In 2009, Z. Mekhalif et al. [138] used organodiphosphonic acid monolayer to modify the Ta_2O_5 surface. In 2010, Y. Lin et al. [139] studied the Ta_2O_5 for low voltage electrowetting using multilayer hydrophobic materials. The focus of their work was to reduce the actuation voltage by use of Parlyene and Cytop as hydrophobic materials.

In 2011, J. Liu et al. [140] investigated the structural and electrical properties of Ta_2O_5 thin films. The film was prepared by Photo-induced CVD process and the effect of UV-lamp power on the structural and electrical properties were studied. In 2012, C. Kim et al. [141] investigated the Ta_2O_5 dielectric for electrowetting application. The Cytop polymer was used to increase the hydrophobicity of Ta_2O_5. In 2013, C. Kim et al. [142] investigated the use of Ta_2O_5 for electrowetting application. The film of Ta_2O_5 was prepared by anodizing a sputtered Ta_2O_5. The Cytop was used to increase the hydrophobicity of the dielectric Ta_2O_5.

In 2014, L. Mao et al. [143] investigated the hydrophilic Ta_2O_5 nanoparticle. The Ta_2O_5 nanoparticles were covalently bonded with grapheme oxides. H. Chen et al. [144] studied the Ta_2O_5 for electrowetting application. The Ta_2O_5 was deposited by RF magnetron sputtering system. The Cytop hydrophobic coating was used to increase the

hydrophobicity of Ta_2O_5. Y. Chang et al. [145] studied the Ta_2O_5 for bio application. The tantalum oxide was deposited using the magnetron sputtering system and used as hydrophilic surface for in-vitro anti-bacterial analysis purpose.

2.2.2.4 Titanium oxide (TiO_2)

In 2002, Textor et al. [146] demonstrated surface modification of TiO_2 surface with Self assembled monolayer. Alkane phosphate was used to create pattern of titanium oxide. Fadeev et al. [147] studied the TiO_2 modification with different types of monolayer. The octadecylsilanes with different head group and phosphoric acid monolayer with titanium dioxide were investigated. Their work was focused on the structure, kinetics and mechanism of the growth of the monolayer.

In 2003, Diebold et al. [148] studied the surface science of titanium oxide. The review presented in 2003 was on the adsorption and reaction of a wide variety of inorganic molecules as well as organic molecules. Paz et al. [149] studied the effect of metallic micro domains on the modified TiO_2 surface. The formation of Octadecyltrichlorosilane monolayers on titanium dioxide was studied in structures consisting of microdomains of TiO_2 and metal such as gold and platinum. In 2008, Xiao et al [150] demonstrated the alkanephosphate monolayer to modify the surface properties of TiO_2.

In 2009, C. Hsich et al. [151] demonstrated the superhydrophobic coating of TiO_2 nanosphere on Indium tin oxide (ITO) surface. The TiO_2 nanosphere was deposited using the chemical vapor deposition techniques. The contact angle of $\approx 166^o$ was observed after the deposition.

In 2010, Y. Li et al. [152] investigated the making of superhydrophobic surface using nano-TiO_2 modified hydrophobic coating. Room temperature vulcanized (RTV) silicone rubber coating was used to improve the surface hydrophobicity of TiO_2.

In 2011, W. Xu et al. [153] reported the superhydrophobic behaviour of TiO_2 by facial method. The first method used the TiO_2 nanoparticles and was prepared by sol-gel method to change the wettability behaviour and second method was dispersion of TiO_2/Polystyrene on silicon substrate. L. Raimondi et al. [154] investigated the hydrophobic behaviour of TiO_2 hybrids. The TiO_2 powder was prepared by sol-gel synthesis. The surface of nano-TiO_2 was functionalized with siloxane molecules. In

2012, N. Ishida et al. [155] reported the hydrophilic behaviour of TiO_2 surface. The hydrophilic behaviour of TiO_2 was obtained by reactive oxygen species generated by air plasma removes the surface organic contaminates, leading to hydrophilic behaviour. H. Yamashita et al. [156] reported the hydrophobic behaviour of TiO_2 nanocomposite. The $TiO_2$was deposited using the magnetron sputtering. The polytetrafluoroethylene was used as hydrophobic coating.

In 2013, A. Lyons et al. [157] investigated the TiO_2-polymer nanocomposite surface. The high-density polyethylene (HDFE) substrate with lamination process was used at temperature of 138°C for making the pore structures. In 2014, G. Chagas et al. [158] reported the wetting properties of polypropylene materials using the TiO_2 nanoparticles which gave a contact angle $\geq$150°.

The literature on surface modification of dielectric materials as outlined above with use of hydrophobic materials exemplifies the progress and scientific advancement in the field of synthesis of artificial hydrophobic and superhydrophobic dielectric surfaces. The materials such as Teflon, Cytop and various variety of self-assembled monolayer are used for altering the surface properties of dielectric materials. The superhydrophobic behaviour of dielectric materials though still is in nascent stage of research for high-*k* dielectric materials. The higher water contact angle had been reported for Al_2O_3 and TiO_2 dielectric materials and high-k dielectric material had shown the superhydrophobicity when their surfaces modified with plasma and monolayer.

2.4 Polymer Materials

A wide variety of polymer material has been studied and reported in literature to create superhydrophobic surfaces. Due to ease of fabrication silicon and polymers materials like poly-dimethyl-siloxane (PDMS), poly-methyl-methacrylate (PMMA), and SU8 are more used to create a superhydrophobic surface. SU8 is the material of choice for Bio-MEMS and microfluidics devices as it allows for simple processing, shorter fabrication times, and optical transparency.

In 2004, Shirtcliffe [159] investigated the superhydrophobic behaviour of SU8. Their work presented the high aspect ratio pattern in thick SU8 and its surface treatment with easily available fluorocarbon hydrophobic coating to produce the superhydrophobic pattern. M. Calleja et al. [160] studied the hydrophilic behaviour of SU8. The harmless

solution ethanolamine was used to reduce the contact angle of SU8. The reduced contact angle leads to increase in the capillary pressure in the SU8 microchannel.

In 2006, M. Newton et al. [161] reported the superhydrophobic SU8 for electrowetting application. The SU8 was patterned in the form of cylindrical pillars and modified with Teflon which was widely used material to achieve superhydrophobic surface. N. Allbritton et al. [162] studied the modification of SU8 monomer. The SU-8 monomer was polymerized using the UV exposure and chemical modification with polyethylene glycol for cell attachment and growth.

In 2007, CK. Chung et al. [163] studied the effect of oxygen plasma treatment on the surface property of exposed and unexposed SU8 photo resist. The work focused on reducing the shrinkage-induced non-uniformity problem to fabricate the smooth monolithic MEMS structures. N. Allbritton et al. [164] described the surface grafting of SU8 for bio-MEMS applications. The epoxide group presents on the SU8 surface got converted to hydroxyl group by oxidation with high concentration of cerium ammonium nitrate (CAN) and nitric acid. After oxidation of SU8 the surface was grafted by water soluble polymers like poly-acrylic acid and polyarcylamide which served as sites for cell attachment in Bio-MEMS. Stark et al. [165] studied the effect of oxygen plasma on surface energy, topography and surface chemistry of SU8 photo resist.

In 2008, M. Avram et al. [166] had carried out theoretical and experimental study of surface modification of SU8 by plasma treatment. It was found that the surface became more hydrophilic after oxygen plasma whereas CF_4 based plasma improves the hydrophobicity of SU8. Desai et al. [167] reported the surface modification of SU8 for enhanced biofunctionality. The polyethylene glycol was used to modify the SU8 surface. Metze et al. [168] reported the hydrophobic behaviour of SU8 for microfluidics chip. The SU8 surface was modified using the Octadecyltrichlorosilane to gain the hydrophobic surface.

In 2009, Stark et al [169] studied the wetting behaviour of SU8 by plasma and chemical process. The argon and oxygen based plasma was used for the study of hydrophilic behaviour of SU8. The cerium ammonium nitride was used to make the surface hydrophilic.

In 2010, Tseng et al. [170] introduced the electrokinetic separation of protein in modified SU8 microchannel. The high energy UV irradiation in ozone rich environment was used to modify the inner or outer structure of SU8 embedded channels.

In 2012, Yang et al. [171] reported the superhydrophobic behaviour of SU8 by patterning the surface. Uniform woodpile structures were prepared using prism holographic lithography and after patterning the surface was modified using the SF_6 plasma to achieve the superhydrophobic surface.

In 2013, Rasmussen et al [172] studied the SU8 surface properties by texturing using combined chemistry of oxygen and SF_6 plasma. In 2014, C. Rickel et al. [173] developed the superhydrophobic surfaces on Si_3N_4 membranes with a tailored pattern of SU8 photo resist pillars and obtained contact angle of 151.2^o.

The above discussion on polymer SU8 surface modification describes the research on attaining superhydrophobic behaviour using photolithography with chemical modification and plasma treatments separately. The superhydrophobicity with combination of plasma and self-assembled monolayer is not discussed in literatures. As a combinatorial method is developed and tried on silicon and dielectric surface in this thesis to investigate its effect on wettability of surface, we also examined the developed method for SU8 surfaces.

2.5 Gap in existing Research and Investigations

Numerous methods and materials have been studied to achieve the super hydrophobicity and in that context a WCA greater than 150°. Most of the research work is oriented towards the preparation of superhydrophobic surfaces by composition of roughness and chemical treatment of surfaces mostly separately. From the literature review still a few significant gaps exits in studied on wettability of silicon, dielectric materials and SU8. A few of them are figured out and addressed in this thesis and are detailed below:

1. Among many a texturing and deposition techniques available in literature for enhancement of WCA, the reported literature lacks a common strategies and method developed for important materials in MEMS microfluidics like, silicon, dielectric and polymers. We have developed simple technique without any patterning to increase the hydrophobicity of silicon, dielectric materials and polymer surfaces.

2. The silicon hydrophobicity is enhanced by the composition of texturing either by chemical or plasma and surface modification with hydrophobic coating. The synergism of physical texturing and chemical modification is rarely attempted to make superhydrophobic surfaces of silicon especially the investigation on many possible ways to achieve chemical and plasma texturing combined with SAM has not been done comprehensively. We are reporting the formation of superhydrophobic surfaces by combined effect of texturing and organosilane modifications. Further, various combinations of methods for texturing are used here, that is by chemical etching using alkaline hydroxide solution like, potassium hydroxide (KOH) and Tetramethylammonium hydroxide (TMAH) and by plasma treatments using Reactive ion etching (RIE) based fluorine plasma of SF_6 and O_2. The back side of silicon surface and piranha cleaned surface is also used for the study.

3. The dielectric materials are widely used in Microelectronic and Microfluidics area. From the literature, the hydrophobicity of dielectric materials without any patterning has not been discussed and elaborated. Very few studies are available on making high-*k* dielectric materials superhydrophobic despite their increasing importance in MEMS and NEMS devices. We have developed and proposed a very simple and bulk production method without any mask patterning for preparing hydrophobic surface for both high-*k* and low-*k* dielectrics. The dielectric hydrophobic surfaces are produced by combination of plasma and organosilane modification. The combinatorial method is similar to what has been developed for silicon surface treatments.

4. The hydrophobic behaviour of widely used SU8 polymers in Microfluidics application is also investigated by combined effect of patterning and hydrophobic coating. This has not been investigated in literature so far. The present study showed that the hydrophobic behaviour of SU8 by various combination of SF_6 and O_2 plasma has significant improvement in WCA. The surface chemistry of OTS SAM and SU8 which is rarely attempted in literature has also been studied in this thesis work.

2.6 Organization of Thesis

The wettability of the solid surface is an important physical phenomenon and it has been known that surface topography plays a major role in the hydrophobic behavior of the surface. Much literature has concluded that heterogeneous wetting enhances hydrophobic nature of the surfaces. The hydrophobic surfaces are widely used for self-cleaning, low adhesion, non-wetting and electrowetting application. Exceptionally hydrophobic surfaces not only need to be constructed from low energy materials, they require highly developed surface microstructures which acts to enhance the surface hydrophobicity further. The hydrophobicity surface via, texturing and hydrophobic coating suggest most easiest and cost effective way for the fabrication of superhydrophobic surface. This thesis focus on the fabrication of surfaces with high water contact angle ($>150^o$)in the range of making superhydrophobic surfaces.

The work in this thesis details the fabrication of the superhydrophobic surfaces via combined effect of texturing and deposition of organosilane monolayer. A wide variety of materials namely silicon, dielectric (low-*k* and high-*k*) and SU8 polymer are used for the investigations in this thesis. The roughening of the surfaces is tailored by chemical (TMAH, KOH) and plasma (SF_6 and O_2) texturing of the surfaces. The texturing of materials makes the surface more hydrophilic. The use of the hydrophobic coating on textured surface enhances the hydrophobicity of the surfaces which is significantly more in comparison to hydrophobic coatings done on untextured surface. This is one important finding of this thesis. The hydrophobic coating like an organosilane monolayer is the easiest, cost effective and less time consuming method for the deposition. There are no studied available on whether similar approaches for making the superhydrophobic surface for silicon, dielectric and polymer materials. This work, investigated the similar approaches for improvement of the hydrophobicity of the materials using easiest and cost effective methods.

In Chapter 3 we present a combined method of texturing and chemical modification in order to produce superhydrophobic silicon surface. Chemical and plasma textured method are used to make silicon surface rough followed by the organosilane monolayer deposition. Condition for wetting and non-wetting are analyzed and produced surfaces are tested for their wetting behaviour, characterized with Raman, AFM, XPS and WCA and surface roughness are also measured and discussed.

In Chapter 4 investigation on high-k dielectric materials with new method to prepare the superhydrophobic surface is presented. The WCA and surface roughness measurement for all dielectric materials are discussed in this chapter. The surface characterizations are done with Raman, AFM, XPS and WCA and surface roughness are also measured and discussed.

In Chapter 5, a similar study as is done for silicon and dielectric materials in Chapter 3 and Chapter 4 is presented for SU8 polymer. The effects of fluorine and oxygen plasma in preparing of superhydrophobic SU8 surfaces are described. Wettability behaviour of plasma activated SU8 after monolayer deposition is discussed. The WCA, surface roughness measurement, Raman spectroscopy and XPS result are discussed.

Finally conclusion for all experimental work is given in Chapter 6 with scope for future work.

References:

1] Thomas Young (1805) An Essay on the Cohesion of Fluids, Philosophical Transactions of the Royal Society of London, (95), pp. 65-87.

2] A. Carre and K. Mittal (2009) Superhydrophobic surfaces, CRC Press.

3] K. Mittal (2004) Polymer Surface Modification: Relevance to adhesion, CRC Press.

4] Karin Hermansson, Ulf Lindberg, B. Hok and G. Plamskog, (1991) Wetting properties of Silicon surfaces, IEEE transaction, pp.193-195.

5] D. Oner and Thomas J. Mc Carthy (2000) Ultrahydrophobic surfaces. Effects of topography length scales on wettability, Langmuir, (16), pp.7777-7782.

6] Zen Yoshimitsu, Akira Nakajima, Toshiya Watanabe, and K. Hashimoto (2002) Effects of surface structure on the hydrophobicity and sliding behaviour of water droplets, Langmuir, (18), pp.5818-5822.

7] T. Sun, G. Wang, Huan Liu, L. Feng, Lei Jiang, and Daoben Zhu (2003) Control over the wettability of an aligned Carbon nanotube films, Jl. American chemical society, (125), pp.14996-14997.

8] T. sun, G. Wang, L. Feng, B. Liu, Y. Ma, Lei Jiang and Daoben Zhu (2004) Reversible Switching between superhydrophilicity and superhydrophobicity, Angewandte chemie, (43), pp. 357-360.

9] R. Furstner and W. Barthlott (2005) Wetting and self-cleaning properties of artificial superhydrophobic surfaces, Langmuir, (21), pp. 956-961.

10] L. Lacroix, M. Lejeune, L. Ceriotti, M. Kormunda, T. Meziani, P. Colpo and Francois Rossi (2005) Tuneable rough surfaces: A new approach for elaboration of superhydrophobic films, Surface Science, (592), pp.182-188.

11] M. Callies, Y. Chen, Frederic Marty, Anne Pepin and Davic Quere (2005) Microfabricated textured surfaces for superhydrophobicity investigations, Microelectronics engineering, (78-79), pp. 100-105.

12] E. Martines, K. Seunarine, H. Morgan, N. Gadegaard, Chris D.W. Wikinson and Mathis O.Riehle (2005), Superhydrophobicity and superhydrophilicity of regular Nanopatterns, ACS Nano letters, (5), pp.2097-2103.

13] L. Zhu, Y. Xiu, J. XU, Dennis W. Hess, CP. Wong (2006) Optimizing geometrical design of superhydrophobic surfaces for prevention of Miecroelectromechanical system stiction, Electronic Components and Technology conference, pp. 1129-1135.

14] L. Zhu, Yanying Feng, X.Ye, Z. Zhou (2006) Tuning wettability and getting superhydrophobic surface by controlling surface roughness with well-designed microstructures, Sensor and Actuators, (130-131), pp.595-600.

15] T. Baldacchini, J. E. Carey, Ming Zhou and E. Mazur (2006) Superhydrophobic surfaces prepared by micro structuring of silicon using a femtosecond laser, Langmuir, (22), pp. 4917-4919.

16] B. Bhushan and Y. Jung (2007) Wetting study of patterned surfaces for superhydrophobicity, Ultra microscopy, (107), pp. 1033-1041.

17] M.F. Wang, N. Raghunathan and B. Ziaie (2007) A Nonlithographic Top-down Electrochemical Approach for creating hierarchical (Micro-Nano) Superhydrophobic silicon surfaces, Langmuir, (23), pp.2300-2303.

18] L. Cao, H.Hu and Di Gao (2007) Design and fabrication of Micro-textures for Inducing a superhydrophobic behaviour on hydrophilic materials, Langmuir, (23), pp. 4310-4314.

19] Y. Xiu, L. Zhu, Dennis W. Hess and CP. Wong (2007), Hierarchical Silicon Etched structures for Controlled Hydrophobicity/Superhydrophobicity , ACS Nano Letter, 7 (11), pp. 3388-3393.

20] B. Bhushan, K. Koch and Y. Jung (2008) Nanostructures for superhydrophobicity and low adhesion, Soft Matter, (4), pp. 1799-1804.

21] Y. Jung, B. Bhushan (2008) Dynamic Effects of Bouncing Water droplets on superhydrophobic surfaces, Langmuir, (24), pp.6262-6269.

22] V. Jikinen, L. Sainiemi and S. Franssila (2008) Complex droplets on chemically modified silicon nanograss, Advanced Materials, (20), pp.3453-3456.

23] L. Cao, T. Price, M. Weiss, Di Gao (2008) Super Water-and Oil-repellent surfaces on intrinsically hydrophilic and oleophilic porous silicon films, Langmuir, (24), pp.1640-1643.

24] Y. Xiu, S. Zhang, V.Yelundur, A. Rohatgi, Dennis W. Hess and CP. Wong, Langmuir, (24), pp.10421-10426.

25] G. Piret, Y. Coffinier, C. Roux, O. Melnyk, R. Boukherrou (2008), Bimolecular and nanoparticle transfer on patterned and heterogeneously Wetted superhydrophobic silicon Nanowire surfaces, (24),pp. 1670-1672.

26] D. Qi, Nan Lu, H. Xu, B. Yang, C. Huang, M. Xu, L. Gao, Z. Wang and L. Chi (2009) Simple approach to wafer -scale self-cleaning antireflective silicon surfaces, Langmuir, 25(14), pp.7769-7772.

27] J. Wang, F. Liu, H. Chen and D. Chen (2009) Superhydrophobic behaviour achieved from hydrophilic surfaces, Applied physics letters, 95, pp. 084104-3.

28] M. Barberoglou, V. Zorba, E. Stratakis, E. Spanakis, P.Tzanetakis, S.H. Anastasia C. Fotakis (2009) Bio-inspired water repellent surfaces produced by ultrafast laser structuring of silicon, Applied surface sciences, (255), pp. 5425-5429.

29] Y. Chang Wei, H. Fei, H. Feng (2009), Effect of upper contact line on sliding behaviour of water droplet on superhydrophobic surface, Chinese Science Bulletin, 54(5), pp. 727-731.

30] X. Li, B. Tay, P. Meile, A. Brioude and D. Cornu (2009) Fabrication of Silicon pyramid/nanowire binary structure with superhydrophobicity, Applied surface science, (225), pp. 7147-7152.

31] Y. Song, R. Premachandran Nair, M. Zou, Y.A. Wang (2010) Adhesion and friction properties of micro/nano-engineered superhydrophobic/hydrophobic surfaces, Thin solid films, (518), pp. 3801-3807.

32] Yan Liu, Y. Xiu, Dennis W. Hess and CP. Wong, (2010) Silicon surface structure-controlled oleophobicity, Langmuir, 26(11), pp. 8908-8913.

33] R.T. Rajendra Kumar, K. Mogensen and P. Boggild (2010), Simple approach to superamphiphobic overhanging silicon nanostructures, Jl. Of Physical Chemistry C, (114), pp.2936-2940.

34] L. Chen, Z. Xiao, Philip CH Chan and Yi-Kuen Lee (2010) Static and dynamic characterization of robust superhydrophobic surfaces built from nano-flowers on silicon micro-post arrays, Jl. Micromechanical and Micro engineering, (20), pp. 105001-8.

35] D. Sarkar, M. Farzaneh and R. Paynter (2010), Wetting and superhydrophobic properties of PECVD grown hydrocarbon and fluorinated-hydrocarbon coatings, (256), pp. 3698-3701.

36] S. Cho, T. An, J. Kim, J. Sung and G Lim, (2011) superhydrophobic nanostructure silicon surfaces with controllable broadband reflectance, Chemical communication, (47), pp.6108-6110.

37] Yang He, C. Jiang, H. Yin, W. Yuan (2011), Tailoring the wettability of patterned silicon surfaces with dual-scale pillars: from hydrophilicity to superhydrophobicity, Applied surface science, (257), pp. 7689-7692.

38] J. Seo, S. Lee, J. Lee and T. Lee (2011), Guided transport of water droplets on superhdyrophobic-hydrophillic patterned Si nanowires, applied materials and interfaces, (3), 4722-4729.

39] K. Jradi, D. Laour, C. Daneault and B. Chabot (2011), Control of the chemical and physical behaviour of silicon surfaces for enhancing the transition from hydrophilic to superhydrophobic surfaces, Colloids and surfaces A: Physicochemical and Engineering Aspects, 374, 33-41.

40] M. Dawood, H. Zheng, NA. Kurniawan, KC. leong, Y. Foo, R. Rajagopalan, S. Khan and W. Choi (2012) Modulation of surface wettability of superhydrophobic substrates using Si nanowire arrays and capillary-force-induced nanocohesion, Soft Matter, (8), pp. 3549-3557.

41] Bin Su, S. wang, Yuchen Wu, Xiao Chen, Yanlin Song and L. Jiang (2012) Small molecular Nanowire arrays assisted by superhydrophobic pillar structured surfaces with high adhesion, Advanced materials, (24), pp.2780-2785.

42] D. Zhang, F. Chen, Q. Yang, J. Young, H. Bian, Y. Ou, J. Si, X. Meng and X. Hou (2012) A Simple Way to achieve pattern-dependent tunable adhesion in superhydrophobic surfaces by femtosecond laser, Applied materials and interface, (4), pp. 4905-4912.

43] Zhibo Ma, C. Jiang, X. Li, Y. Fang and W. Yuan (2013) Controllable fabrication of periodic arrays of high-aspect -ratio micro-nano hierarchical structures and their superhydrophobicity, Jl. Micromechanics and micro engineering, (23), pp.095027-9.

44] J. Groten and J. Ruhe (2013) Surface with Combined microscale and nanoscale structures: A Route to mechanically stable superhydrophobic surfaces, Langmuir, (29), pp.3765-3772.

45] S. Wiedemann, A. Plettl, P. Walther and P. Ziemann (2013) Freeze fracture approach to directly Visualize wetting transitions on nanopatterned superhydrophobic silicon surfaces: more than a proof of principle, Langmuir, (29), pp. 913-919.

46] B. Kiraly, S. Yang and T. J. Huang (2013) Multifunctional porous silicon nanopillar arrays: antireflection, superhydrophobicity, photoluminescence and surface-enhanced Raman scattering, Jl. of Nanotechnology, (24), pp.245704-10.

47] T.P.Nguyen, R.Dufour, V.Thomy, V. senez, B. Rabah, Y. Coffinier, (2014) Fabrication of superhydrophobic and highly olephobic silicon-based surfaces via electroless etching method, Applied surface science, (295), pp. 38-43.

48] V. Kondrashov and J. Ruhe, (2014), Microcones and Nanograss: Towards Mechanically Robust superhydrophobic surfaces, Langmuir, (30), pp. 4342-4350.

49] W. Zhang, X. Fan, S. Sang, P. Li, Gang Li, Y. Sun, J.Hu (2014) Fabrication and characterization of silicon nanostructures based on metal-assisted chemical etching, Jl. Korean of chemical engineering, 31(1), pp.62-67.

50] Y.Kim, Y.Chung, Y.Tian, C. Carraro and R. Moboudian (2014), Two-fluid wetting behaviour of a hydrophobic silicon nanowire array, Langmuir, 30, 13330-13337.

51] X.M.Yang, Z. Zhong, E.M.Diallo, Z.H.Wang and W.S.Yue (2014) Silicon wafer wettability and aging behaviour: impact on gold thin-film morphology, Materials Science in Semiconductor Processing, 26, 25-32.

52] G.Vereecke, X.Xu, W.K.Tsai, H.Yang, S.Armini, T.Delande, G.Doumen, F.Kentie, X.Shi, I.Simms, K.Nafus, F.Holsteyn, H.Struyf and S.Gendt, (2014), ECS Journal of Solid state science and technology, 3(1), N3095-3100.

53] T.Nguyen, R.Dufour, V.Thomy, V.Senez, R.Boukherroub and Y.Coffinier, (2014), Applied surface science, 295, 38-43.

54] V.Kumar, K.N.Bhat and NN. Sharma (2014), Surface modification of textured silicon and its wetting behaviour, Journal of adhesion science and technology, Doi:10.1080/01694243.2014.9868335.

55] V.Kumar, NN.Sharma, 2014, A Study on hydrophobicity of silicon and a few dielectric materials, Micro and Smart Devices and System, pp 265-283.

56] T.L.Chu, (1969), Dielectric Materials in Semiconductor Devices, 6(25), pp.25-33.

57] R.K.sharma, A. Kumar and J.M.Anthony, (2001), Advances in High-k Dielectric Gate Materials for Future ULSI devices, JOM, 6, pp.53-55.

58] G. Bersuker, O. Zeitzoff, G. Brown and H.R. Huff (2004), Dielectric for future transistor, Materials today, pp. 26-33.

59] S. Hall, O. Buiu, I. Mitrovic, Y. Lu, W. Davey,(2007),Review and perspective of High-k dielectric on silicon, J of Telecommunications and information technology (110), pp.33-42.

60] X. Sun, C. Di and Y. Liu, (2010), Engineering of the dielectric-semiconductor interface in organic field-effect transistor, (20), pp.2599-2611.

61] H. Liu, S. Darmatilleke, D.K. Maurya, A. Tay, (2010), Dielectric materials for electrowetting-on-dielectric actuation, (16), pp.449-460.

62] R.G. Frieser (1974) Characterization of thermally grown SiO_2 surfaces by contact angle measurements, Jl. of Electrochemical Society, 669-672.

63] R.Thomas, F.B. Kaufman, J.T. Kirleis and R.A. Belsky (1996) Wettability of polished silicon oxide surfaces, J. Electrochemical Society, 143(1), 643-648.

64] H.Fujii, M.Yamamoto, S.Hara and K.Nogi (1999) Effect of gas evolution at solid-liquid interface on contact angle between liquid Si and SiO_2 , J of material science, (34), pp.3165-3168.

65] A.Hozumi, Y.Yokogawa, T.Kameyama, H.Sugimura, K.Hayashi, H.shirayama and O.Takai (2001), Amino-terminated self -assembled monolayer on a SiO_2 surface formed by chemical vapor deposition, J of vacuum science and technology A, 19(4) pp.1812-1816.

66] A.Jeong, S.Mankoo and D.Kim (2000) Characterization of hydrophobic SiO_2 powders prepared by surface modification on wet gel, J of Sol-Gel science and technology, (19), pp.483-487.

67] R.Sfez, L.D. Zhong, I.Turyan, D.Mandler, S.Yitzchaik (2001) Polyaniline monolayer self-assembled on hydroxyl terminated surfaces, (17), pp.2556-2559.

68] T.Ye, D.Wynn, R.Dudek and E.Borguet (2001) Photoreactivity of alkylsiloxane Self assembled monolayers on silicon oxide surfaces, Langmuir, (17), pp.4497-4500.

69] A.Salleo, M.L.Chabinyc, M.S.Yang and R.A.street (2002) Polymer thin film transistor with chemically modified dielectric interfaces, Applied physics letters, 81(23), pp. 4383- 4385.

70] H.Klauk, M.Halik, Z.Ute, G.Schmid, W.Radlik and W.Weber (2002) High-mobility polymer gate dielectric pentacene thin film transistors, Applied physics letters, 92(9), pp. 5259-5263.

71] Y.Wang and M. Lieberman (2003) Growth of Ultrasmooth octadecytricholoro silane self-assembled monolayers on SiO_2, Langmuir, (19), pp.1159-1167.

72] Y.Wu, H. Sugimura, Y. Inoue and O. Takai (2003) Preparation of hard and ultra-water-repellent silicon oxide films by microwave plasma-enhanced CVD at low substrate temperatures, Thin solid films, (435), pp.161-164.

73] A. Kawai and J. Kawakami (2003) Characterization of SiO_2 Surface treated by HMDS vapor and O_2 plasma with AFM tip, J of photopolymer science and technology, 16(5), pp 665-668.

74] Z. Yuan, WL. Huang and K. Mukai (2004) Wettability and reactivity of molten silicon with various substrates, Applied physics A, (78), 617-622.

75] S.Tsoi, E.Fok, J.C.Sit and J.Veinot (2004) Superhydrophobic, high Surface Area, 3-D SiO2 Nanostructures through Siloxane -base Surface functionalization, Langmuir, (20), pp. 10771-10774.

76] T. Soeno, I. Kohei, S. Shiratori (2004) Ultra-water-repellent surface: fabrication of complicated structure of SiO_2 nanoparticle by electrostatic self -assembled films, Applied surface science, (237), pp.543-547.

77] K.Wu, T.C.Bailey, C. Willson and J. Ekerdt (2005) Surface hydration and its effects on fluorinated SAM formation on SiO_2 surfaces, Langmuir, (21), 11795-11801.

78] D. Janssen, R. Palma, S.Verlaak, P.Heremans and W.Dehaen (2006) Static solvent contact angle measurements, surface free energy and wettability determination of various self assembled monolayers on silicon dioxide, Thin solid films, (515), pp.1433-1438.

79] Y.Tang, X.Xu, J.Fang, Y.Liang and H.Ji, (2006), The growth and superhydrophobicity of a perfluorocarbon Nanoneedle array on an SiO_2 surface, 5(4), 415-419.

80] C.Franco, N.Cioffi, N.Ditaranto, MS.Vitello, M.Sibilano, L.Torsi and G. Scamarcio (2007) Functionalized interface by plasma treatments on silicon and silicon dioxide substrates, Thin solid films, (515), pp.7195-7202.

81] D.Aronov, G.Rosenman, Z.Barkay (2007) Wettability study of modified silicon dioxide surface using environmental scanning electron microscopy, J of applied physics, (101), pp. 084901-5.

82] H.Lu, F. Bottausci, J.Fowler, A.Bertozzi, M.Carl and CJ.Kim (2008) A study of EWOD-driven droplet by PIV investigation, (8), pp.456-461.

83] A.Tuteja, W.Choi, J.Mabry, M.Gareth and R.Cohen (2008) Robust omniphobic surfaces, PNAS, 105(47), pp.18200-18205.

84] J. Yoon (2008) Open-surface digital Microfluidics, J of Biotechnology, (2), pp.94-100.

85] C.P. Smits, P. Hal, M. Leeuw (2008) Bottom-up organic integrated circuits, Nature Letter , (455), pp. 956-959.

86] Y.Ito, A.Virkar, S.Mannsfed, Z.Bao (2009) Crystalline Ultrasmooth Self-assembled monolayers of alkylsilanes for organic Field-effect transistor, J of American Chemical Society, (131), pp.9396-9404.

87] C. Celle, J. Simonato, D.Vuillaume (2009), Self-assembled monolayers for electrode fabrication and efficient threshold voltage control of organic transistor with amorphous semiconductor layer, Organic Electronics, (10), pp. 119-126.

88] F. Zhang, K. Sautter, D. Findley, R. Davis, M. Linford (2010) Chemical Vapor deposition of three aminosilanes on Silicon dioxide: Surface Characterization, stability, effects of silanes concentration, and cyanine dye adsorption, Langmuir, 26(18), pp. 14648-14654.

89] C. Belgardt, T. Baumgartel and B. Christan (2010) Self-assembled monolayers on silicon oxide, Pysica status solidi C, 7(2), pp. 227-231.

90] Y. Liu, P. Lai, R. Yao, L. Deng (2011), Influence of Octadecyltrichlorosilane surface modification on electrical properties of polymer thin-film transistors studied by capacitance-voltage analysis, IEEE transactions on Device and materials Reliability, 11(1), pp. 60-65.

91] R. Diebold, D.R. Clarke (2012) Smooth, aggregate-free self-assembled monolayer deposition of silane coupling agents on silicon dioxide, Langmuir, 28, pp. 15513-15520.

92] Y. Mhaisagar, B. Joshi and AM. Mahajan (2012) Surface modification of spin-coated SiO2 xerogel thin films by TMCS silylation, Bulletin materials science, 35(2), pp.151-155.

93] H. Park, S.Yoon and Y. Do (2012) Superhydrophobic of 2D SiO2 hierarchical micro/nanorod structures fabricated using two-step micro/nanosphere lithography, 22, 14035-14041.

94] D.Xu, M.Wang, X.Ge, M.H. Lam, X.Ge (2012) Fabrication of raspberry SiO2/polystyrene particles and superhydrophobic particulate films with high adhesive force, 22, 5784-5791.

95] D. Cui, W. Li and T. Li and H. Zhang (2011) Development of a simple method for the fabrication of superhydrophobic surfaces with NH_4VO_3 and SiO_2, 70, 105-108.

96] S. Arscott (2013) Wetting of soap bubbles on hydrophilic, hydrophobic and superhydrophobic surfaces, Applied Physics letters, (102), pp. 254103-4.

97] V. Gupta, N. Madaan, D. Jensen, S.Kunzler and M. Linford (2013)Hydrogen plasma treatment of silicon dioxide for improved silane deposition, Langmuir, (29), 3604-3609.

98] L. Jinhua and W. Rui (2014), Preparation of Nano-SiO2/Amino-modified polysiloxane hybrid superhydrophobic Coating, Journal of Wuhan University of Technology-Material Science Education, 35-39.

99] M. Han, X. Zhang, L. Li, C. Peng, L. Bao, Y. Xiong, W. J. Xu (2014), Dual-switchable surfaces between hydrophobic and superhydrophobic fabricated by the combination of chemistry and RAFT, Journal of express polymer letters, 8(7), 528-542.

100] J. Lin, C. Zheng, W. Ye, H. Wang, DY. Feng, Q. Li and B. Huan (2014) A Facile dip-Coating approach to prepare SiO_2/Fluropolymer Coating for superhydrophobic and Superoleophobic fabrics with self-cleaning property, Journal of Applied Polymer Science, 41458-41466.

101] L. Zhefeng, L. Xianye (2014) ADO-phosphoric acid self-assembled monolayer modified dielectric for organic thin film transistors, Journal of Semiconductors, 35(10), 104001-4.

102] F. Meiners, J. Ross, I Brand, A. Buling, M. Neumann, P. Koster, J. Christopher's and G. Wittstock, Modification of Silicon oxide surfaces by monolayers of an oligoethlyene glycol-terminated perfluoroalkylsilane. Colloids and Surfaces A: Physicochemical and engineering aspects, 449, 31-41.

103] R. Ortiz, A. Faccheti and T. Marks, (2010), High-k Organic, Inorganic and Hybrid Dielectric for Low-Voltage Organic Field-Effect Transistors, American Chemical society, (110), pp.205-239.

104] A. Fadeev, R. Helmy, and S. Marcinko (2002) Self-assembled Monolayers of Organosilicon Hydrides Supported on Titanium, Zirconium and Hafnium dioxide, Langmuir, (18), pp.7521-7529.

105] O. Acton, G. Ting, H. Ma and A. Jen (2008) Low-voltage high-performance C60 thin films transistors via low-surface energy phosphoric acid monolayer/hafnium oxide hybrid dielectric, Applied physics letters, (93), 083302-3.

106] C. Wei, F. Adriyanto, Y. Lin, Y. Li, T. Huang, D. Chou and Y. Wang (2009) Pentacene-Based Thin-films Transistors with a solution -process Hafnium oxide insulator, IEEE Electron device letters, 30(10), 1039-1041.

107] G. Ting, O. Acton, H. Ma, J. Ka and A. Jen (2009) Study on the formation of self-assembled monolayers on Sol-gel processed Hafnium oxide as dielectric layers, Langmuir, (25), 2140-2147.

108] C. Hsieh, Y. Chen, K.Lu, G.Lin and J.Lou (2010) Characteristics of the Fluorinated high-k Inter-poly dielectric, IEEE Electron device letters, 31(12), 1446-1448.

109] Y. Liu, L. Deng, R. Yao and P. Lai (2010) IEEE Transaction on device and materials reliability, 10(2), 233-237.

110] K. Liu, J.R. Tsai, W.Lin, C. Li, J. Chen (2011) Defect passivation by O_2 plasma treatment on high-k dielectric HfO2 films at room temperature, Thin solid films, (519), pp.5110-5113.

111] I. Guha, J. Kedzierski and B. Abedian (2011) Low-voltage electrowetting on a lipid bilayer formed on hafnium oxide, applied physics letters, (99), 024105-3.

112] A. Durov (2011), Wetting of Hafnium Dioxide by pure metals, Powder metallurgy and metal ceramics, 50 (7-8), pp. 552-556.

113] R. Renaudot, V. Agache, L. Jalabert, M. Kumemura, D. Collard, H. Fujita (2012) Performances of High-K dielectric materials (Al_2O_3, HfO_2, ZrO_2) for liquid dielectrophoresis microfluidics devices, International conference on Miniaturized System for chemistry and life sciences, pp. 905-908.

114] M. Lee, N. Zina, A. Errachid (2012) A Novel biosensor based on hafnium oxide: Application for early stage detection of human interleukin-10, Sensor and actuators B, (175), pp.201-207.

115] H. Ma, O. Acton, D. Hutchins, N. Cernetic and A. K.Jen (2012) Multifunctional phosphoric acid self -assembled monolayers on metal oxides as dielectrics, interface modification layers and semiconductors for low-voltage high-performance organic field-effect transistors, Physical chemistry chemical physics, 14(41), 14081-14402.

116] O. Acton, G. Ting, P. Shamberger, F. Ohuchi, H. Ma and A. Jen (2012), Dielectric surface-controlled Low-voltage Organic Transistors via n-Alkyl phosphonic acid Self-assembled monolayers on high-k metal oxide, 2(2), 511-520.

117] V. Dave, P. Dubey, H.Gupta and R. Chandra (2013) Effects of sputtering gas on structural, optical and hydrophobic properties of DC-sputtered hafnium oxide thin films, Surface & Coatings Technology, (232), pp. 425-431.

118] R.K.Jain, Y.K.Gautam, V.Dave, A.Chawla and Ramesh Chandra (2013) A Study on structural, optical and hydrophobic properties of oblique angle sputter deposited HfO_2 films, Applied surface Science, (283), pp. 332-338.

119] J.Shim, J.A.Rivera, R.Bashir (2013) Electron beam induced local crystallization of HfO_2 nanopores for biosensing applications, RSC Nanoscale, (5), 10877-10893.

120] B.Branch, M.Dubey, A. Anderson, K.Artyushkova, J.Baldwin, D.Petsev and A.Dattelbaum (2014) Investigating phosphonate monolayer stability on ALD oxide surfaces, Applied surface science, (288), pp.98-108.

121] C.Bram, C.Jung and M.stratmann (1997) Self assembled molecular monolayers on oxidized inhomogeneous aluminum surfaces, Fresenius J. Analytical Chemistry, (358), pp.108-111.

122] L.Majewski, R.Schroeder, M.Grell, P.A. Glarvey and M.Turner (2004) High capacitance organic field-effect transistors with modified gate insulator surface, J of applied physics, (96), pp. 5781-5787.

123] C.F.Herrmann, W.D.Frank, V.M.Bright and S.M.George (2005) conformal hydrophobic coatings prepared using atomic layer deposition seed layers and non-chlorinated hydrophobic precursors, J Micromechanics and microengineering, (15), pp.1-9.

124] L.N.Mitchon and J.M.White (2006) Growth and analysis of octadecylsiloxane monolayers on Al_2O_3 (0001), Langmuir, (22), pp.6549-6554.

125] M.S.Lim, Ke Feng, A.Raman, A.Timperman (2007) Adsorption and desorption of stearic acid Self-assembled monolayers on aluminum oxide, Langmuir, (23), pp.2444-2452.

126] S. Sun and G. Leggett (2007) Micrometer and Nanometer scale photo patterning of Self assembled monolayers of phosphonic acids on aluminum oxide, 7(12), pp.3753-3758.

127] W.Cho, S. Park, S. Jon and I. Choi (2007) Water-repellent coating: formation of polymeric self-assembled monolayers on nanostructure surfaces, Jl. of Nanotechnology, 18, 395602-395609.

128] P. Thissen, M. Valtiner, G. Grundmeier (2009) Stability of phosphonic Acid Self-assembled monolayers on Amorphous and Single - Crystalline aluminum oxide surfaces in aqueous solution, Langmuir, 26(1), 156-164.

129] J. Buijnsters, R.Zhong, N. Tsyntsaru, J.P.Celis (2013) Surface Wettability of Macroporus Anodized Aluminum Oxide, Applied Materials and Interface, 5, 3224-3233.

130] O. Zubir, I. Barlow, G. Leggett and N. Williams (2013) Fabrication of molecular nanopatterns at aluminum oxide surfaces by nanoshaving of self-assembled monolayers of alkyphosphonates, Nanoscale, 5, 11125-11131.

131] E. Jenner, C. Barbier and B. Dusro, Durability of hydrophobic coatings of superhydrophobic aluminum oxide, Applied Surface Science, 282, 73-76.

132] M.Psarski, J.Marczak, J.Grobelny and G.Celichowski (2014), Superhydro- phobic Surface by Replication of Laser Micromachined pattern in Epoxy/Alumina Nanoparticle composite, Journal of Nanomaterials, 2014, 1-11.

133] D.Kalblein, H.Ryu, F.Ante, B.Fenk, K.Hahn, K.Kern and H.Klauk (2014) High-performance ZnO Nanowire Transistors with aluminum top gate electrodes and naturally formed hybrid Self-assembled monolayer/AlO_x Gate dielectric, ACS Nano, 8(7), 6840-6848.

134] H.C.Lu, N.Yasuda, G. Alers (1999), Structural properties of thin films of high dielectric constant materials on silicon, Microelectronic Engineering, (48), pp.287-290.

135] M.Textor, L.Ruiz, R.Hofer, G.Hahner and N.Spencer (2000), Structural Chemistry of self-assembled monolayers of Octadecylphosphoric acid on Tantalum oxide surfaces, Langmuir, (16), pp. 3257-3271.

136] R.D. Palma, W.Laureyn, F.Frederix, K.Bonroy, G.Maes (2007), Formation of Dense Self-assembled Monolayers of (n-Decyl) tricholosilane on Ta/Ta_2O_5, Langmuir, (23), pp.443-451.

137] Y.Li, W.Parkes, A.Stokes, A.Collin, N.Hutcheon, A.Walton (2008), Anoidic Ta_2O_5 for CMOS compatible low voltage electrowetting-on-dielectric device fabrication, Solid state electronics, (52), pp. 1382-1387.

138] C. Arnould, C. Volcke, P. Thiry, J. Delhalle, Z. Mekhalif (2009), Titanium modified with layer-by-layer sol-gel tantalum oxide and an organodiphophonic acid: A coating for hydroxyapatite growth, J of colloid and interface science, (336), pp. 497-503.

139] Y.Lin, R.Evans, E.Welch, B.Hsu, A. Madison, R. Fair (2010), Low voltage electrowetting-on-dielectric platform using multi-layer insulators, Sensor and Actuators B: Chemical, (150), pp.465-470.

140] J. Liu, A.Wei, X. Zhao and H. Zhang (2011), Structural and electrical properties of Ta2O5 thin films prepared by photo-induced CVD, Bulletin of Materials Science, 34(3), pp. 443-446.

141] L. Huang, B. Koo and C. Kim (2012) Evaluation of Anodic Ta_2O_5 as the dielectric layer for EWOD devices, IEEE MEMS 2012, pp. 428-431.

142] L. Huang, B.Koo and C.Kim (2013) Sputtered-Anodized Ta_2O_5 as the dielectric layer for electrowetting-on-dielectric, Journal of Microelectromechanical System, 22(2), pp.253-255.

143] L. Mao, S. Zhu, J. Ma, Dian Shi, Y. Chen , Z. Chen, C. Yin, Y. Li and D. Zhang (2014) Superior H_2 production by hydrophilic ultrafine Ta_2O_5 engineered covalently on graphene, Nanotechnology, 25 , pp. 215401-215410.

144] H. Chen and C. Fu (2014) Annealing effect of high dielectric materials for low voltage Electrowetting on dielectric (EWOD), Modern Applied Science, 8(3), pp.10-23.

145] Y. Chang , H. Huang, H. Chen, C. Lai and C. Wen (2014) Antibacterial properties and cytocompatibilty of tantalum oxide coatings, Surface and coating technology, 259, pp. 193-198.

146] R. Michel, J. Lussi, G.Csucs, G. Danuser, B. Ketterer, J. Hubell, M. Textor and N.Spencer (2002), Selective Molecular assembly patterning: A New approach to micro and nanochemical patterning of surfaces for biological applications, Langmuir, pp. A-E.

147] R. Helmy and A.Y. Fadeev (2002) Self assembled monolayers supported on TiO2 comparison of $C_{18}H_{37}SiX_3$ (X=H, Cl, OCH_3), $C_{18}H_{37}Si$ $(CH_3)_2Cl$, and $C_{18}H_{37}PO$ $(OH)_2$, Langmuir, (18), pp.8924-8928.

148] U. diebold (2003), The surface science of titanium dioxide, Surface Science report, (48), pp.53-229.

149] H. Haick, Y. Segatelian and Y. Paz (2003), Effect of Metallic microdomains on the Chemisorptions of Octadecyltrichlorosilane onto Titanium dioxide, Langmuir, (19), pp.2540-2544.

150] H. Liu, N. Venkataraman, N.Spencer, M. Textor and S. Xiao, Structural Evolution of self assembled alkanephosphate monolayers on TiO_2, Chemical physical chemistry, (9), pp. 1979-1981.

151] C. Hsieh, M. Lai and Y. Cheng (2009) Fabrication and superhydrophobicity of fluorinated titanium dioxide nanocoating, Journal of Colloid and Interface Science, 340, 237-242.

152] W. Li, Y. Li and X. Wang (2010) Nano-TiO_2 modified superhydrophobic surface coating for Anti-ice and Anti-flashover of Insulating layer, IEEE conference on Power and Energy Engineering, pp. 1-4.

153] Z. Chen, S. Pan, H. Yin, L. Zhang, E. OU, Y. Xiong and W. Xu (2011) Facile synthesis of superhydrophobic TiO_2/polystyrene core-shell microspheres, eXpress polymer letters, 5(1), pp. 38-46.

154] D. Meroni, S. Ardizzone, G. Cappellettti, M. Ceotto, M.Ratti, R. Annunziata, M. Benaglia and L. Raimondi (2011) Interplay between chemistry and texture in hydrophobic TiO2 hybrids, Journal of physical chemistry, 115, pp. 18649-18658.

155] N. Ishida and D. Fujita (2012) Superhydrophilic TiO_2 surfaces generated by reactive oxygen treatment, Journal of Vacuum Science and Technology A, 30, pp. 051402-5.

156] T. Kamegawa, Y. Shimizu and H. Yamashita (2012) Superhydrophobic surfaces with photocatalytic self-cleaning properties by nanocomposite coating of TiO_2 and polytetrafluoroethylene, Advanced materials,(24), pp. 3697-3700.

157] Q. Xu, Y. Liu, F. Lin, B. Mondal and A. Lyons (2013) Superhydrophobic TiO_2-polymer Nanocomposites surface with UV-Induced Reversible wettability and Self-cleaning properties, Applied Materials and Interface, 5, 8915-8924.

158] G. Chagas, D. Weibel (2014) Photochemistry treatment on superhydrophobic polypropylene surfaces to improve wettability and adhesion properties, American Symposium on polymer, 1-4.

159] N. Shirtcliffe, S. Aqil, C. Evans, G. Mchale, M. Newton, C. Perry and P. Roach (2004), The use of high aspect ratio photoresist (SU-8) for superhydrophobic pattern prototyping, J of Micromechanics and Microengineering, (14), pp.1384-1389.

160] M. Nordstrom, R. Marie, M. Calleja and A. Boisen (2004) Rendering SU-8 hydrophilic to facilitate use in micro channel fabrication, J of micromechanics and microengineering , (14) , pp. 1614-1617.

161] D. Herbertson, C. Evans, N. Shirtcliffe, G. Mchale, M. Newton (2006) Electrowetting on superhydrophobic SU-8 patterned surfaces, Sensor and Actuators A, (130-131), pp.189-193.

162] Y. Wang, M. Bechman, C. Sims, GP. Li and N. Allbritton, (2006), simple photo grafting Methods to chemically Modify and Micropattern the surface of SU-8 Photoresist, Langmuir, (22), pp.2719-2725.

163] CK. Chung and YZ. Hong, (2007), Surface modification of SU8 photoresist for shrinkage improvement in a monolithic MEMS microstructure, J Micromechanics and microengineering, (17), pp.207-212.

164] Y. Wang, J. Pai, H. Lai, C. Sims, M. Bechman, G. Li and N. Allbritton (2007) surface graft polymerization of SU-8 for Bio-MEMS applications, J Micromechanics and micronengineering, (17), pp.1371-1380.

165] F. Walther, P. Davydovskaya, S. Zurcher, M. Kaiser, H. Herberg, A. M. Gegler and R.W.Stark (2007), Stability of the hydrophilic behaviour of SU-8 oxygen plasma activated SU-8.

166] M. Avram, A. Avram, A. bragaru, A. Ghiu, C. Iliescu, (2008), Plasma surface modification for selective hydrophobic control, Raman J of information Science and Technology, 11(4), pp. 409-422.

167] S. Tao, K. Popat, J. Norman and T. Desai, (2008), Surface Modification of SU-8 for enhanced biofunctionality and Nonfouling properties, Langmuir, (24), pp.2631-2636.

168] J. Schumacher, A. Grodrian, C. Kremin, M Hoffmann and J. Metze, (2008), Hydrophobic coating of microfluidics chips structured by SU-8 polymer for segmented flow operation, J of Micromechanics and Micromachining, (18), pp.055019-6.

169] F. Walther, T. Drobek, A. Gigler, M. Kaiser, T. Shimitsu, R. Stark, (2010), Surface hydrophillization of SU-8 by plasma and wet chemical processes, Surface and interface analysis, (42), pp.1735-1744.

170] C. Chang, CS. Yang, L. Lan, P. Wang and F. Tseng, (2010), Fabrication of a SU-8 based polymer-enclosed channel with a penetrating UV/Ozone-modified interior surface for electrokinetic separation of proteins, (20), pp. 115031-11.

171] S. Park, J. Moon, H. Jeon and S. Yang, (2012), Anisotropic wetting and superhydrophobic on holographically featured 3D nanostructured surfaces, Soft matter, (8), pp. 4567-4570.

172] K.H. Rasmussen, S. Keller, F. Jensen, A. Jorgensen, O. Hansen, (2013), Su-8 etching in inductively coupled oxygen plasma, Microelectronic engineering, (112), pp.35-40.

173] G. Marinaro, A. Accardo, F.D. Angelis, T. Dane, B. Weinhausan, M. Burghammer, C. Riekel (2014) A Superhydrophobic chip based on SU-8 photoresisit pillar suspended on a silicon nitride membrane, RSC Technical innovation, 14, 3705-09.

Chapter 3

Wetting behaviour of Silicon

3.1 Overview

The Wettability of solid surfaces especially that of silicon surface, plays a very important role in microfluidics devices. This property of solid surfaces is governed by both the chemical composition and the micro/nano structure on the surfaces [1-8]. The surface wettability is determined by measuring the contact angle (θ_c) of liquid droplet on a solid surface. Among the four categories of wettability as mentioned in Chapter 1 section 1.1, the superhydrophobic surfaces with θ_c >150° have attracted great attention because of their importance in devices where the contact angle of the fluid with the device surface determines the performance and durability of the surface and hence the devices. These surfaces promise useful applications which require self-cleaning, non-wetting and low adhesion [9-11]. Superhydrophobic surfaces can be prepared either by enhancing the surface roughness through surface texturing or by chemically modifying the surface. The chemical modification of surface by self-assembly of organosilane is one of the efficient strategies to synthesize superhydrophobic surface and is achieved due to lowering of the surface energy [12-14]. The Octadecyltrichlorosilane (OTS, $Cl_3Si\ (CH_3)_{17}$), self-assembled monolayer (SAM) is one such organosilane used for realizing superhydrophobic surfaces [15-16], and this has been widely investigated on silicon surface, because of its wide range of applications in molecular electronics devices and microfluidics [17-21]. The superhydrophobicity of silicon surfaces achieved using the chemical texturing followed by chemical modification with depositions of self-assembled monolayer has been reported in literature. Eric Mazur et al. had shown the silicon texturing using laser followed by silane monolayer to obtain the θ_c equal to 160° [22]. C. P. Wong et al. and Jie Hu established the chemical texturing of silicon using alkaline solution and metal assisted etching to obtain superhydrophobic silicon surface [23-24]. B. T. Tay et al. reported the θ_c of 162° by metal assisted silicon etching followed by SAM [25]. However, the synergism of physical texturing and chemical modification to realize superhydrophobic surfaces of silicon has not been reported in published literature. Further, to the best of our knowledge, a comprehensive study involving the investigation on many possible ways

to achieve chemical and plasma texturing combined with SAM on silicon surface has not been addressed. In this chapter, we present the results of a study aimed at achieving wettability for superhydrophobic surfaces of silicon by combined effect of various methods of texturing and organosilane modifications. For this purpose, we compare the results obtained using various combinations of texturing methods, namely, chemical etching using potassium hydroxide (KOH) and Tetra methyl ammonium hydroxide (TMAH) and plasma treatments using Reactive ion etching (RIE) in gas plasma of SF_6 as well as in O_2 plasma.

3.2 Experimental Details

From the literature review, conceptually at least there is a possibility of enhancement of WCA by combining texturing and deposition of SAMs. We conceived of exploring various texturing methods with OTS SAM deposition to investigate the change in wettability behaviour of silicon surface. The experimental details of the combined method and comparison with texturing and SAM deposited surface separately are given in next subsection.

We prepared silicon surface samples by (i) simply cleaning with piranha (ii) cleaning with piranha and later dipping in HF (iii) Etching (texturing) cleaned silicon surface with (a) KOH (b) TMAH and (c) a combination of KOH and TMAH (iv) texturing with plasma treatment in the environment of (a) SF_6 (b) O_2 and (c) a combination of SF_6 and O_2 and lastly (v) modified all pervious samples with deposition of OTS SAM. For each type of surfaces, we prepared 4-5 samples for obtaining an average value to conclude.

3.2.1 Cleaning and sample preparation

First we have taken single side polished silicon (100) wafers with a resistivity of (3-10) ohms-cm, and orientation, <100> were used in all experiments for producing the textured surface. Though the wafer is fresh, they still are not clean, so before starting fabrication process we have to clean the wafer properly. A two step process for cleaning is considered with DI water rinsing and followed by piranha cleaning.

DI Water rinsing: Wafer is rinsed with DI Water for 10 minutes. A large fraction of ionic impurities present on the wafer surface is removed and wafer become free from all ionic impurities expect HO^+ and OH^-.

Piranha cleaning: After DI water rinsing; the wafers are cleaned using Piranha solution. Piranha solution contains H_2SO_4:H_2O_2 in the ratio of 3:1 by volume. The wafers are dipped in the solution for 15 min. Organic impurities and alkali ions are removed due to strong oxidizing property of the solution. The surface of silicon is passivated with (OH) groups making it hydrophilic. After piranha cleaning the wafers are dipped in dilute HF (HF: DI water: 1:50) at room temperature to remove the native oxide. This is followed by N_2 blow drying. The completion of etching of the native oxide layer is confirmed by the appearance of hydrophobic Si surface. Three set of samples were prepared for the experimental work.

3.2.2 Silicon surface without any texturing

The first set of cleaned silicon wafers prepared as identified in Table 3.1 are: (i) Polished silicon surface piranha cleaned but did not go through the HF dip and designated as 'PR' (ii) Polished silicon surface piranha cleaned followed by HF dip and DI rinse, designated as 'HF' (iii) The unpolished backside surface of silicon wafer subjected to only HF dip to remove the native oxide, designated as 'BS'. The details of time, temperature and concentration parameter are given in Table 3.1.

Table 3.1: Parameter details for PR, HF and BS samples

Sample ID	Treatment methods	Time	Temperature (°C)	Concentration
PR	Piranha (H_2SO_4 : H_2O_2)	30 Minutes	25°	1:3
HF	Piranha + HF	30 sec + 10 sec	25°	10% Dilute HF
BS	Back Side	-	-	-

3.2.3 Chemical texturing of silicon surface

There are many chemicals and mixtures that etch silicon anisotropically including the alkali metal hydroxides, ammonium hydroxides, ethylenediamine mixed with pyrochatechol (EDP). Many of these are still the subject of research and in practice only potassium hydroxide (KOH), tetramethylammonium hydroxide (TMAH) are regularly used in MEMS manufacturing. KOH and TMAH are close to each others. KOH is simply the hydroxide of potassium and TMAH is an organic hydroxide.

One set of prepared sample, after the piranha cleaning followed by HF dip is used to perform the chemical texturing using commonly used etchant solutions tetramethylammonium hydroxide (TMAH) and potassium hydroxide (KOH) with iso-propylalcohol (IPA). The silicon samples were protected from the back side of silicon to avoid the etching from the back side. The plasma enhanced chemical vapor deposition (PECVD) system is used for protection from back side. The silicon dioxide of 1μm is deposited on the back side of silicon surface. The silicon texturing and cleaning was carried out in chemical wet bench shown in Appendix A. After SiO_2 deposition, the silicon samples were textured using three different methods detailed in following section:

(a) KOH texturing: In order to texture the silicon surface with alkaline solution KOH+IPA etching is performed. The solution was prepared by dissolving the KOH 50 g pellets in 80 ml DI water. The IPA (5%) was added in KOH solution (10%) to make the surface rough with uniform density of pyramids. The samples were dipped into prepared KOH solution for 10 minutes. The temperature of KOH solution was set at 80°C which was set through a control panel of Wet bench. The process parameter details with sample ID for KOH (K) are listed in Table 3.2.

(b) TMAH texturing: Another cleaned sample was subjected to TMAH texturing on the surface. The 5% of 25% TMAH solution from MERCK was used for experiment. After TMAH the 5% of IPA was added to TMAH solution. The 80°C was the temperature for the texturing of silicon which was carried out for 10 minutes to make the surface silicon rough. The process parameter details with sample ID for TMAH (T) are listed in Table 3.2.

(c) KOH and TMAH texturing: Another cleaned sample was used to perform the texturing by combined effect of both TMAH and KOH etching. The samples first textured using KOH 10% concentration with IPA (5%) for 10 minutes. Then KOH textured sample was dipped in TMAH (5%) solution for 10 more minutes. The process parameter details with sample ID for combine texturing (KT) are listed in Table 3.2.

After texturing with alkaline solution the samples were cleaned using standard RCA1 and RCA2 cleaning to remove metallic contamination. The RCA1 solution is prepared by mixture of DI water: NH_4OH: H_2O_2 in a proportion 5:3:3 respectively. The samples

were dipped in the solution for 20 minutes keeping the solution at a temperature of around 60°C. After RCA1 the samples were cleaned with RCA2 solution. The RCA2 solution was prepared by mixing of DI water: HCl: H_2O_2 in a proportion 5:3:3 respectively. The wafers were dipped in the solution for 20 minutes at a temperature of around 60ºC. The RCA cleaning was followed by dipping in 10% dilute HF for 10 sec, to remove the native oxide. The process parameter used in different chemical texturing are enlisted in Table 3.2.

Table 3.2: Parameter details of used chemical textured methods

Sample ID	Texturing methods	Time	Temperature (°C)	Concentration
K	KOH	10 Min.	80°C	10%
T	TMAH	10 Min.	80°C	5%
KT	KOH + TMAH	10 Min. + 10Min.	80°C	10%+5%

3.2.4 Plasma texturing of silicon surface

Over the past ten years, most of the plasma texturing process was done using the RIE plasma source image of RIE setup as shown in Appendix A. Texturing by RIE plasma can be performed with or without patterning the surface. Plasma texturing reduce the silicon loss due to pyramid formation via a chemical etch which requires only tens of micron of silicon consumption. The third set of piranha with HF dipped sample was used for plasma texturing. We tried investigating the texturing of silicon surface by using three different gases for plasma treatment as follows:

(a) SF_6 texturing: The piranha cleaned samples were first textured with SF_6 plasma which is widely used for etching of the silicon surface. The sample after piranha clean directly was used for SF_6 texturing. The SF_6 texturing was performed for 60 sec. at 50W. The detail of process parameter is enlisted in Table 3.3 with S sample ID name for SF_6 texturing.

(b) O_2 texturing: Another piranha cleaned sample was used for oxygen plasma texturing. The O_2 plasma will not make much effect on the surface topography of silicon but it makes more hydroxylated group on the silicon surface. The parameters details are listed in Table 3.3 with sample name O for oxygen plasma texturing.

Table 3.3: Parameter details of used plasma textured methods

Sample ID	Texturing methods	Time	Temperature (°C)	Concentration
S	SF_6	60 sec	10°	25 sccm
SO	SF_6+O_2	60 sec	10°	25 + 15 sccm
O	O_2	60 sec	10°	15 sccm

(c) SF_6 and O_2 texturing: The piranha cleaned samples were also used for a combined SF_6 and O_2 texturing. We employed 25 sccm gas flows for SF_6 and 15 sccm O_2 gas flow at 50W, with chamber pressure 50 mtorr for 60 sec duration. The optimized parameters used in different plasma treatment are enlisted in Table 3.3 with SO sample ID for combine plasma (SF_6 + O_2) texturing.

3.2.5 Deposition of OTS SAM on textured silicon

After texturing and cleaning, the OTS was deposited on all the textured silicon surfaces prepared by different methods including chemical and physical. The OTS deposition was carried out in homemade glove box. The details of glove box are given in Appendix A. Before OTS deposition, samples were dehydrated at 110°C for 20 minutes. In the mean time solution was prepared in glove box in argon environment with mixing of 40 ml toluene and 1% of OTS solution to allow the OTS uniformly self-assembles on the textured surfaces. After dehydration, samples were dipped in prepared solution for 2 hours without any disturbance in argon environment. After 2 hours, samples were rinsed with toluene and rinsed samples were then dried in Nitrogen.

3.2.6 Characterization tool

There were all type of textured silicon surface identified as PR, HF, BS, K, T, KT, S, O, SO and these variants were also prepared with OTS depositions. In order to investigate their wettability behaviour, we characterized the different aspect of the surfaces by different tools. The different characterization tools are detailed in Appendix A. The prepared silicon surfaces were characterized by atomic force microscope (AFM) BRUKER to obtain the information on topography of the textured and OTS SAM modified textured silicon surface. A qualitative assessment of surface was also obtained from their SEM images. The surface roughness measurements for untextured, textured

and OTS modified textured surfaces with corresponding rms roughness were obtained with AFM in tapping mode. The static water contact angles on all samples were recorded using contact angle goniometer (data physics) under ambient condition (21°±2°C) and relative humidity of 48-50% with deionized water. We also studied the chemical properties of the surfaces using the Raman spectra and XPS spectra.

3.3 Results and Discussion

Effects of surface texturing on wetting properties were studied by comparing the surface topography, WCA of the textured surfaces with cleaned silicon surface and textured surface before and after OTS SAM modifications. The chemical properties after OTS SAM modification were studied using the Raman spectra and XPS results.

3.3.1 Surface topography by AFM/SEM

The surface morphologies of samples were observed by a BRUKER Dimension icon scan asyst atomic force microscope (AFM) in tapping mode as discussed in pervious section.

3.3.1.1 Silicon surface treated with cleanser (untextured)

The one set of silicon wafers without any texturing namely BS and sample cleansed with HF and PR have the rms roughness shown in Figure 3.1(a). The rms roughness for PR is 0.16±0.05 nm which is greater than the HF treated sample. After HF cleaning, roughness value decrease to 0.09±0.05 nm. Whereas the BS sample followed by HF dip were found to be rougher with rms roughness 485±3 nm without any treatment. The surface morphology for the BS, HF and PR are shown in Figure 3.2(a1-a3) respectively. The Figure 3.2(a1) shows the surface morphology for BS sample. It can be observed from the Figure 3.2(a1) BS sample consist of rough surface without any texturing. The Figure 3.2(a2) shows the surface morphology for the HF treated surface. The Figure 3.2(a2) shows that the HF treated sample makes the surface very smooth a small spike was observed on the surface after HF treatment. The texturing on the surface without any texturing method can be seen very easily. The Figure 3.2(a3) shows the surface morphology for the PR treated surface. Figure 3.2(a3) shows a very smooth surface .The corresponding SEM images were also obtained and illustrated in Figure 3.2(b1-b3) respectively and confirm the observation made based on AFM results.

The surface morphology were also measured after OTS SAM depostion and are given in Figure 3.1(b). It is observed that the rms roughness further increase after OTS SAM depsotions. The change in roughness for BS samples increased to 710±3 nm from 485±3 nm as shown in Figure 3.1(b). The change in roughness was also observed for HF sample with OTS and having a value of 18.6±2 nm. For PR sample with OTS, the rms roughness increased to 9.52±2 nm after OTS SAM from 0.16±0.05 nm without OTS SAM modification. All the obtained values are shown in Figure 3.1(b).

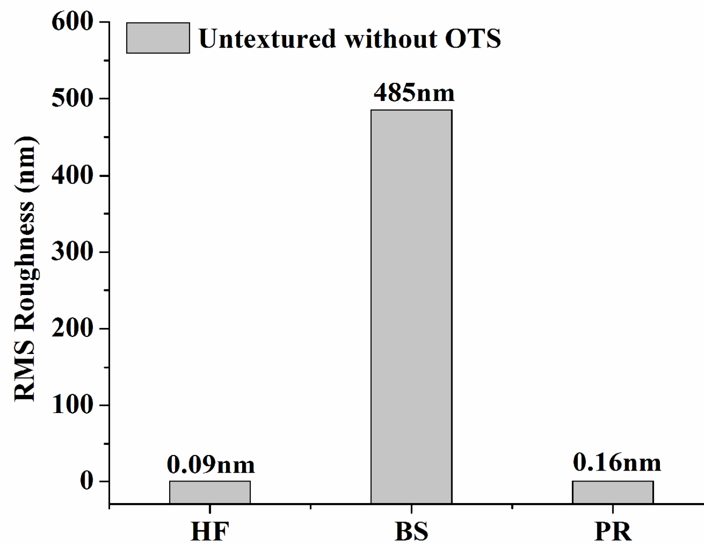

(a)

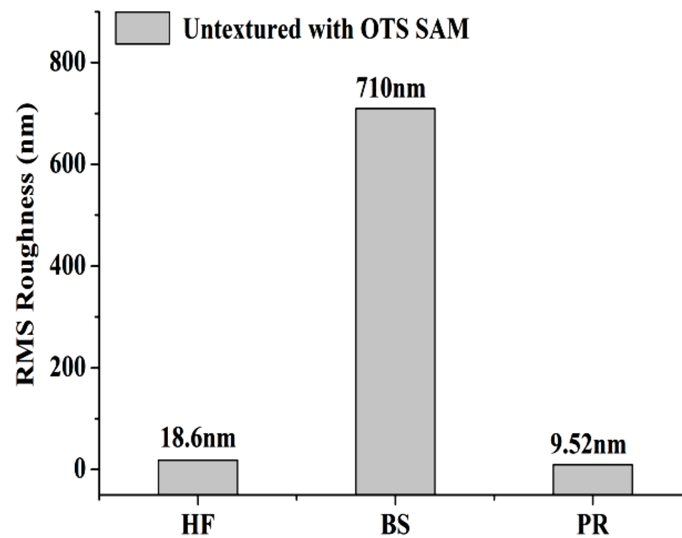

(b)

Figure 3.1: Atomic force morophology values (a) untextured silicon surface without OTS SAM (b) untextured silicon surface with OTS SAM

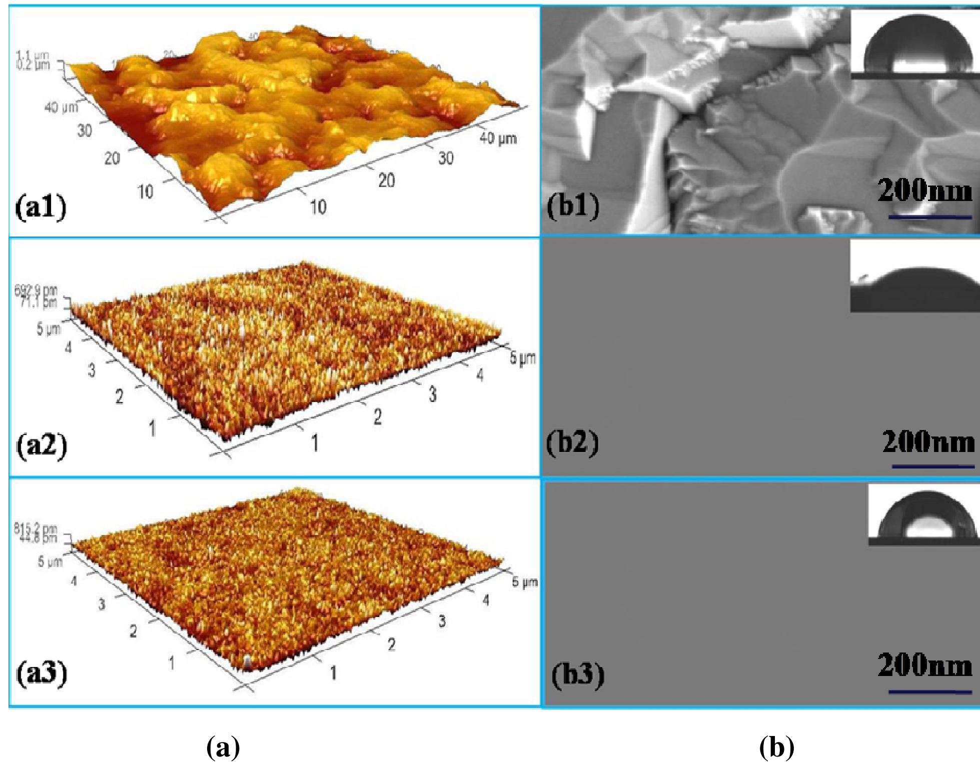

Figure 3.2: Atomic force morphology (a) Untextured silicon surface (a1) BS (a2) PR (a3) HF; Scanning electron microscope images (b) Untextured silicon surface with contact angle inset (b1) BS (b2) PR (b3) HF

The corresponding surface morphology are shown in Figure 3.3(a1-a3). The Figure 3.3(a1) shows the morphology for BS sample. The Figure 3.3(a2) shows the AFM image for PR sample. It can be observed for PR sample surface that their are more spikes which make the surface rough. The Figure 3.3(a3) shows the surface morphology for HF sample. The Figure 3.3(a3) shows more spikes formation on the surface as comapred to PR sample which makes HF sample more rougher in comparison to PR samples.

The corresponding SEM images also shown in Figure 3.3(b1-b3). The Figure 3.3(b1) shows SEM image for BS sample. From the Figure 3.3(b1), the formation of dense monolayer on the surface after OTS SAM modifcation is clearly seen. Figure 3.3(b2) SEM image shows for the PR sample which indicate the formation of monolayer but less dense as comapred to BS sample. The Figure 3.3(b3) shows the SEM image for the HF samples. The Figure 3.3(b) indicate the formation of monolayer but as smooth and dense as compared to PR samples.

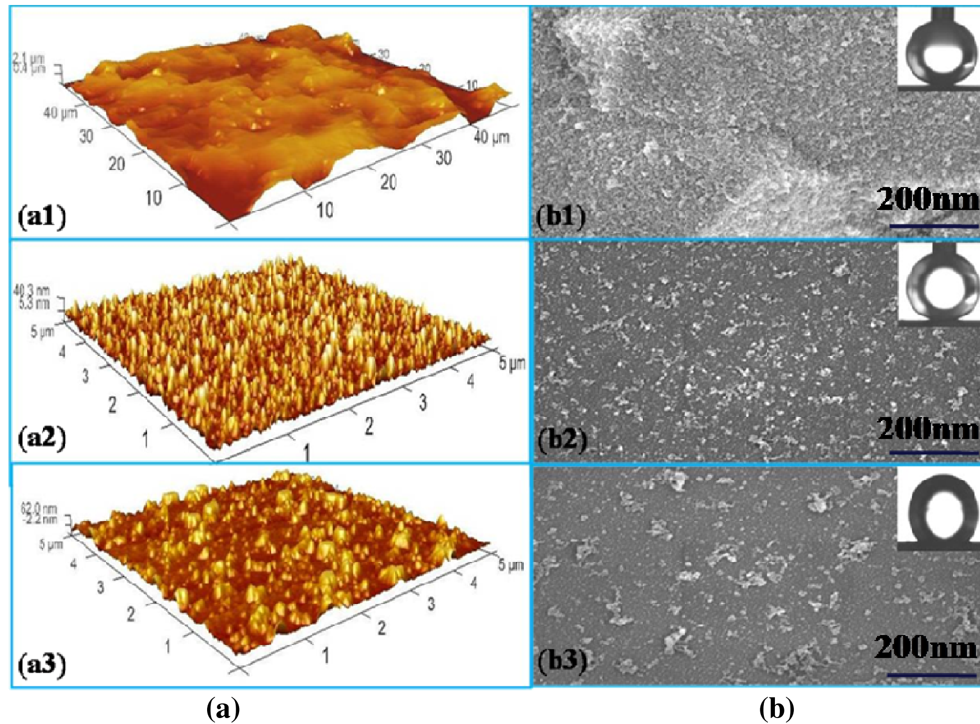

Figure 3.3: Atomic force morphology (a) Untextured silicon surface (a1) BS (a2) PR (a3) HF; Scanning electron microscope images (b) Untextured silicon surface with contact angle inset (b1) BS (b2) PR (b3) HF

3.3.1.2 Chemically textured silicon surface

The chemical texturing causes more significant effect on surface topography in comparison to plasma texturing. The texturing of silicon by chemical alkaline solution such as Potassium hydroxide (KOH), Tetramethylammoniahydroxide (TMAH) are commonly used solution for textured silicon surface in solar cell application. KOH etching solution is cost and time efficient but result in the potassium ion contaminations on surfaces. TMAH is well known etchant solution and is widely used in microelectronics due to its no alkali ions, non-volatile, nontoxic and good anisotropic etching characteristics.

Addition of Isopropyl (IPA) to alkaline etchants is done to improve the uniformity of the random pyramid texturing of the surface. After alkaline chemical etching with KOH, TMAH and combination of KOH and TMAH (surfaces K, T and KT), the rms roughness of textured surfaces increases significantly in comparison to those surfaces which were only HF treated. The obtained rms value of roughness are shown in Figure 3.4. The rms roughness for K sample increased from 0.09±0.05 nm for HF to 758±2 nm for

10 mintues texturing where as for T sample, roughness increased to 838±2 nm as shown in Figure 3.4(a). The sample with a combined treatment of KOH and TMAH (KT) had a lower roughness value of 704±2 nm.

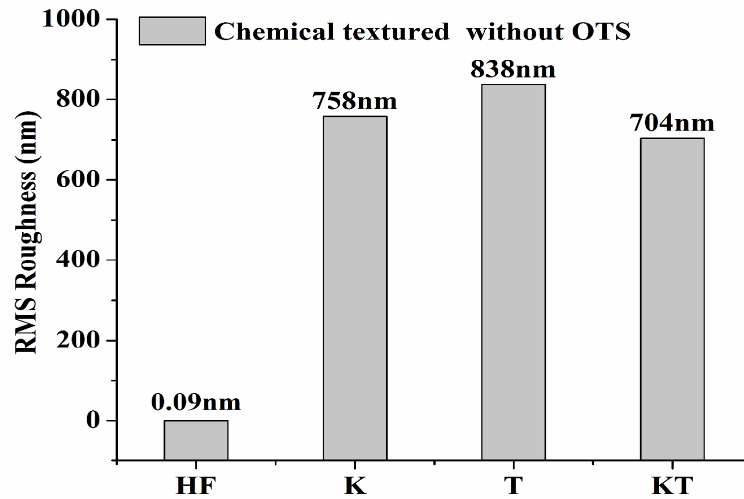

(a)

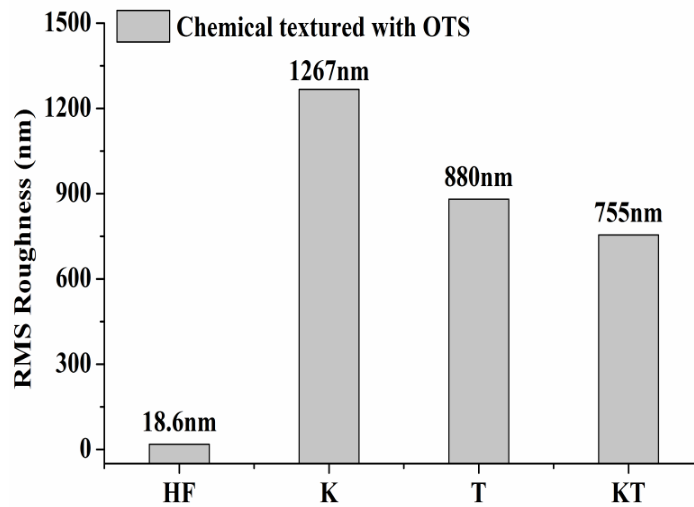

(b)

Figure 3.4: AFM RMS Roughness (a) chemical textured silicon surface without OTS modification (b) chemical textured silicon surface with OTS modified

The corresponding surface morphology for K sample and for T sample is shown in Figure 3.5(a1) and 3.5(a2) which shows the formation of random pyramids on the silicon surface. The rms roughness for KT sample is 704±2 nm [refer Figure 3.4(a)] which is less as compared to K and T sample but the density of pyramid found is more as is seen from surface morphology in Figure 3.5(a3). The SEM images of textured samples is shown in Figure 3.5(b). The density and pyramid formation is clear from the SEM

images. The foramtion of pyramid is least in TMAH as shown in Figure 3.5(b1) as compared to KOH as shown in Figure 3.5(b2). The density of pyramid is increased due to combine etching of TMAH and KOH as shown in Figure 3.5(b3).

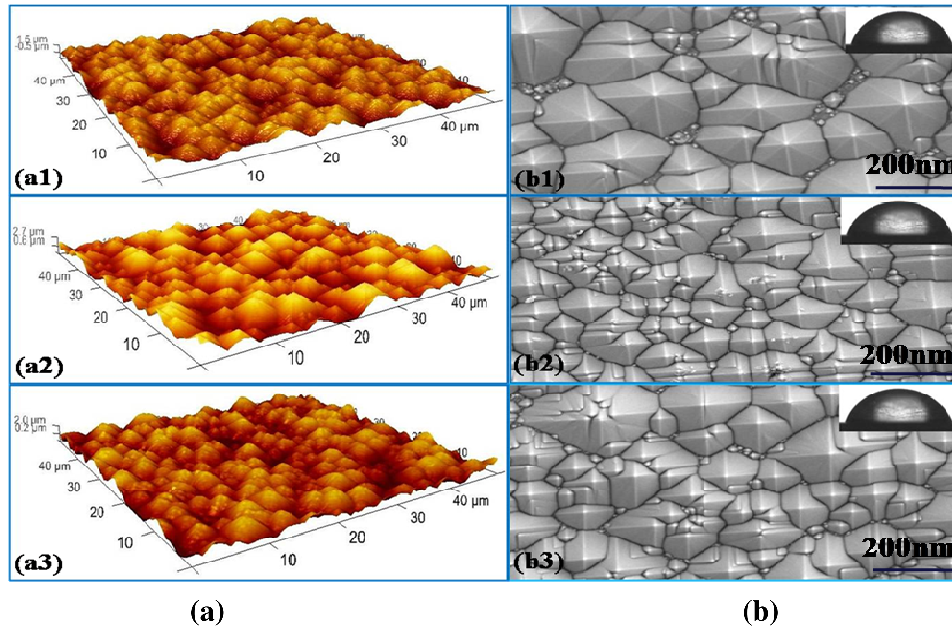

(a) (b)

Figure 3.5: Atomic force morphology (a) chemical textured silicon surface (a1) K (a2) T (a3) KT; Scanning electron microscope images (b) chemical textured silicon surfaces with contact angle inset (b1) K (b2) T (b3) KT

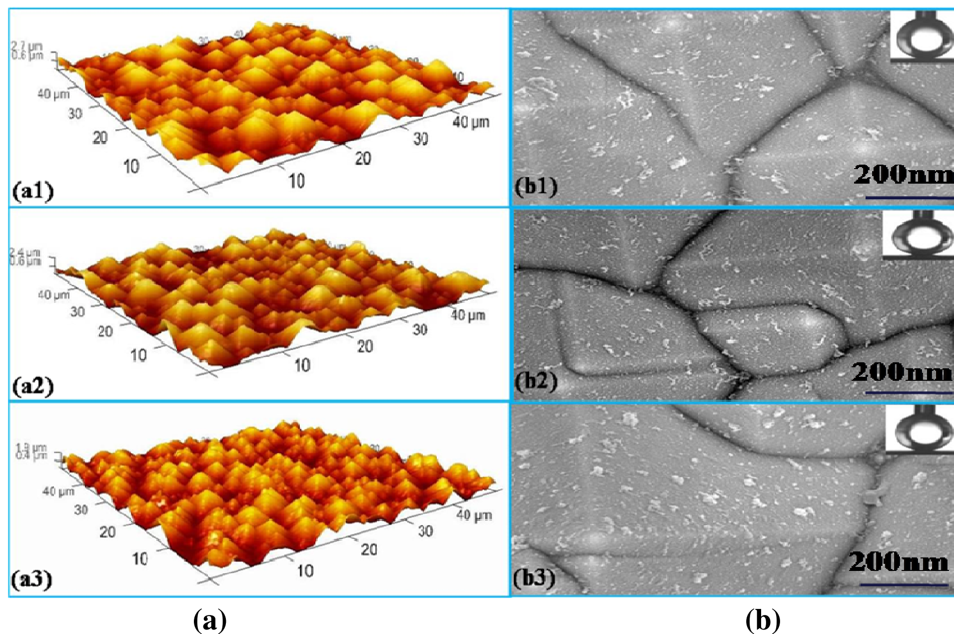

(a) (b)

Figure 3.6: Atomic force morphology (a) chemical textured OTS Modified silicon surface (a1) K (a2) T (a3) KT; Scanning electron microscope images (b) chemical textured OTS modified silicon surfaces with contact angle inset (b1) K (b2) T (b3) KT

The surface modification with OTS SAM further increased the surface rms roughness. The values of rms roughness after OTS deposition on chemically textured silicon surface are shown in Figure 3.4(b). Comparing roughness without OTS and with OTS sample, rms roughness increase from 758±2 nm to 1267±4 nm for K sample [refer Figure 3.4 (b)] which is significantly higher as compared to other textured methods. The rms roughness for T sample increased to 880±2 nm and for KT sample change to 755±2 nm as in Figure 3.4(b). The surface topography after OTS modification shown in Figure 3.6(a) with sequence of (a1) for K, (a2) for T, and (a3) for KT samples. The change in roughness is due to formation of island on the surface shown in SEM images in Figure 3.6(b) in sequence of (b1-b3) respectively.

3.3.1.3 Plasma textured silicon surfaces

The plasma texturing of silicon surface was carried out using fluorine based plasma. The parameters for plasma texturing were chosen to cover the minimum effect on topography and to achieve significant change in wettability. The rms roughness values for plasma textured silicon surface are shown in Figure 3.7(a). The SF_6 plasma for 60 sec at 50 W make small pyramid on silicon surface which make the surface rougher (Sample S). The corresponding surface morphology for plasma textured samples are shown in Figure 3.7(a) which shows the formation of random pyramids on the silicon surface. The obsereved value of roughness increase from 0.09±0.05 nm for HF sample to 1.20±0.5 nm for 60 sec. texturing where as for O sample roughness increased but less than as compared to S samples to 0.10±0.2 nm as shown in Figure 3.7(a).

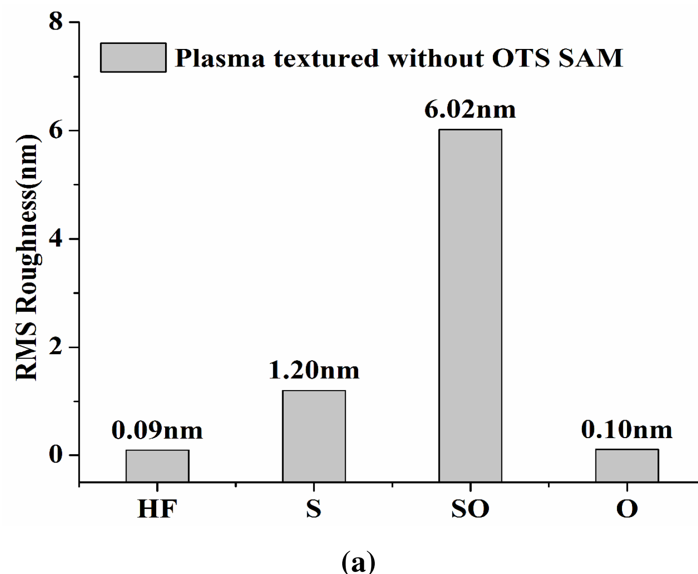

(a)

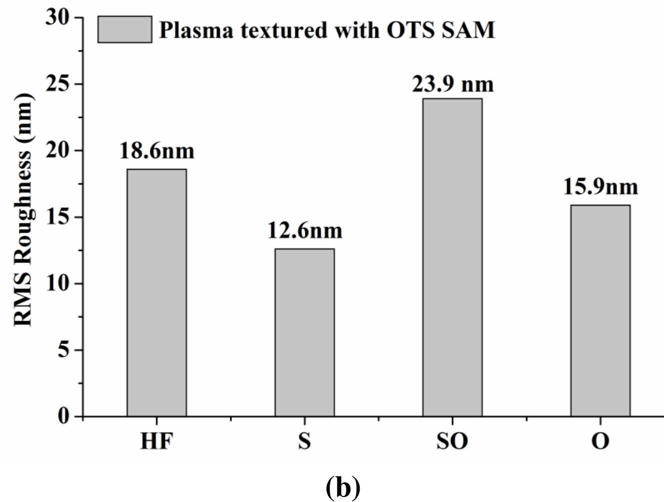

(b)

Figure 3.7: Atomic force morphology values (a) plasma textured without OTS SAM (b) plasma textured with OTS SAM

The corresponding SEM images are shown in Figure 3.8(b1) for S sample and Figure 3.8(b2) for O sample. The rms roughness for SO sample is 6.02±0.5 nm [refer Figure 3.8(a)] which is greater as compared to both S and O sample and the the density of pyramid found is also more as is seen from surface topography Figure 3.8(b3).

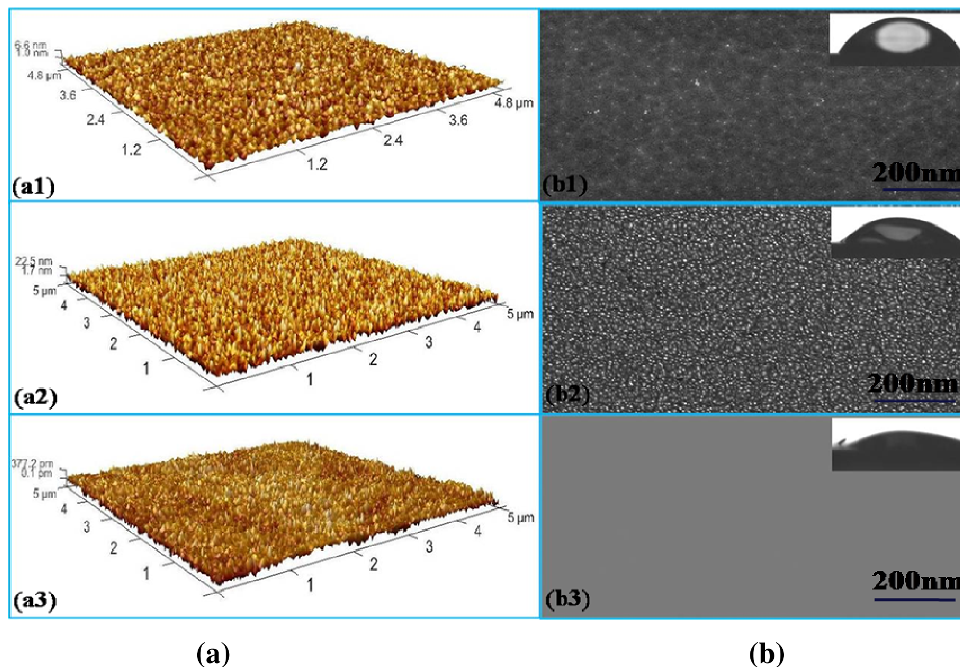

(a) (b)

Figure 3.8: Atomic force morphology (a) plasma textured silicon surface (a1) S (a2) O (a3) SO; Scanning electron microscope images (b) plasma textured silicon surfaces with contact angle inset (b1) S (b2) O (b3) SO

Further, the plasma textured surfaces of silicon were deposited with OTS SAM. The value of rms roughness after OTS deposition on plasma textured silicon surface are shown in Figure 3.7(b). Comparing roughness without OTS and with OTS sample, rms roughness increase from 6.02±0.5 nm to 23.9±2 nm for SO sample [refer Figure 3.7(b)] The surface roughness after OTS SAM modification also increased to 12.6±2 nm for S and to 15.9±2 nm for O as shown in Figure 3.7(b). Corresponding surface morphologies are shown in Figure 3.9(a1) and 3.9(a2) respectively.

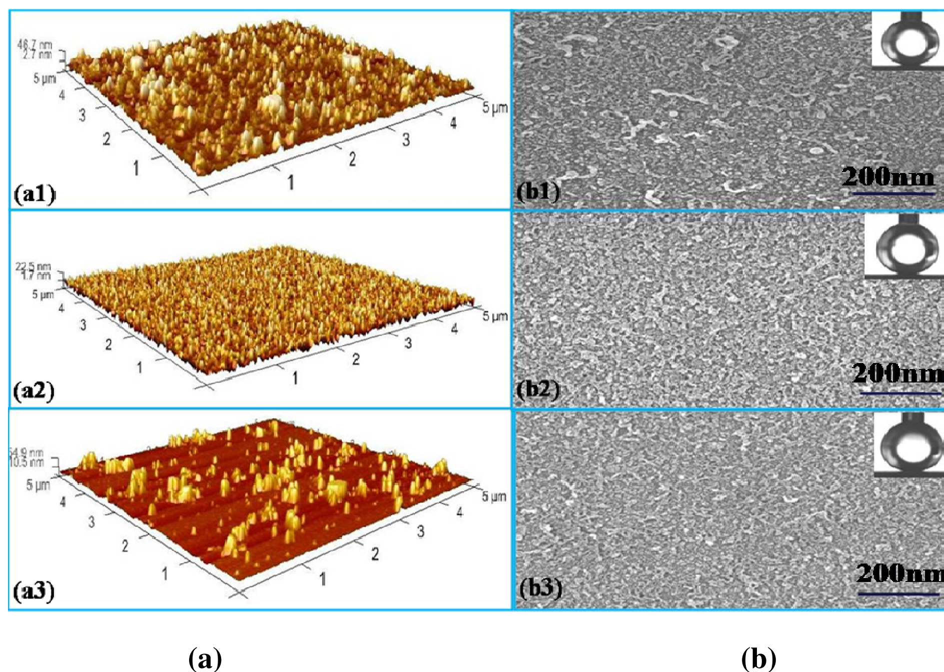

(a) **(b)**

Figure 3.9: Atomic force morphology (a) plasma textured OTS modified silicon surface (a1) S (a2) O (a3) SO. Scanning electron microscope images (b) plasma textured OTS modified surfaces with contact angle inset (b1) S (b2) O (b3) SO

The change in roughness is due to formation of island on the surface shown in SEM images in Figure 3.9(b) in sequence of (b1-b3). The Figure 3.9(b1) for S sample shows the dense formation of monolayer where as Figure 3.9(b2) for SO sample shows formation of even more dense monolayer. The Figure 3.9(b3) for O sample indicates that formation of monolayer is less dense as compared to other plasma textured surface.

3.3.2 Contact angle measurements

The static water contact angles on all samples were recorded using contact angle goniometer (Data Physics) under ambient condition (21°±2^oC) and relative humidity of 48-50% with deionized water. The WCA of each sample was measured five times across

the sample surface using sessile drop method by dispensing 5μl drop of DI water on the sample surface. The contact angles of five different sites for 4-5 samples of each type were averaged and the corresponding results for each type of samples are given in Figure 3.10. The results are discussed in next sections.

3.3.2.1 *Silicon surfaces treated with cleanser (untextured)*

It is observed from the results of our experiments that the WCA >150° in superhydrophobic range can be achieved by synthesizing hydroxylated group on the surface, obtained from piranha treatment without HF treatment [refer to silicon surface as seen with the sample PR in Figure 3.5(a)] after coating with OTS, indicating that the surface chemistry plays a very important role for piranha treated surfaces as compared with textured silicon surface. Here it may be noted that the PR sample showed $\theta_c \leq 10^o \pm 2^o$ just after the piranha treatment as compared to the θ_c = 86° ±2° for HF sample which had undergone both piranha and HF treatment.

The lower contact angle for piranha treated surface is consistent with the presence of more hydroxyl group (-OH) over the surface [26]. These hydroxyl group terminated at surfaces act as anchoring sites for OTS depostion. After OTS SAM deposition the OH group from OTS solution react with these hyroxylated group forming a Si-O-Si bond on the surface which change the surface wettability. As a consequence, the θ_c for PR sample increrase to 156°±2°.The θ_c for HF sample increrase to 132°±2° after OTS SAM modifications by this syergatic combination which is greater than reported value of 109° ±1° in [26]. It is also interesting to note that the θ_c on the intrinsically hydrophobic BS sample without any texturing treatment also increases from a value of θ_c = 94°±2° as shown in Figure 3.5(a) to 162°±2° with OTS SAM deposition as shown in Figure 3.10(b) respectively.

3.3.2.2 *Chemical textured surface*

The texturing of silicon with alkaline chemical make the surface more hydrophillic (WCA <90°) and droplet may penetrate in to rough surface which may enhance the hydrophilicity. By, comparing the WCA for HF sample which is 86.2^o±2° with K sample, WCA reduce to 69.7^o±2°, 81.2^o±2° for T sample and 74.7^o±2° for KT sample as shown in Figure 3.10(a). It is obvious that WCA for HF is better in comparison to others.

The HF treated and all other methods though achieved less WCA in comparsion to BS which gives the WCA of 94°±2° [refer Figure 3.10(a)] which is a hydrophobic surface. The WCA of textured surface increase significantly after modification of OTS SAM. The change in WCA given in Figure 3.10(b). By, comparing the WCA of HF sample which 132°±2° with K sample increase to 163°±2°, 161°±2° for T sample and 162°±2° for KT sample. The highest WCA achieved is for the K sample and is 163°±2°. From Figure 3.10 (a) and 3.10 (b), the WCA of all textured silicon surface which is hydrophilic i.e. $<90^o$ increases to $\geq 150^o$ with OTS SAM, which is in the range of superhydrophobic surface.

3.3.2.3 *Plasma textured surface*

It is observed that the texturing by chemical provide more roughness in comparison to plasma treated surfaces. The chemically textured surfaces consumed microns of silicon and results in formation of large size of pyramid as is clear from surface topography from Figure 3.10(a1) to (a3). The plasma texturing reduce the silicon loss with less consumption of silicon [refer Figure 3.13(a1) to (a3)]. After texturing hydrophobicity of the silicon surface increases with OTS in comparison to untreated surface with OTS SAM improving the importance of surface texturing.

The SF_6 plasma for 60 sec at 50W make small pyramid on silicon surface which make the surface hydrophillic with $\theta_c = 55^o$±2° as shown in Figure 3.10(a). Further rms roughness value increase for diluted SF_6 with O_2 plasma in comparison to surface prepared by only SF_6 plasma treatment making surface more hydrophillic with θ_c=25°±2° and is as given in Figure 3.10(a).

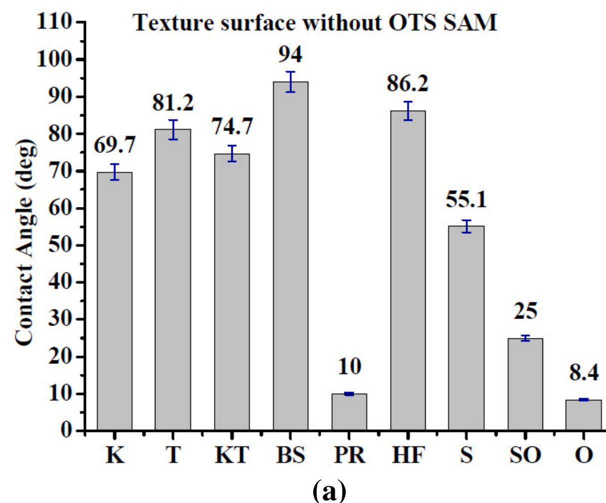

(a)

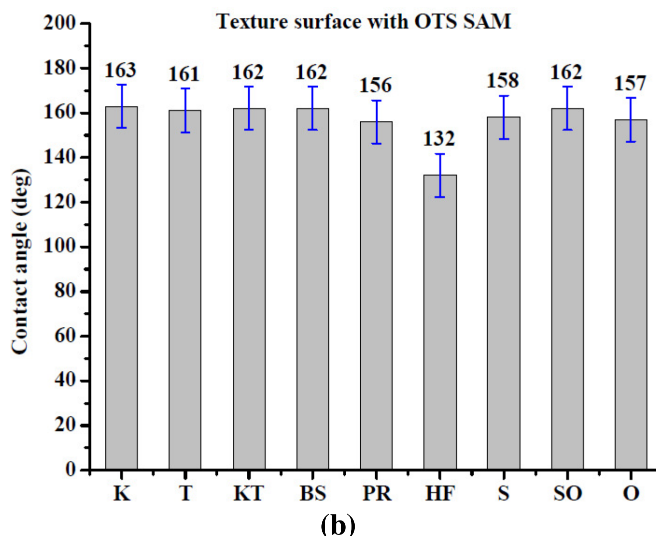

Figure 3.10: Water contact angle (a) untextured, chemical and plasma textured silicon (b) OTS modify untextured, chemical and plasma textured silicon surface

The surface treated with O_2 plasma remained smooth with rms roughness 0.10±0.2 nm of as shown in Figure 3.7(a) which makes surface further hydrophillic with $\theta_c < 10^o \pm 2^o$ [refer Figure 3.10(b)]. The contact angle significantly increases after OTS SAM depsotion on the plasma treated samples. It can be observed from Figure 3.10(b) that the contact angle for plasma treated SO sample increased from $25^o \pm 2^o$ to $162^o \pm 2^o$ where as the value of contact angle increased for S sample to $158^o \pm 2^o$ and for O to $157^o \pm 2^o$.

3.3.3 Raman spectra

To confirm the presence of the chemical bond on the surfaces after OTS SAM modification, the Ramana spectra was taken and observed. The Raman spectra of after OTS SAM deposited silicon surfaces are shown in Figure 3.11. The Figure 3.11 shows the three spectra of the sample prepared through different routes. The Figure 3.11(a) shows the spectra for first set of sample namely that of HF, PR and BS. Figure 3.11(b) shows the spectra for second set of samples K,T and KT. The Figure 3.11(c) shows the spectra for S, O and SO for plasma textured suraface.

The spectra of interest at peak location 2850 cm^{-1}, 2880 cm^{-1} are due to stretching of C-H group. Similarly, the observed peak at 3044 cm^{-1} are peak of =(C-H) in all OTS SAM deposited textured and untextured silicon surfaces. The spectra for cleanser surafce are shown in Figure 3.11(a). The Figure 3.11(a1) shows the spectra for HF sample. The

Figure 3.11(a2) shows the spectra for the PR sample and Figure 3.11(a3) shows the spectra for HF smaples. It can be observed from the Figure 3.11 that no chnage was observed in peak for BS, HF and PR samples.

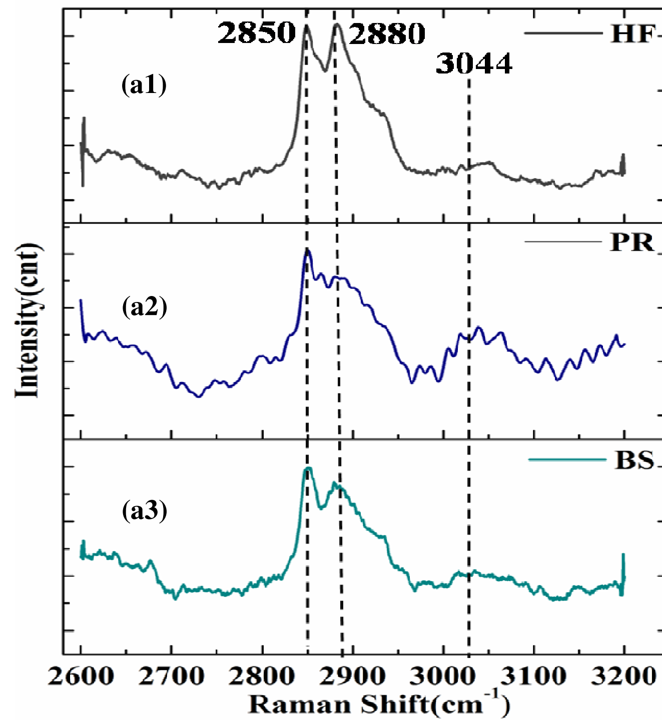

(a)

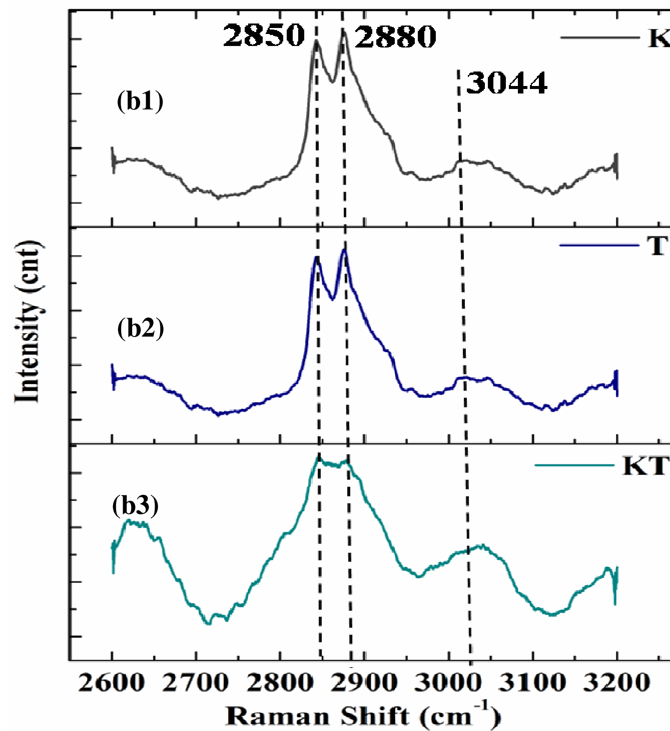

(b)

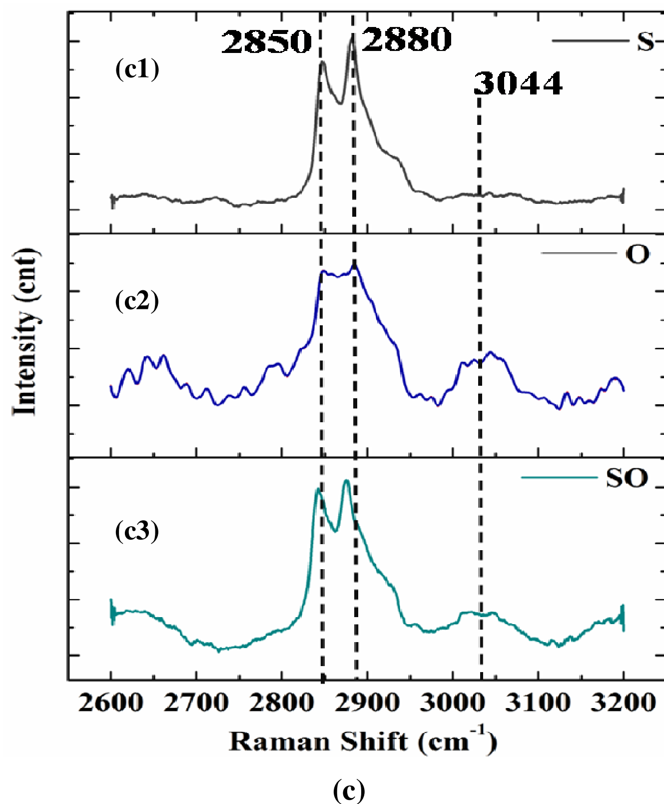

(c)

Figure 3.11: Raman spectra information (a) Untextured silicon with piranha cleaned surface (b) Chemical textured silicon surface (c) Plasma textured silicon surface

The spectra for chemically textured surfaces are shown in Figure 3.11(b). The Figure 3.11(b1) shows the spectra for the K samples and Figure 3.11(b2) for T samples. It can be observed from the spectra that there is no change observed in peak location for both K and T sample after OTS SAM modifcation. The Figure 3.11(b3) shows the spectra for KT samples which also shows the same peak location as K and T samples. The spectra for plasma textured samples are shown in Figure 3.11(c). The Figure 3.11(c1) shows the spectra for S sample and Figure 3.11(c2) shows the spectra for O sample. The same peak location are observed as in chemically textured surface K and T sample. The Figure 3.11(c3) shows the spectra for SO sample. There are no changes observed after OTS depositions on untextured, chemically and plasma textured silicon surface on chemical bonding on the surfaces.

3.3.4 X-Ray photoelectron spectra

Figure 3.12 compares the XPS survey scans of the untextured, chemically and plasma treated surfaces with an OTS SAM modification. The XPS of OTS modified surfaces

were performed with a Kratos Axis Ultra DLD with monochromatic AlKα excitation (1486.6eV). The sample surface was etched by argon ion source to eliminate the surface contamination. The XPS spectra of the OTS SAM for untextured silicon surface are nearly identical to textured OTS modified surface. The Figure 3.12(a) shows the spectra for first set of samples namely HF, PR and BS. Figure 3.12(b) shows the spectra for second set of samples K,T and KT. The Figure 3.12(c) shows the spectra for S, O and SO for plasma textured suraface.

The modified surface shows the significant peak at 480eV and 280eV corresponding to C1s and O1s peak. The Peak C-1s at 480eV implies that much thicker hydrocarbon layer form on the silicon surface, which improve the hydrophobicity of self assembled monolayers. The intensity of the peak of C-1s is higher as compared to the relative intensity of O-1s and Si-2p as in Figure 3.12(b) for chemically textured surfaces. The intensity of the peaks for plasma treated OTS modified surface as in Figure 3.12(c) and untextured silicon surface are shown in Figure 3.12(a). Not much difference in the peak location and intensity of the peaks are observed in XPS of all types of surfaces. There is no evidence for the Chlorine (Cl) peaks from OTS modified surfaces which indicate complete hydrolysis of the trichlorosilane, and surface reactions with textured surface OH group and methyl group chain of OTS SAM solution thereby enhancing WCA.

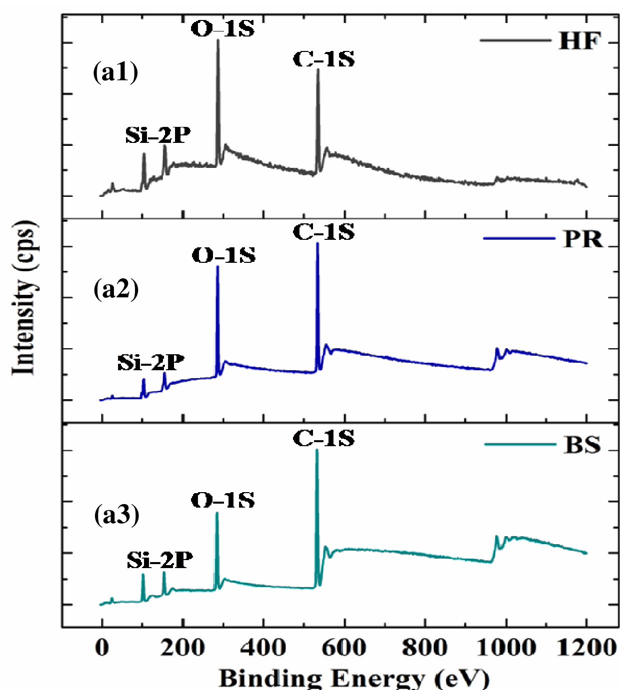

(a)

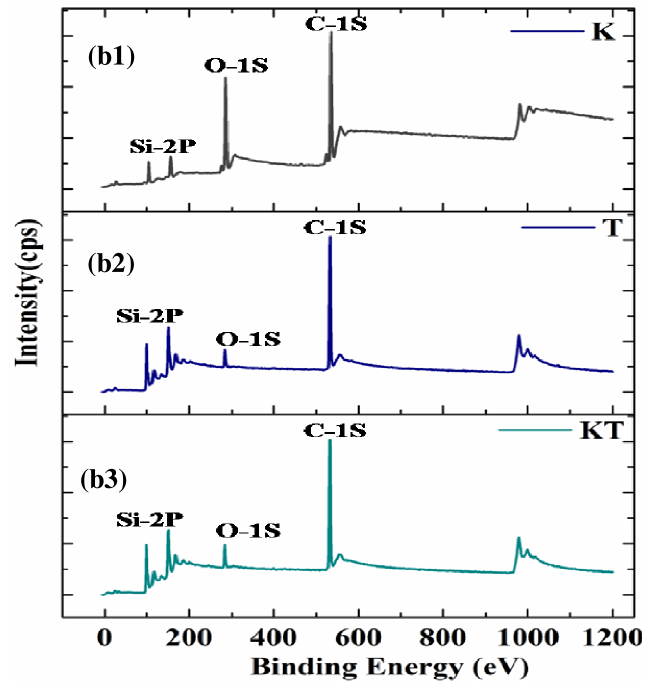

(b)

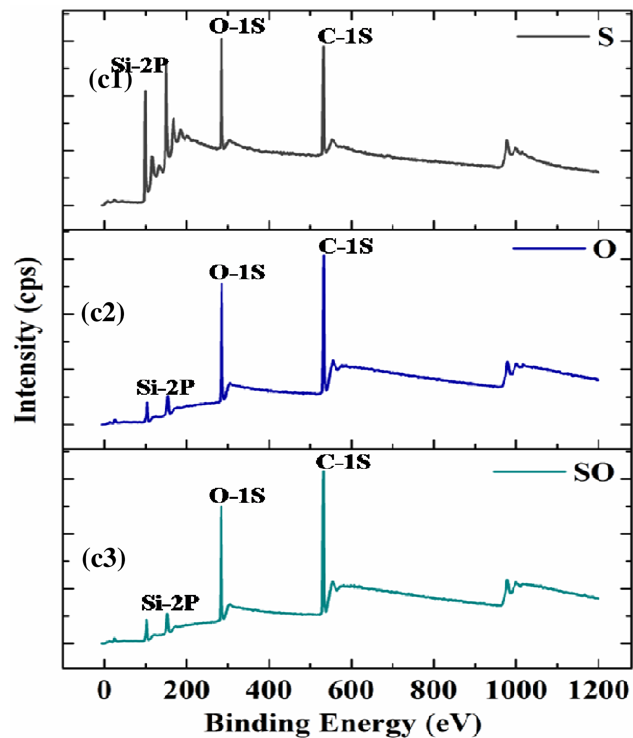

(c)

Figure 3.12: XPS spectra information (a) Untextured silicon with piranha cleaned surface (b) Chemical textured silicon surface (c) Plasma textured silicon surface

3.4 Conclusion

1. The surfaces of silicon with WCA >150° is superhydrophobic regime were prepared by combined effect of chemical and plasma micro/nano texturing and OTS surface modification. The texturing of the surface was carried out using the chemical etchant TMAH and KOH, plasma chemistry of SF_6 and O_2 plasma and cleanesers like Piranha, HF for making experimental samples of silicon surface to study roughness and wettability.

2. It was observed from the AFM results that the TMAH etching gives the maximum roughness of 838±2 nm in comparison with KOH chemical etchant. Similarly, the combined plasma of SF_6 and O_2 provide more rough surface as compare to separately treated SF_6 and O_2 plasma. The surface roughness further increased after the OTS SAM modification because of formation of Islands on the surface. After modification with OTS SAM, the K sample (KOH textured sample) provided a more rough surface with roughness value of 1267±4 nm. The surface modification of combined plasma SF_6 and O_2 also provided maximum roughness value of 23.9±2 nm.

3. The plasma texturing was performed for very less time (60 sec) in order to have minimum effect on topography of silicon. This enables acheivement of high roughness and also provide higher WCA.The surface roughness also increased in the OTS SAM modified HF and PR treated samples.

4. Both of the texturing i.e. chemically and plasma methods provides the surface hydrophillic nature. After being modified by OTS, the silicon surfaces shows superhydrophobic surface with high WCA greater than 150°. For the first time, we have shown that WCA=162°±2° can be achieved on the unpolished BS of silicon provided it is coated with OTS SAM after only a dip in HF and DI water rinse. Piranha cleaned (PR) silicon surface without any texturing showed WCA 156°±2° in the range of superhydrophobicity when OTS is deposited on the surface, provided it did not receive any HF treatment.

5. The wetting behaviour of untextured, chemical and plasma textured silicon changes after OTS SAM modifcation. The WCA >150° was observed for each type of silicon sample. The chemical texturing makes the surface hydrophilic. The texturing reduce the contact angle from 86.2^o±2° for HF sample to 69.7^o±2° for K sample, 81.2^o±2° for T sample and 74.7^o±2° for KT sample. After OTS SAM the WCA increase from

132°±2° for HF sample to 163°±2° for K sample, 161°±2° for T sample and 162°±2° for KT sample. The highest WCA achieved is for the K sample and is 163°±2°.

6. The plasma texturing reduce the contact angle from 86.2^o±2° for HF sample to 8.4^o±2° for O sample, 55.1^o±2° for S sample and 25°±2° for SO sample. The change in WCA also observed after plasma textured and OTS SAM deposition. The WCA increased from 132°±2° for HF sample to 157°±2° for O sample, 158°±2° for S sample and 162°±2° for SO sample. The highest WCA achieved is for the K sample and is 163°±2°.

7. The surface treated with piranha and O_2 plasma process is the most effective way to produce to superhydrophobic surfaces without consumption of much silicon in comparison to chemical and plasma methods.

8. The presence of C-H group in Raman spectra confirm the presence of monolayer on the surface. It can be concluded from the Raman spectra the all type of surfaces shows the same peak with no change observed in peak location for OTS SAM modify samples.

9. The XPS also confirm the presence of C and O on the OTS SAM modified surface. There was no evidence for the Chlorine (Cl) peaks from OTS modified surfaces confirming the complete hydrolysis of silane in OTS.

Refernces:

1] Jose Bico, Uwe Thiele, David Quere (2002) Wetting of textured surfaces" Journal of Colloids and surfaces, (206) pp. 41-46.

2] Reinhard Lipowsky, peter lentz, Peter S. Swain (2000) Wetting and dewetting of structured and imprinted surfaces, Journal of colloids and surfaces, (161), pp.3-22.

3] Lichao Gao, Thomas J. McCarthy, (2009), Wetting and superhydrophobicity Langmuir, (25), pp. 14100-14104.

4] Y.Yan, N.Gao, W. Barthlott, (2011), Mimicking natural superhydrophobic surfaces and grasping the wetting process: A review on recent progress in preparing superhydrophobic surface, Advance in colloid and Interface surfaces, (169), pp. 80-105.

5] Z. Zhu,Yang Wang, Qiu-Sheng Liu, J. Chang Xie (2012), Influence of Bond Number on behaviour of liquid drops deposited onto Solid substrates, Jl Microgravity Science Technology, (24), pp.181-188.

6] Jian-Lin Liu, Xi-Qiao, G.Wang and Shou-Wen Yu (2007), Mechanism of superhydrophobicity on hydrophilic substrate, Journal of Physics condensed Matter, (19), 356002-14.

7] Xianmin XU, X. Wang, (2010), Derivation of the Wenzel and Cassie equations from a phase field model for two phase flow on rough surface, Jl. of applied mathematics, 70, no. 8, pp. 2929-41.

8] Ben Wang, Yabin Zhang, Lei Shi, Jing Li and Zhiguang Guo, (2012), Advances in the theory of superhydrophobic surfaces, Jl. Materials chemistry, (22), 20112-2017.

9] Reiner Fuestner, Wilhelm Barthlott, (2005) Wetting and self-Cleaning properties of artificial superhydrophobic surfaces, Langmuir, (21), 956-961.

10] Bharat Bhushan, Yong Chae Jung, and Kerstin Koch, (2009), Self-Cleaning efficiency of artificial superhydrophobic surfaces, Langmuir, (25), 3240-3248.

11] Yewang Su, B. Ji, Y. Huang, K. Hwang, (2010) Nature's design of hierarchical superhydrophobic surfaces of a water strider for low adhesion and low energy dissipation, Langmuir, 26(24), 18926-18937.

12] George M. Whiteside, Paul E. Laibinis, (1990),Wet chemical approaches to the Characterization of organic surfaces: Self Assembled Monolayer, Wetttting, and the physical-organic chemistry of the Solid-Liquid interface, Langmuir, 6(1), pp. 87-96.

13] Claudia Haensch, Stephanie Hoeppener, Ulrich S. Schubert, (2010) Chemical modification of self assembled silane based monolayers by surface reactions Chemical Society review, (39), 2323-2334.

14] J. Justin Gooding, Freya Mearns, Wenrong Yang, Jingquan Liu, (2003), Self-Assembled Monolayers into the 21st Century: Recent advances and applications, Electroanalysis, 15(2), 81-96.

15] E.Martines, Kris Seunarine, Hywel Morgan, N.Gadegaard, C. Wilkinson, and M.Riehle, (2005) Superhydrophobicity and superhydrophilicity of regular nanopatterns, American chemical society Nano Letters, (10), 2097-2103.

16] Y. Song, Rahul premachandrannair, Min Zou, Y. Wang, (2009) Superhydrophobic surfaces produced by applying a self-assembled monolayers to Silicon Micro/Nano textured surfaces, Nano Research, (2) 143-150.

17] J. Takeya, T. Nishikawa, T. Takenobu, S. Kobayashi, and Y. Iwasa, C. Goldmann, C. Krellner, and B. Batlogg (2004) Effects of polarized organosilane self-assembled monolayers on organic single-crystal field-effect transistors, Applied physics letters, 85(21), pp. 5078-5080.

18] Nick R. Glass, R. Tjeung, Peggy Chan, Leslie Y. Yeo, and James R. Friend, (2011), Organosilane deposition for microfluidics applications, Biomicrofluidics, (5), 036501.

19] Sara A. DiBenedetto, Antonio Facchetti, M. Ratner, T. J. Marks, (2009), Molecular Self-assembled monolayers and multilayers for organic and Unconvential inorganic thin-film transistor applications, Advanced Materials, (21), pp.1407-1433.

20] D. Aswal, S.Lenfant, D.Guerin, J.V. Yakhmi, D. Vuillaume, (2006), Self Assembled monolayers on silicon for molecular electronics, Analytica Chemica Acta, 568, 84-108.

21] Luciano Miozzo, AbderrahimYassar, Gilles Horowitz, (2010), Surface engineering for high performance organic electronics devices: the chemical approach, Journal of Materials chemistry, (20), 2513-2538.

22] TommasoBaldacchini, James E. Carey, Ming Zhou, Eric Mazur, (2006) Superhydrophobic surfaces prepared by Microstructuring of Silicon using a Femtosecond Laser, Langmuir, (22), 4917-4919.

23] Yonghaoxiu, Lingbo Zhu, D. Hess, C. P. Wong, (2007), Hierarchical silicon etched structures for controlled hydrophobicity/Superhydrophobicity" Nano Letters, (7), pp.3388-3393.

24] W. Zhang, Xuge Fan, S. Sang, Pengwei Li, Gang Li,Y. Sun, and Jie Hu, (2014) Fabrication and characterization of silicon nanostructures based on metal-assisted chemical etching, Korean Jl. Chemical Engineering, 31(10), 62-67.

25] Xiaocheng Li, Beng Kang Tay, Philippe Miele, Arnaud Brioude, David Cornu, (2009), Fabrication of silicon pyramid/nanowire binary structure with superhydrophobicity, Applied surface science, (255), 7147-7152.

26] Mingji Wang, Kenneth M. Liechti, Qi Wang, J. M. White, (2005), Self-assembled silane Monolayer: Fabrications with Nanoscales uniformity, Langmuir, (21),1848-1857.

Chapter 4

Wetting behaviour of Dielectric Materials

4.1 Overview

Dielectric materials serve as an important functional material in the manufacturing of silicon integrated circuits (ICs). The SiO_2 is first adopted and highly used dielectric material for semiconductor device technology [1]. Though the usage of SiO_2 with film thickness in micron and sub-micron ranges have been widely reported and accepted in semiconductor and MEMS devices, it is also well know that when the physical thickness of SiO_2 approaches to 2 nm the tunneling current increases exponentially and dominates the leakage current. The considerable improvement in device technology from last few decades has been accompanied by an intense reduction in the thickness of SiO_2 dielectric. The scaling down of film thickness limits the uses of SiO_2 dielectric. To continue the downward scaling, high-*k* dielectric materials are being actively investigated, as an alternative solution to the aforementioned problem [2-4]. However, usage of the high *k* (k >7) materials is a major challenge because of reliability, thermal and chemical stability and for making an ideal contact with silicon substrate [5-8].

Recently, it has been shown that conventional dielectric interface contains large density of electron-interface trap states [9]. The dielectric materials can contain a hydroxyl group (-OH) and water content, resulting in the trap-sites on the surface of dielectrics [10-11]. The presence of -OH group limit the device performance. The neutralization of these polar groups is possible by using surface modification methods, including the use of self-assembled monolayer (SAM) on dielectric interface. The alkanetrichlorosilanes and alkanephosphonic acids and hexamethyldisilazane (HMDS) among others have been extensively studied for oxide surface modifications [12-17]. In this chapter, we are reporting functionalization of low *k* (SiO_2) and high-*k* (HfO_2, Al_2O_3, Ta_2O_5 and TiO_2) oxides using Octadecyltrichlorosilane (OTS, $Cl_3Si\ (CH_3)_{17}$) SAM in synergism with texturing and alone. Further, the surface characteristic of these functionalized surfaces is compared with the original non-functionalized surfaces. The method for modification on all types of dielectric has been kept similar to the one used in previous chapter for modification of silicon surface. In case of plasma treatment, the effect of fluorine plasma

on the quality of monolayer is also discussed. We have shown that the formation of smooth, denser and high quality monolayer with increased hydrophobicity and contact angle >150° is achieved by combine texturing and OTS SAM deposition. The modified surface were characterized using the Atomic force microscope (AFM), Scanning electron microscope (SEM), Raman spectroscopy, Contact angle and X-ray photoelectron spectroscopy.

4.2 Experimental Details

From the literature review, there are very less investigation available for enhancement of WCA by combining texturing and deposition of SAMs for dielectric materials. We conceived of exploring plasma texturing combined with OTS SAM deposition to investigate the change in wettability behaviour of oxide surfaces. The experimental details of the combined method and comparison with texturing and SAM deposited oxide surface separately are given in next subsections.

We prepared oxide surface samples by (i) texturing with plasma treatment in the environment of SF_6 (ii) modified all textured and untextured samples with deposition of OTS SAM. For each type of surfaces, we prepared 4-5 samples for obtaining an average value of WCA, rms roughness and other morphological feature to conclude. The samples were prepared with similar approach as was done for silicon. For the clarity, we repeat the experiment details with changes whenever applicable in next subsections.

4.2.1 Sample preparation

First we have taken single side polished silicon (100) wafers with a resistivity of (3-10) ohms-cm, and orientation, <100> were used in all experiments for producing the textured surface. Though the wafer is fresh, they still are not clean, so before starting fabrication process we have to clean the wafer properly. A two-step process for cleaning is considered with DI water rinsing and followed by piranha cleaning.

(a) **DI Water rinsing**: Wafer are rinsed with DI Water for 10 minutes. A large fraction of ionic impurities present on the wafer surface is removed and wafer becomes free from all ionic impurities except HO+ and OH-.

(b) **Piranha cleaning**: After DI water rinsing; the wafers are cleaned using Piranha solution. Piranha solution contains H_2SO_4:H_2O_2 in the ratio of 3:1 by volume. The wafers are dipped in the solution for 15 min. Organic impurities and alkali ions are removed due

to strong oxidizing property of the solution. The surface of silicon is passivated with (OH) groups making it hydrophilic. After piranha cleaning the wafers are dipped in dilute HF (HF: DI water: 1:50) at room temperature to remove the native oxide. This is followed by N_2 blow drying. The completion of etching of the native oxide layer is confirmed by the appearance of hydrophobic Si surface. Two set of 4-5 samples for each type of oxide were prepared for the experimental work of which one set is used for OTS SAM modification and other set is used for plasma and OTS SAM modification.

4.2.2 Dielectric depositions

4.2.2.1 *Low-k dielectric materials*

The first set of cleaned samples was used for deposition of low-*k* dielectric (SiO_2) materials. After the HF dip, sample was loaded for oxidation at 1000°C with a flow of nitrogen atmosphere. When the chamber reaches the temperature of 500°C, the wafers are loaded into it. A dry-wet-dry oxidation process was used. Initial dry oxidation was performed for 15 minutes to realize the better contact on the interface. Now, the wet thermal oxidation was performed at same temperature for three hours. Finally, again dry oxidation was performed for 15 minutes. Wet oxidation is a fast process, but is not so perfect and results in a relatively porous silica films. On the other hand, a comparatively very slow process dry oxidation is most perfect one. So we have made a sandwich of dry-wet-dry oxidation for the uniformity and high oxidation rate with oxide thickness of the samples 1.01 micron. The thickness was measured using ellipsometry. The SiO_2 substrate was then cut in to small pieces of sizes 1 cm × 1 cm for further experiments.

4.2.2.2 *High-k dielectric materials*

Second set of cleaned samples were used for deposition of High-*k* dielectric materials. We used sputtering deposition method to deposit high-k dielectric materials like HfO_2, Al_2O_3, TiO_2 and Ta_2O_5.The sputtering deposition method of metal and oxide materials is a well-established technique. In sputtering plasma discharge is initiated using either a DC or RF field in an inert gas, usually Argon (Ar), at low pressure. Materials to be sputtered are held on a target plate and the substrate to be coated is placed on a substrate holder in close proximity to the target. When the RF power is applied between the target and substrate, electric field is created from substrate to target. Ar gas is ionized due to the

collisions between the electrons coming from the power supply and argon atoms and plasma is generated. Magnetic field is created by magnets located under the target. Electrons are trapped on the surface of target by magnetic field to increase the collisions and to keep the plasma going continuous. Ionized argon atoms move through the target by means of electric field. They give their energy to target atoms in order them to cause to move to the substrate surface.

A Tecport sputtering system was used for deposition of high-*k* dielectrics. Thin film of dielectric materials namely Hafnium oxide (HfO_2), Aluminium oxide (Al_2O_3), Titanium oxide (TiO_2) and Tantalum (Ta_2O_5) were prepared in RF (13.56MHz) magnetron system with target of respective material. The films were deposited on piranha cleaned, HF dipped samples loaded for sputtering. The sputtering of dielectric materials was carried out at 150W RF power with Ar environment with pressure 2.2×10^{-2} mbar. The deposition was carried out at room temperature and no external substrate heating was provided for deposition. Table 1 gives the details of used process parameter for dielectric deposition with measured thickness. The sputtered dielectric substrate was then cut in to small pieces of sizes 1cm×1cm for further experiments. The parameters given in Table 4.1were optimized for obtaining the superhydrophobic surface after a number of experiments. For the process time of 30 min kept constant, chamber pressure also kept at 2.2×10^{-2} mbar, the thickness of deposited film with variation on different samples are given in Table 4.1.

Table 4.1: Deposition parameter details for high-k dielectric materials [19]

Materials	Chamber Pressure (mbar)	Process Time (Minutes)	Dielectric constant (*k*)	Measured Thickness (nm)
HFO_2	2.2×10^{-2}	30	25	120.6±3
Al_2O_3	2.2×10^{-2}	30	9	120.4±3
Ta_2O_5	2.2×10^{-2}	30	26	336.4±3
TiO_2	2.2×10^{-2}	30	80	76.4±3

4.2.2.3 *Plasma texturing of dielectric materials*

Both, low-*k* and high-*k* deposited surfaces were textured by plasma texturing method. Gas plasma textured processes (glow discharges) are extensively used for increasing the surface roughness and modify hydrophobicity of organic and inorganic materials. The main advantage of this versatile technique is that it is confined to the surface layer of a material without affecting its bulk properties. Moreover, it is a dry (solvent free), clean and time-efficient process with a large variety of controllable process parameters (e.g. discharge gas, power input, pressure, textured time) within the same experimental setup.
We conducted experiments for texturing of dielectric surfaces by the use of plasma surface textured in a fluorinated environment. An empirical investigation of the various parameters that affect the results of the plasma textured such as gas composition, duration of plasma, effect of RF power etc. was carried out the surface modification process. The process gas is introduced into the plasma chambers at moderately low pressures (10-50 mtorr) at 50W of RF power. When RF energy is supplied to the electrode pair of the plasma chamber, it accelerates stray electrons, increasing their energy to the limit where they can break chemical bonds in the process gas and generate additional ions and electrons. The duration of the RIE process was restricted to 60 sec.

4.2.2.4 *Deposition of OTS SAM on textured dielectrics*

In order to form high quality SAM it is very important to ensure a high level of cleanliness to minimize contamination. The Octadecyltrichlorosilane (OTS) SAM was deposited on all untextured and plasma textured oxide surfaces. Before OTS deposition samples were dehydrated at 110°C for 20 minutes. In the meantime solution was prepared in glove box in argon environment with mixing of 40 ml toluene and 1% of OTS solution to allow the OTS uniformly self-assembles on the textured surfaces. After dehydration, samples were dipped in prepared solution for 2 hours without any disturbance in argon environment. After 2 hours, samples were rinsed with toluene and rinsed samples were then dried in Nitrogen.

4.2.2.5 *Characterization tool*

All type of textured oxide surface was characterized for properties like contact angle, surface roughness and chemical properties using the Raman and XPS spectroscopy. In order to investigate their wettability behaviour, we characterized the different aspect of

the surfaces by different tools. The prepared silicon surfaces were characterized by atomic force microscope (AFM) BRUKER to obtain the information on topography of the textured and OTS SAM modified textured silicon surface. The surface roughness measurements for untextured, textured and OTS modified textured surfaces with corresponding rms roughness were obtained with AFM in tapping mode. The static water contact angles on all samples were recorded using contact angle goniometer (data physics) under ambient condition ($21^{o}\pm2^{o}C$) and relative humidity of 48-50% with deionized water. The details of tool are given in Appendix-A.

4.3 Results and Discussion

Effect of surface texturing on wetting properties were studied by comparing the surface topography, WCA of the textured oxide surfaces with OTS SAM modified oxide surfaces. The chemical properties after OTS SAM modification were studied using the Raman spectra and XPS results.

4.3.1 Surface topography by AFM/SEM

The surface morphologies of samples were observed by a BRUKER Dimension icon scan asyst atomic force microscope (AFM) in tapping mode as discussed in pervious section.

4.3.1.1 *Untextured OTS modified oxide surface*

The surface roughness measurements on all type of oxide surfaces before and after the OTS modification are shown in Figure 4.1.The roughnes value shown are averaged out value of measurment taken at five different sites of 4-5 samples of each type. It is observed that Al_2O_3 gives the maximum roughness 0.74±0.2 nm as compared to other oxide surfaceswhere as the SiO_2 which is having the minimum roughness 0.19±0.2 nm as compared to other dieletrics shown in Figure 4.1(a). The surface roughness values for other oxides was 0.27±0.2 nm, 0.34±0.2 nm, 0.30±0.2 nm and 0.19±0.2 nm for HfO_2, TiO_2, Ta_2O_5 and SiO_2 respectively. The corresponding surface morphologies are shown in Figure 4.2(a). The Figure 4.2(a1) for HfO_2 shows very small spikes on the surface. The Figure 4.2(a2) gives the surface morphology for Al_2O_3 which indicates the spikes are larger as comapred to HfO_2 and which increases the surface roughness. The Figure 4.2(a3) shows the surface morphology for TiO_2 which also shows the smooth

surface as compared to HfO_2 and Al_2O_3. The Figure 4.2(a4) shows the surface topography for the Ta_2O_5. It is observed from Figure 4.2(a4) that the untreated surface of Ta_2O_5 is smooth in comparison to other dielectric materials. The Figure 4.2(a5) shows the surface topogrpahy for the SiO_2 surface. The surface of the SiO_2 is very smooth as compared to all other oxides surfaces.

It may be noted that the surface roughness increased in all the samples which were subjected to OTS modification as shown in Figure 4.1(b). For example, the rms roughness of untextured HfO_2 0.27±0.1 nm increased with OTS SAM to 17.8±2nm. This is attributed to the formation of islands on oxide surface after OTS SAM. This is illustrated from surface morphology image in Figure 4.2(b1) with OTS modification. The formation of island on surface can be alsobe seen from SEM image shown in Figure 4.2(c1). In similar manner the surface roughness for other dielectric were also increased. Figure 4.1(a) shows the rms roughness of untextured Al_2O_3 was 0.74±0.2nm (which is maximum as compared to other untextured oxides) also increased to 11.7±0.2 nm after OTS SAM. Where as for both TiO_2 and Ta_2O_5 not much change in rms roughness value was observed after OTS SAM modification. The rms roughness of TiO_2 changed from untextured surface value of 0.34±0.2 nm to 12.7±0.2 nm and Ta_2O_5 changedfrom 0.30±0.2 nm to 13.8±0.2 nm.The rms roughness after OTS modification also increased for SiO_2 surface from 0.19±0.2 nm to 18.2±0.2 nm.

The corresponding surface morphology after OTS SAM modification of other oxide surfaces are shown in Figure 4.2(b2-b5). The Figure 4.2(b1) shows the surface morphology for the HfO_2 which indicates the formation of islands on the surface. The Figure 4.2(b2) shows the morphology for Al_2O_3 which also shows the formation of islands but formation of islands is more dense as comapred to $HfO_2$and provides smooth surface.The Figure 4.2(b3) for TiO_2 and Figure 4.2(b4) for Ta_2O_5which indicates the formation of islands after depsotion of OTS SAM. The Ta_2O_5 indicates more spikes onthe surfaces which increases the roughness as compared to TiO_2. The Figure 4.2(b5) shows the surface morphology for SiO_2 which indicates more islands formation as compared to other dielectric surfaces.The corresponding SEM images are also shownin Figure 4.2(c1) for HfO_2, 4.2(c2) for Al_2O_3, 4.2(c3) for TiO_2,4.2(c4) for Ta_2O_5 and 4.2 (c5) for SiO_2 respectively.

4.3.1.2 *Plasma textured OTS modified oxide surface*

The plasma texturing of oxide surfaces was carried out using fluorine (SF_6) based plasma. The parameter for plasma texturingwere choosen to have minimum effect on topography and achieve significant change in wettability. The rms roughness values for plasma textured oxide surface are shown in Figure 4.1(b). The plasma texturing was carried out for 60 sec. After plasma texturing the rms roughness for oxide (HfO_2) surface increased from 0.27±0.1 nm (untextured surface) to 2.47±0.5 nm as shown in Figure 4.1(b) where not much change was observed for rms roughness of TiO_2 and Ta_2O_5 oxide surface. The observed value of rms roughness for TiO_2 (after plasma) changed from 0.29±0.1 nm (untextured surface) to 0.34±0.1 nm and for Ta_2O_5 changed from 0.25±0.1 nm (untextured surface) to 0.30±0.1 nm resspectively shown in Figure 4.1(b).The surface roughness was 0.74±0.1 nm for untextured Al_2O_3 and changed to 2.5±0.1 nm for plasma textured surface whereas the SiO_2 roughness also increased from 0.19±0.1 nm to 0.29±0.1 nm after plasma texturing.The corresponding surface morphologies are shown in Figure 4.3(a1-a5) for HfO_2, Al_2O_3, TiO_2,Ta_2O_5, and SiO_2 respectively.

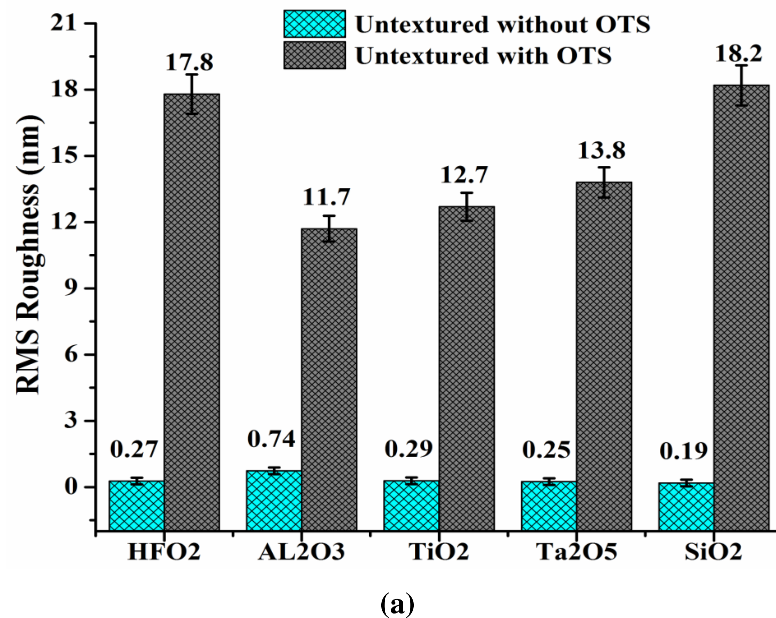

(a)

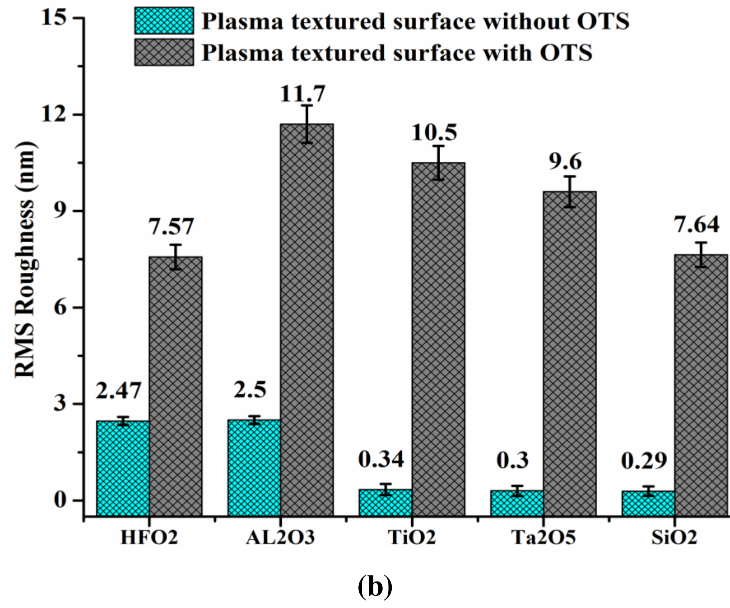

(b)

Figure 4.1: Surface roughness by AFM (a) Plasma untextured dielectric surface with and without OTS SAM (b) Plasma textured dielectric surface with and without OTS SAM

Further, the plasma textured oxide surfaces were deposited with OTS SAM.The change in rms roughness value was observed to be insignificant for TiO_2 and Ta_2O_5 after the plasma texturing but after OTS modification roughness the value increased substantially. The value of rms roughness after OTS deposition on plasma textured oxide surface are shown in Figure 4.1(b).Comparing roughness with and without OTS modified oxide surface, rms roughness increased with OTS SAM, for example the roughness of HfO_2 (plasma textured) increased from 2.47±0.5 nm to 7.57±0.5 nm as shown in Figure 4.1(b). The corroseponding surface morophologies are shown in Figure 4.3(b1).

From Figure 4.1(b) it can be observed that the roughness for the other oxide surfaces also increased. The change in rms roughness value of Al_2O_3 incresed significantlly from 2.5±0.1nm to 11.7±0.1nm.The corroseponding surface morphology is shown in Figure 4.3(b2). The rms roughness for TiO_2 increased from 0.34±0.1 nm (plasma textured) to 10.5±0.5 nm which is less as compare to untextured OTS SAM modified surface (12.7±0.5nm). The corroseponding surface morphology shown in Figure 4.3(b3).The rms roughness of Ta_2O_5 after OTS modification also increased from 0.30±0.1 nm to 9.6±0.5 nm which is less from untextured OTS SAM modified roughness (13.8±0.5 nm) and is given in Figure 4.1(b).The corroseponding surface morphology shown in Figure 4.3(b4). The OTS SAM modifcation on plasma textured surface make

surface smooth as compared to untextured OTS SAM modify surface. The roughness after plasma textured increased from 0.19±0.1 nm to 0.29±0.1 nm and after OTS modification the roughness incaresed from 0.29 ±0.1 nm (plasma textured) to 7.64±0.1 nm which is less as compared to untextured OTS modified SiO_2 surface. The corroseponding surface morphology is shown in Figure 4.3(b5).

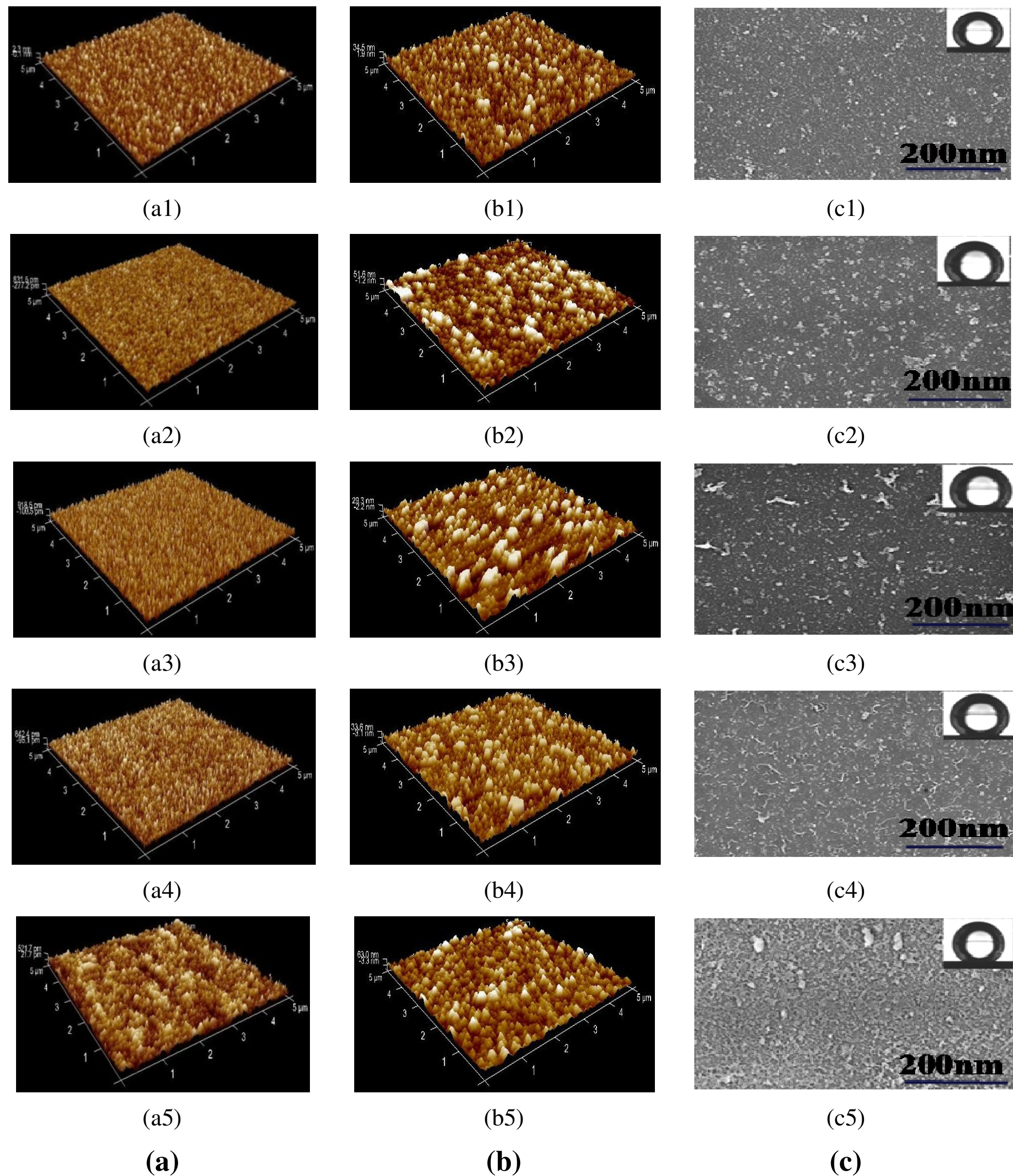

Figure 4.2: Atomic force morphology (a) for untextured oxide surface (b) for OTS modify untextured oxide surface (c) Scanning electron microscope images for untextured OTS modify oxide surface with contact angle inset (1) HfO_2 (2) Al_2O_3 (3) TiO_2 (4) Ta_2O_5 (5) SiO_2

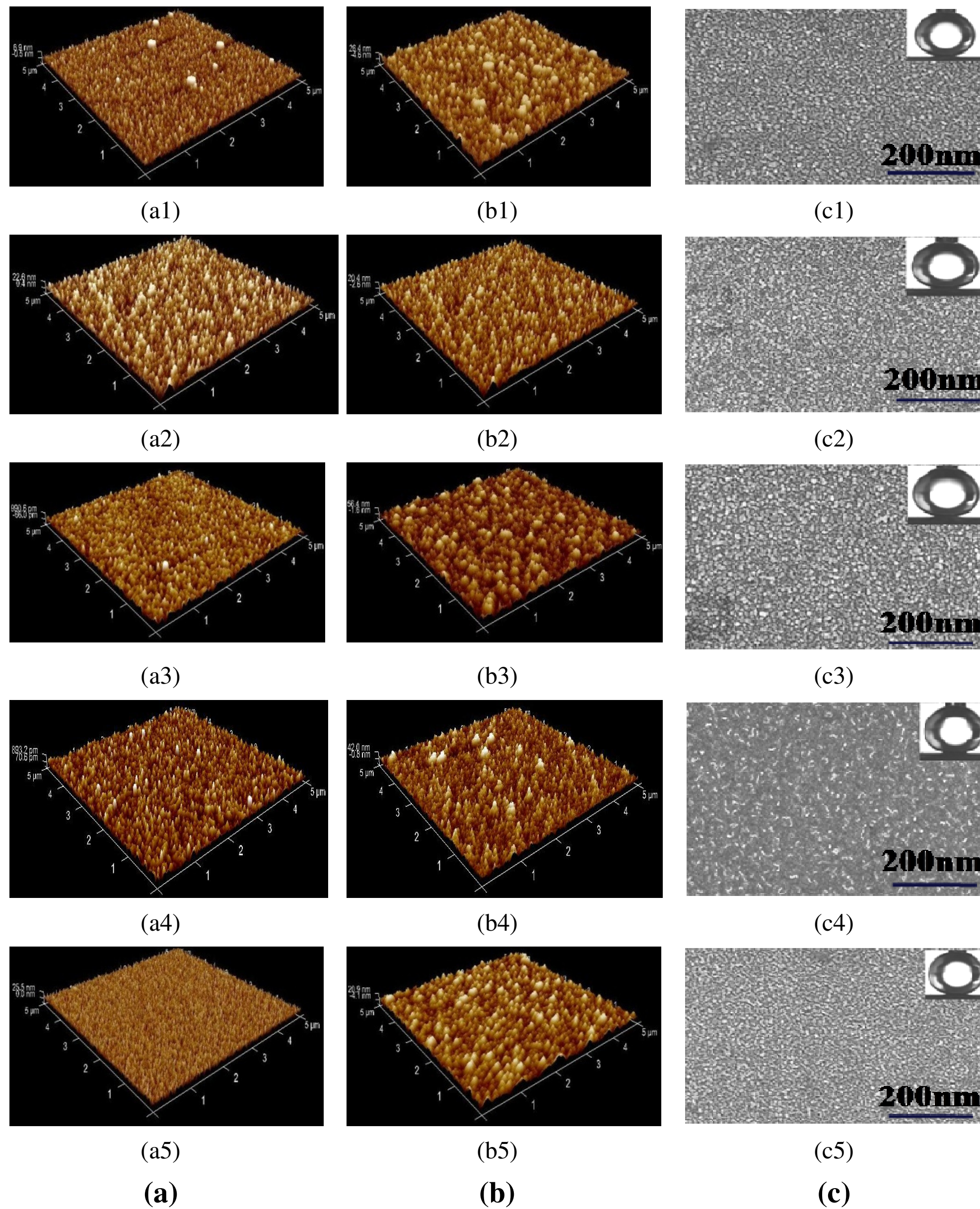

Figure 4.3:Atomic force morphology (a) for plasma textured oxide surface (b) for OTS modify plasma textured oxide surface (c) Scanning electron microscope images for plasma textured OTS modify oxide surface with contact angle inset (1) HfO_2 (2) Al_2O_3 (3) TiO_2 (4) Ta_2O_5 (5) SiO_2

The change in roughness is due to formation of island on the surface as is visible from the SEM images in Figure 4.3(c) in sequence of (c1-c5). Figure 4.3(c1) shows the SEM image of HfO_2 oxide surface. From the Figure 4.3(c1) it is observed that formation of island which is smooth and there is dense formation of monolayer. From Figure 4.3(c2), showing the SEM image of Al_2O_3, the formation of smooth and dense monolayer is

observed. Figure 4.3(c3) shows the SEM images of TiO_2 oxide surface and Figure 4.3(c4) shows the SEM image of Ta_2O_5 surface which indicate the formation of smooth and dense monolayer. Figure 4.3(c5) SEM image of the SiO_2 surface indicates the uniform and dense monolayer deposition. The observations indicate that denser and smooth monolayer forms after plasma texturing on oxide surfaces in comparison with untextured OTS modified oxide surface.

4.3.2 Contact angle measurement

4.3.2.1 Untextured OTS modified oxide surface

The contact angle (θ_c) of a sessile water drop on a trichlorosilane SAM is an appropriate and conventional criteria of SAM quality, a large contact angle indicate hydrophobic and hence dense film. A drop of de-ionized water of 5µl was used to obtain the contact angles on all type of oxide surfaces namely untextured, plasma textured, OTS deposited untextured and OTS deposited textured surface. Measurements were performed with water drop at five different location on each SAM coated samples. The contact angle of unmodified and OTS SAM modified oxide surface are shown in Figure 4.4(a). The contact angle of untextured and unmodified SiO_2 and HfO_2 was observed to be 62.7 ± 2° and 86.0 ± 2° respectively. From Figure 4.4(a) it can be observed that all the oxide surfaces are intrinsically hydrophilic. The observed WCA are 65.1 ± 2°, 75.1 ± 2° and 62.7 ± 2° for Al_2O_3, TiO_2 and Ta_2O_5 respectively.

The WCA of untextured oxide surface increases significantly after modification of OTS SAM. The WCA for modified surface are given in Figure 4.4(a). The WCA of SiO_2sample was $62^o \pm 7^o$ before OTS modification which increased to $132^o \pm 4^o$ after OTS SAM modification. There was no significantly change observed after the OTS SAM modification for other oxide surfaces. The changed in contact angle was $131.6^o \pm 2^o$ for HfO_2, 134.7 ± 2° for Al_2O_3, 132.9 ± 2° for TiO_2, 133 ± 2° for Ta_2O_5 respectively. It can be conclude that the WCA of all untextured OTS SAM modified oxide surfaces (which are hydrophilic i.e. $\theta_c < 90^o$) increases to $>90^o$ with OTS SAM, and thereby lower the wettability of oxide surface making them hydrophilic.

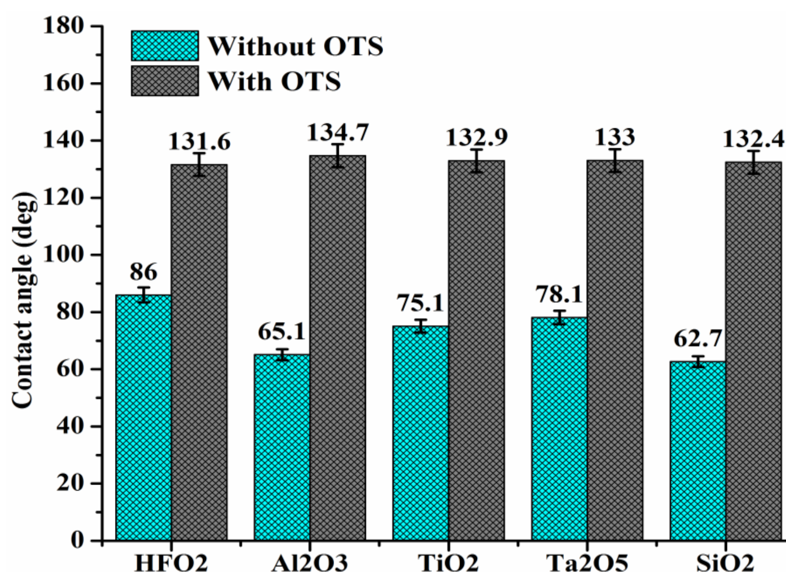

Figure 4.4: Water contact angle for untextured oxide surface with and without OTS SAM

4.3.2.2 Plasma textured OTS modified oxide surface

The effects of plasma texturing on wetting properties were studied by comparing the θ_c of the textured and untextured oxide surfaces before and after OTS SAM modifications. It is seen that in all the cases, after the plasma texturing the contact angle θ_c decrease and make the surface further hydrophilic (θ_c<< 90°) as compared to untextured oxide surface and are given in Figure 4.5. The contact angle of HfO_2surface after plasma reduces to 45.9± 2° from 86.0± 2° that was for untextured surface. The other oxides surfaces the value of contact angle also reduces to 44.6± 2°, 56.9± 2°, 55.5± 2° and 19.5± 2° after plasma texturing as compare to untextured surface 65.1± 2°, 75.1± 2°, 78.1± 2° and 62.7± 2° for Al_2O_3, TiO_2, Ta_2O_5 and SiO_2 respectively. It can be concluded that the surface of SiO_2 become more hydrophilic as compared to other oxide surfaces.

It was observed that the θ_c significantly increased after functionalization with OTS SAM on textured oxide surface and value are given in Figure 4.5. It may be noted that the θ_c on the HfO_2 surface increased from 45.9±2° to only 155.7±2° after OTS SAM modification. The other oxides surface value of contact angle also increased to 160.5±2°, 156.3±2°, 159.2±2° and 157.7±2° after OTS SAM modification on plasma textured surface compared to untextured OTS SAM modified surface which had value of 134.7±

2°, 132.9± 2°, 133± 2° and 132.4± 2° for Al_2O_3, TiO_2, Ta_2O_5 and SiO_2 respectively. The maximum change in contact angle was observed in Al_2O_3 oxide surface. The change in contact angle after OTS modification with plasma textured surface indicates the formation of denser monolayer on the oxide surface.

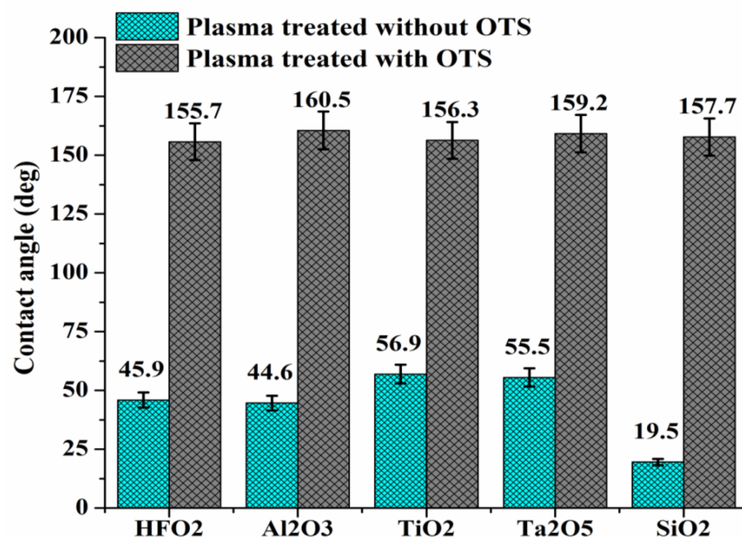

Figure 4.5: Water contact angle for plasma textured oxide surface with and without OTS SAM

4.3.3 Raman spectra

The surface chemistry of different samples was characterized using LAB RAM Raman spectroscopy (The details of the instruments are given in appendix A). The Raman spectra after OTS SAM modified oxide surfaces with and without plasma texturing are shown in Figure 4.6. The spectra of interest at peak location 2850 cm^{-1} and 2880 cm^{-1} are due to stretching of C-H group. The spectra observed for untextured SiO_2 OTS SAM modified oxide surfaces are shown in Figure 4.6(a1). Figure 4.6 shows the spectra of for the other untextured OTS SAM modified oxide surfaces Figure 4.6(a2) for Al_2O_3, 4.6(a3) for HfO_2, 4.6(a4) for TiO_2, 4.6(a5) Ta_2O_5. It can be observed from the spectra that there are no changes were observed in peak location for oxide surfaces.

The Raman spectra were also observed for plasma textured OTS SAM modified oxide surfaces as shown in Figure 4.6(b). By comparison, from Figure 4.6(a) and Figure 4.6(b) there are no changes observed after OTS depositions on untextured and plasma textured oxide surface on chemical bonding on the surfaces. The spectra of interest at peak location 2850 $cm^{-1}$and 2880 cm^{-1} are due to stretching of C-H group. The spectra observed for untextured SiO_2 OTS SAM modified oxide surfaces are shown in

Figure 4.6(b1). Figure 4.6(b) shows the spectra of for the other untextured OTS SAM modified oxide surfaces like Figure 4.6(b2) for Al_2O_3, 4.6(b3) for HfO_2, 4.6(b4) for TiO_2, and 4.6(b5) for Ta_2O_5. It can be observed from the spectra that there are no changes in peak location for oxide surfaces.

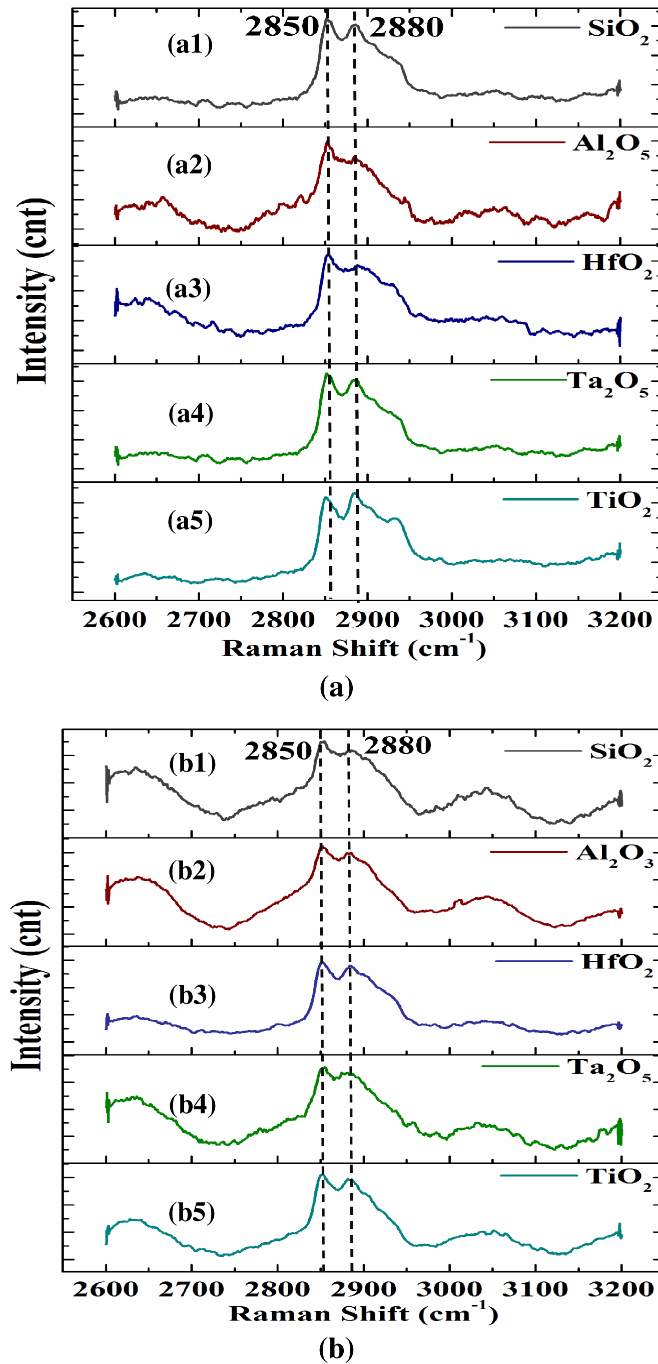

Figure 4.6: Typical Raman spectra of OTS modify (a) untextured surface (b) textured surface

4.3.4 X-ray photoelectron spectra

Figure 4.7 compares the XPS survey scans of the untextured and plasma textured oxide surfaces with an OTS SAM modification. The XPS of OTS SAM modified surfaces were performed with a Kratos Axis Ultra DLD with monochromatic AlKα excitation (1486.6eV). The sample surface was etched by argon ion source to eliminate the surface contamination.

The XPS spectra for OTS SAM modified untextured oxide surface are shown in Figure 4.7(a). The Figure 4.7 (a1) shows the spectra of SiO_2 surface. The modified SiO_2 surface shows the significant peak at 480eV and 280eV corresponding to C-1s and O-1s peak and Si-2p also observed at 180eV.The Figure 4.7 (a2) shows the spectra of HfO_2 surface and same peaks are observed as SiO_2 surface. The intensity of the peaks O-1s and C-1s is less as compared to SiO_2 peaks. The similar peaks are observed for Al_2O_3 as shown in Figure 4.7(a3) and the intensity of the peak O-1s is less as compared to HfO_2 and SiO_2 peaks intensity. Figure 4.7(a4) shows the spectra of Ta_2O_5 and the peak location was observed as others dielectric at 480eV and 280eV corresponding to C-1s and O-1s peak and Si-2p also observed at 180eV. Figure 4.7(a5) shows the spectra of TiO_2 and the similar peak location at 480eV and 280eV corresponding to C-1s and O-1s peak and Si-2p also observed at 180eV. The intensity of O-1s peak is less as compared to the other oxide surface.

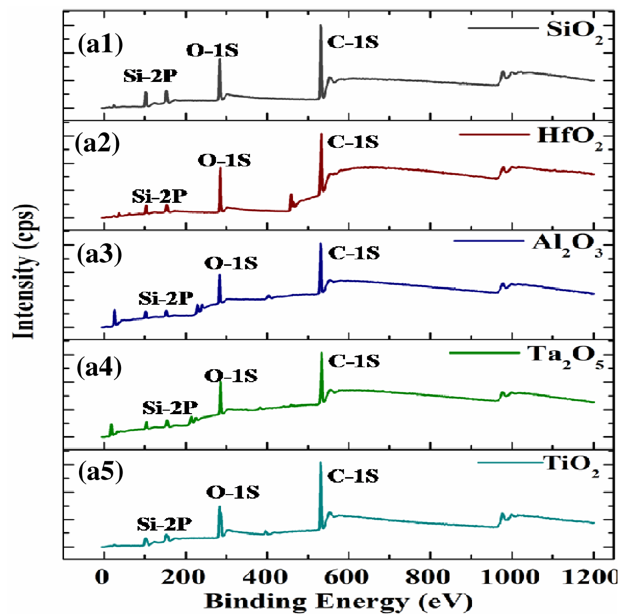

(a)

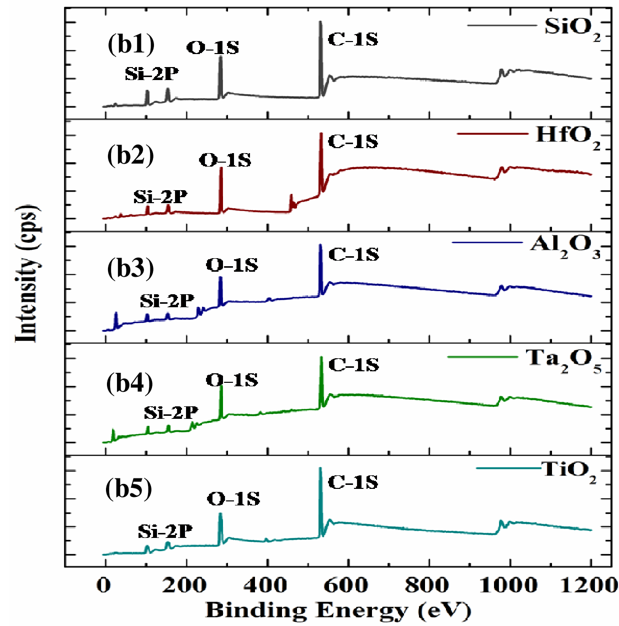

(b)

Figure 4.7: XPS spectra of OTS modify (a) untextured surface (b) textured surface

The XPS spectra for Plasma textured OTS SAM modified oxide surfaces are shown in Figure 4.7(b). The Figure 4.7(b1) shows the spectra of SiO_2 surface. The modified SiO_2 surface shows the significant peak at 480eV and 280eV corresponding to C-1s and O-1s peak and Si-2p also observed at 180eV.The Figure 4.7(b2) shows the spectra of HfO_2 surface and same peaks are observed as SiO_2 surface. The intensity of the peaks O-1s is large as compared to SiO_2 peaks. The similar peaks are observed for Al_2O_3 as shown in Figure 4.7(b3) and the intensity of the peak O-1s is less as compared to HfO_2 and SiO_2 peaks intensity. Figure 4.7(b4) shows the spectra of Ta_2O_5 and the peak location was observed as others dielectric at 480eV and 280eV corresponding to C-1s and O-1s peak and Si-2p also observed at 180eVin which peak intensity is less as compared to other oxide surfaces. Figure 4.7(b5) shows the spectra of TiO_2 and the similar peak location at 480eV and 280eV corresponding to C-1s and O-1s peak and Si-2p also observed at 180eV. The intensity of O-1s peak is large as compared to the Ta_2O_5.There is no evidence for the Chlorine (Cl) peaks from OTS modified surfaces which indicate complete hydrolysis of the trichlorosilane, hence cross-linking and surface reactions between the plasma textured surface and OTS SAM.

4.4 Conclusion

In this chapter, we have demonstrated the assembly of smooth and dense monolayer deposition by combining plasma textured and OTS SAM deposition in low-*k* and high-*k* dielectric oxide surfaces. The monolayer deposition is denser in case apriori plasma texturing is given to oxide surfaces before OTS deposition. We can conclude the following things form above mentioned results:

1. The monolayer deposition was denser in case apriori plasma texturing is given to oxide surfaces before OTS deposition. This is concluded from the AFM and SEM images of the prepared surfaces.

2. The highest water contact angle of θ_c ~160.5^o ±2° was achieved by coating OTS on plasma textured Al_2O_3 dielectric surface.

3. Superhydrophobicity of dielectric surfaces with water contact angle $\theta_c \geq 150.5^o$ was thus far remained unachieved but by methodology presented in this work we have shown to achieve $\theta_c \geq 150.5^o$ invariably on different dielectric surfaces namely, SiO_2, HfO_2, Al_2O_3, Ta_2O_5 and TiO_2. The increase in $\theta_c$is attributed to formation of fluorine trap sites along with -OH traps which contribute to better and denser OTS deposition.

4. After OTS SAM the samples surface chemistry were characterized using the RAMAN. The Raman spectra was observed for each type of prepared samples i.e. cleanser, chemical textured and plasma textured sample. The peak C-H and =(C-H) was observed from the spectra. The presence of hydrocarbon group (C-H) confirm the presence of monolayer on the surface. It can be concluded from the Raman spectra the all type of surfaces shows the same peak and no change was observed in peak location for OTS SAM modify samples.

5. After OTS SAM the samples surface chemistry were also characterized using the XPS. The XPS spectra was observed for each type of samples i.e. cleanser , chemical textured and plasma textured samples.The XPS also confirm the presence of C and O on the OTS SAM modified surface. There was no evidence for the Chlorine (Cl) peaks from OTS modified surfaces confirming the complete hydrolysis of silane in OTS.

References:

1] Jose Bico, Uwe Thiele, David Quere (2002) Wetting of textured surfaces" Journal of Colloids and surfaces, (206) pp. 41-46.

2] Reinhard Lipowsky, peter lentz, Peter S. Swain (2000) Wetting and dewetting of structured and imprinted surfaces, Journal of colloids and surfaces,(161), pp.3-22.

3] Lichao Gao, Thomas J. McCarthy, (2009), Wetting and superhydrophobicity Langmuir, (25), pp. 14100-14104.

4] Y.Yan, N.Gao, W.Barthlott, (2011), Mimicking natural superhydrophobic surfaces and grasping the wetting process: A review on recent progress in preparing superhydrophobic surface , Advance in colloid and Interface surfaces, (169), pp.80-105.

5] Zhi-Qiang Zhu ,Yang Wang ,Qiu-Sheng Liu, Jing-Chang Xie (2012), Influence of Bond Number on behaviour of liquid drops deposited onto Solid substrates, Jl Microgravity Science Technology, (24),pp.181-188.

6] Jian-Lin Liu, Xi-Qiao, Gangfeng Wang and Shou-Wen Yu (2007), Mechanism of superhydrophobicity on hydrophilic substrate, Journal of Physics condensed Matter, (19), 356002-14.

7] X. XU, X. Wang, (2010), Derivation of the Wenzel and Cassie equations from a phase field model for two phase flow on rough surface, Jl. of applied mathematics, 70, no. 8, pp. 2929-41.

8] B.Wang, Y. Zhang, Lei Shi, Jing Li and Zhiguang Guo, (2012), Advances in the theory of superhydrophobic surfaces, Jl. Materials chemistry, (22), 20112-2017.

9] R. Fuestner, W. Barthlott, (2005)Wetting and self-Cleaning properties of artificial superhydrophobic surfaces", Langmuir, (21), 956-961.

10] B. Bhushan, Y. Jung, and K. Koch, (2009), Self-Cleaning Efficiency of Artificial Superhydrophobic Surfaces, Langmuir, (25), 3240-3248.

11] Yewang Su, BaohuaJi, Yonggang Huang, Keh-chih Hwang, (2010) Nature's design of hierarchical superhydrophobic surfaces of a water strider for low adhesion and low energy dissipation", Langmuir, 26(24), 18926-18937.

12] George M. Whiteside, Paul E. Laibinis, (1990),Wet chemical approaches to the Characterization of organic surfaces: Self Assembled Monolayer, Wetttting, and the physical-organic chemistry of the Solid-Liquid interface, Langmuir, 6(1), pp.87-96.

13] Claudia Haensch, Stephanie Hoeppener, Ulrich S. Schubert, (2010) Chemical modification of self assembled silane based monolayers by surface reactions Chemical Society review, (39), 2323-2334.

14] J. Justin Gooding, Freya Mearns, Wenrong Yang, Jingquan Liu, (2003), Self-Assembled Monolayers into the 21st Century: Recent advances and applications, Electroanalysis, 15(2), 81-96.

15] Elena Martines, Kris Seunarine, Hywel Morgan, NikolajGadegaard, Chris D. W. Wilkinson,and Mathis O. Riehle,(2005)Superhydrophobicity and superhydrophilicity of regular nanopatterns, American chemical society Nano Letters, (10), 2097-2103.

16] Yong song, Rahul premachandrannair, Min Zou,Yongqiang Wang, (2009) Superhydrophobic surfaces produced by applying a self-assembled monolayers to Silicon Micro/Nano textured surfaces, Nano Research, (2) 143-150.

17] J. Takeya, T. Nishikawa, T. Takenobu, S. Kobayashi, and Y. Iwasa, C. Goldmann, C. Krellner, and B. Batlogg (2004) Effects of polarized organosilane self-assembled monolayers on organic single-crystal field-effect transistors, Applied physics letters, 85(21), pp. 5078-5080.

18] Nick R. Glass, Ricky Tjeung, Peggy Chan, Leslie Y. Yeo, and James R. Friend, (2011), Organosilane deposition for microfluidics applications, Biomicrofluidics, (5), 036501.

19] Sara A. DiBenedetto, Antonio Facchetti, Mark A. Ratner, Tobin J. Marks, (2009), Molecular Self-assembled monolayers and multilayers for organic and Unconvential inorganic thin-film transistor applications, Advanced Materials, (21), pp.1407-1433.

20] D.K.Aswal, S.Lenfant, D.Guerin, J.V. Yakhmi, D. Vuillaume, (2006), Self Assembled monolayers on silicon for molecular electronics, AnalyticaChemicaActa, 568, 84-108.

21] Luciano Miozzo, AbderrahimYassar, Gilles Horowitz, (2010), Surface engineering for high performance organic electronics devices: the chemical approach", Journal of Materials chemistry, (20), 2513-2538.

22] TommasoBaldacchini, James E. Carey, Ming Zhou, Eric Mazur, (2006) Superhydrophobic surfaces prepared by Microstructuring of Silicon using a Femtosecond Laser", Langmuir, (22), 4917-4919.

23] Yonghaoxiu, Lingbo Zhu, Dennis w. Hess, C. P. Wong, (2007), Hierarchical silicon etched structures for controlled hydrophobicity/Superhydrophobicity" Nano Letters, (7), pp.3388-3393.

24] Wendong Zhang, Xuge Fan, Shengbo Sang, Pengwei Li, Gang Li,Yongjiao Sun, and Jie Hu, (2014) Fabrication and characterization of silicon nanostructures based on metal-assisted chemical etching" Korean Jl. Chemical Engineering, 31(10), 62-67.

25] Xiaocheng Li, Beng Kang Tay, Philippe Miele, Arnaud Brioude, David Cornu, (2009),Fabrication of silicon pyramid/nanowire binary structure with superhydrophobicity,Applied surface science, (255), 7147-7152.

26] Mingji Wang, Kenneth M. Liechti, Qi Wang, J. M. White, (2005), Self-assembled silane Monolayer: Fabrications with Nanoscales uniformity, Langmuir, (21),1848-1857.

Chapter 5

Wetting behaviour of SU8

5.1 Overview

Due to ease of fabrication silicon and polymers materials like poly-dimethyl-siloxane (PDMS), poly-methyl-methacrylate (PMMA), and SU8 are most widely used materials to create a superhydrophobic surface [1-10]. SU8 is the material of choice for Bio-MEMS and microfluidics devices and requires simple processing, less fabrication time and optical transparency [11-14]. SU8 is a negative photo resists and exhibits hydrophobic behaviour with water contact angle (WCA) of approximately 90°. SU8 photo resist consists of EPON^{TM} resin which contains a cyclopentanone, polycarbonate, and photo acid generator [15-16]. The making of SU8 hydrophilic surfaces using oxygen plasma is widely reported in literatures [17-21]. The effect of other plasma such as fluorine (SF_6, CF_4) combined with oxygen plasma had been also investigated for alteration of hydrophobicity of SU8 [22-26] and it has been reported in literature that in SF_6 plasma, SU8 surface become hydrophobic.

In this chapter, we are reporting wetting behaviour of SU8 surface by combination of Octadecyltrichlorosilane (OTS, $Cl_3Si\ (CH_3)_{17}$) self assembled monolayers (SAM) on micro/nano textured surface of SU8. The micro/nano texturing on SU8 surface had been produced by plasma treatment. OTS, self assembled monolayer deposition is one of the most extensively known and widely used ways to influence the chemical and physical properties of various surfaces [27-29]. We have kept the process similar to that we used for treatment of silicon and dielectric in Chapter 3 and Chapter 4 respectively. We have shown that the superhydrophobicity with WCA larger than 150° and hydrophilicity with WCA less than 90° both can be achieved by plasma treated SU8 with and without chemical deposition of organosilane monolayer. To the best of our knowledge, the present work on the wetting property of SU8 by plasma and OTS SAM modification with mask-free generation of superhydrophobic SU8 surfaces is so far the first reporting in available literatures. The experimental details are given in the following sections.

5.2 Experiment Details

From the literature review, the wettability behaviour of SU8 has not been discussed and investigated in detail in published literature when deposited with self-assembled monolayer. We conceived of exploring texturing methods combined with OTS SAM deposition to investigate the change in wettability behaviour of SU8 surface. The experimental details of the combined method and comparison with texturing and SAM deposited surface separately are given in next subsection.

We prepared SU8 polymer surface samples by (i) untextured SU8 (ii) texturing with plasma treatment in the environment of (a) SF_6 (b) O_2 and (c) a combination of SF_6 and O_2 and lastly (iii) modified all textured and untextured samples with deposition of OTS SAM.

5.2.1 Cleaning and sample preparation

First we have taken single side polished silicon (100) wafers with a resistivity of (3-10) ohms-cm, and orientation, <100> were used in all experiments for producing the textured surface. Though the wafers were fresh, they still were not clean, so before starting fabrication process we have to clean the wafer properly. A two step process for cleaning was considered with DI water rinsing and followed by piranha cleaning.

(a) **DI Water rinsing:** Wafers were rinsed with DI water for 10 minutes. A large fraction of ionic impurities present on the wafer surfaces were removed and wafer became free from all ionic impurities except HO^+ and OH^-.

(b) **Piranha cleaning:** After DI water rinsing; the wafers are cleaned using Piranha solution. Piranha solution contains H_2SO_4:H_2O_2 in the ratio of 3:1 by volume. The wafers were dipped in the solution for 15 min. Organic impurities and alkali ions were removed due to strong oxidizing property of the solution. The surface of silicon was passivated with (OH) groups making it hydrophilic. After piranha cleaning the wafers were dipped in dilute HF (HF: DI water: 1:50) at room temperature to remove the native oxide. This was followed by N_2 blow drying. The completion of etching of the native oxide layer was confirmed by the appearance of hydrophobic Si surface.

5.2.2 SU8 coating

After cleaning, the SU8 photoresist was spin coated at 500 rpm for 5 sec followed by 3000 rpm for 30 sec. The coated substrate was then soft baked on a hotplate at 70°C for 2 minutes and then ramped up to 90° C for 2 minutes. The substrate was then allowed to cool down at temperature 25°C. After baking, the SU8 coated silicon substrate was flood exposed to UV light for 10 sec. Immediately after UV exposure, the SU8 substrate was post baked at 70°C for 2 minutes and ramped up to 90°C for 5 minutes. Finally, exposed substrate was developed in SU8 developer (Microchem developer) for 25 sec to make sure that exposed SU8 cross linked appropriate. The SU8 coated substrate was then cut in to small pieces of sizes 1cm×1cm for further experiments. Four sets of samples were used for experimental work, first set was to SU8 coated substrate, second set of samples were prepared by treatment with oxygen plasma, next third set of samples were prepared by SF_6 plasma treatment and fourth set was obtained by combination of SF_6 and O_2 plasma treatment of SU8 surface. All type of sets was further subdivided and half of the samples of each set were deposited with OTS SAM. For each type of surfaces, we prepared 4-5 samples for obtaining an average value to conclude on obtained properties.

5.2.3 Plasma treatments

Plasma treatment of the prepared sample was done using the Reactive ion etching (RIE) plasma source. The plasma treatment of sample surfaces was carried out to achieve a minimum effect on topography of SU8 surface and was done without SU8 patterning. Three different plasma environments were used for changing the surface properties of SU8 surface namely (a) SF_6 (b) O_2 (c) and a combination of SF_6 and O_2. We employed treatment at power of 50 W, with chamber pressure of 100 mtorr. Each plasma treated sample has been assigned a sample ID as S_i (for SF_6), O_i (for O_2) and SO_i (for SF_6 + O_2) plasma, where subscript i stand for the time for which plasma treatment was done. We used i =10, 30, 60 sec. for a study of effect of time of plasma treatment if any was present.

5.2.4 Deposition of OTS SAM

Immediately after the Plasma treatment, OTS SAM deposition was carried out. Few samples of untreated and other three set of plasma treated SU8 surface were used for deposition of OTS SAM. In order to form high quality SAM, it is very important to ensure a high level of cleanliness to minimize contamination which otherwise could lead

to polymerization of the OTS SAM solution. Among many materials available for SAM, OTS is the most common organosilane used in the formation of SAM, mainly because of the fact that in OTS deposition, process is easy, it is readily available, and it forms good, dense layer. The SU8 plasma treated sample were dipped into a toluene/OTS solution to allow the OTS to uniformly self assemble on the sample surfaces, and were held in the glove box for 2 hour to facilitate the SAM. The samples were rinsed sequentially with toluene followed by dried by argon flow. All chemicals used to form self assembled monolayers were purchased from Sigma Aldrich and were used directly without any further treatment. We choose toluene (anhydrous, 99.8%, Aldrich) as the solvent for all of the solutions.

5.2.5 Characterization tool

The surface roughness measurements of untreated, plasma treated and OTS SAM modified surfaces were conducted with Atomic Force Microscope (AFM) BRUKER in tapping mode to obtain the information on topography of the plasma treated SU8 surfaces. SEM image of all surfaces were obtained to qualitatively assess the surface. The static water contact angle on treated surfaces were measured using contact angle goniometer (Data Physics) under ambient temperature ($25\pm1^{o}C$) and relative humidity 48-50% using droplet of 5µl deionized water. The WCA of each sample was measured five times across the sample surface using sessile drop method by dispensing 5µl drop of DI water on the sample surface. The chemical properties after OTS SAM modification were studied using the Raman spectra and XPS results. The details of characterization tool are given in Appendix A.

5.3 Results and Discussion

Effects of surface texturing on wetting properties were studied by comparing the surface topography and WCA of with and without OTS SAM modified SU8 surfaces. The chemical properties after OTS SAM modification were studied using the Raman spectra and XPS results.

5.3.1 Surface topography by AFM/SEM

Few samples from the untreated SU8 and plasma treated SU8 surface with and without OTS SAM modification were used for measurement of surface morphology by AFM and SEM. The details of all type of samples are given in details in subsections.

5.3.1.1 SU8 surface

The surface topography of untreated SU8 surface with and without OTS SAM shown in Figure 5.1 and Figure 5.2 respectively. The untreated SU8 surface exhibits a very smooth surface with an rms roughness value 0.23±0.02 nm as shown in surface morphology AFM images in Figure 5.1(a). The corresponding SEM image of the untreated SU8 is shown in Figure 5.1(b) which exhibits a very smooth SU8 surface. The surface roughness of SU8 surface increases after OTS SAM modification. The roughness after OTS SAM modification increased to 9.7±0.5 nm from 0.23±0.02 nm of unmodified SU8 surface. The roughness increased because of formation of island on the surface and can be visulaized from AFM image and SEM imgae shown in Figure 5.2(a) and Figure 5.2(b) respectively. Form Figure 5.2(a) it can be observed that surface is more rough due to formation of OTS SAM. We can clearly see islands of deposited SAM in Figure 5.2(b). The effects of plasma treatment increase the surface rms roughness and completely changed wettability behaviour of SU8 surfaces which is discussed in next subsections (5.3.1.2, 5.3.1.3, 5.3.1.4).

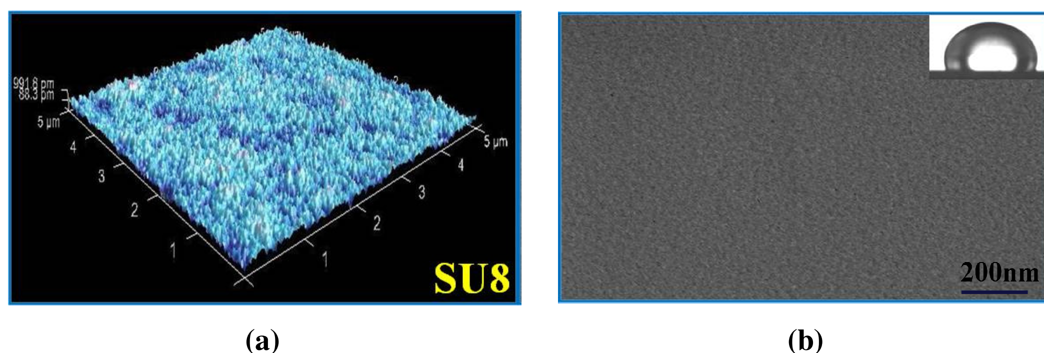

(a) (b)

Figure 5.1: Atomic force morphology wihtout OTS SAM (a) Untreated SU8 surface (b) SEM of untreated SU8

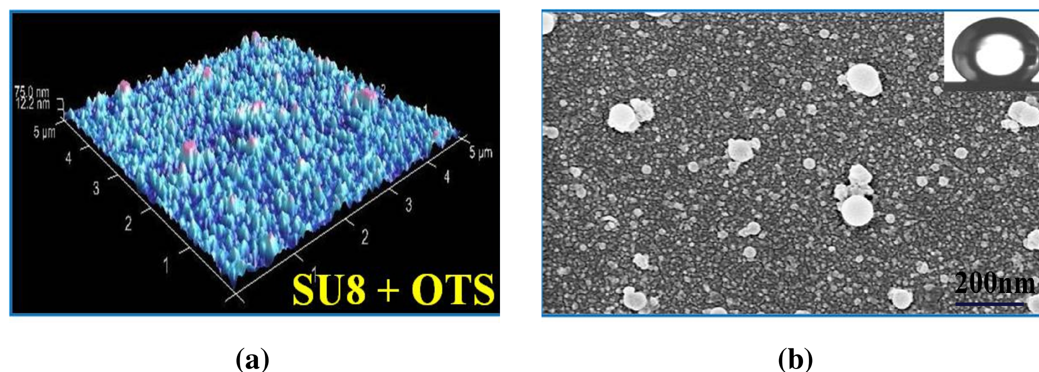

(a) (b)

Figure 5.2: Atomic force morphology with OTS SAM (a) Untreated SU8 surface (b) SEM of untreated SU8

5.3.1.2 Oxygen (O_2) plasma treatment

The oxygen plasma treatment has prominent effect on the surface topography. Oxygen plasma is widely used to enhance the hydrophilic behavior of SU8 [18]. The parameters for the oxygen plasma treatment were chosen to increase surface roughness for improving the hydrophilicity of SU8. The measured surface rms roughness value with and without OTS SAM are given in Figure 5.3. The Figure 5.3(a) shows the value of roughness without OTS SAM and Figure 5.3(b) shows the value of roughness with OTS SAM. The surface roughness was measured after oxygen plasma treatment and the value of rms roughness are shown in Figure 5.3(a) as bar chart for different time of plasma treatment. From Figure 5.3(a), it can be observed that with plasma treatment time 10 sec to 60 sec the roughness value of SU8 surface increased and the rms roughness of the surface changed from 0.23±0.02 nm untreated SU8 to 0.26±0.02 nm, 0.60±0.02 nm and 1.77±0.5 nm depending on the plasma duration as shown in Figure 5.3(a).

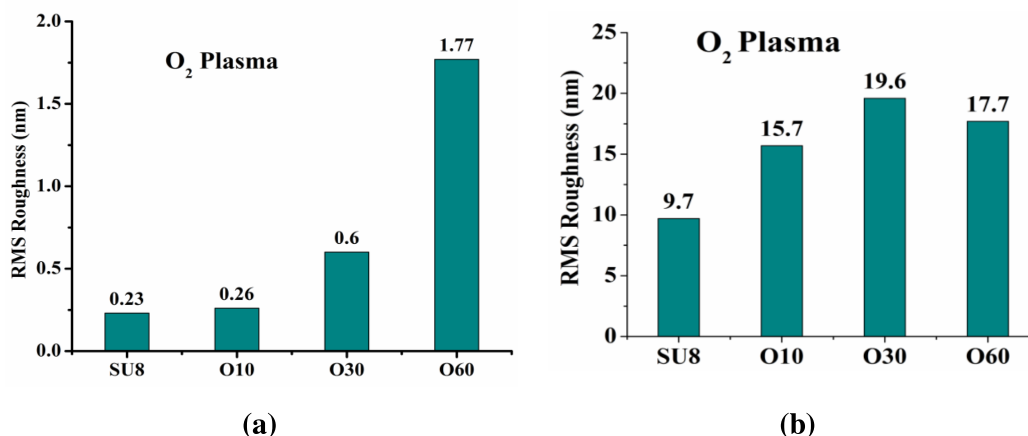

(a) (b)

Figure 5.3: Atomic force morphology (a) untretaed SU8 surface without OTS SAM (b) Plasma treated OTS modify SU8 surface

The corresponding surface topography by AFM are illustrated in Figure 5.4 (a) in sequence of (a1) for O10 (a2) for O30 (a3) for O60 respectively. Figure 5.4(a1) for the O_2 plasma treatment for 10 sec shows the rougher surface as compared to untreated SU8. Figure 5.4(a2) for 30 sec plasma treatment shows creation of more spikes on the surfaces as compared to O10 plasma treatment and untreated SU8 surface. From Figure 5.4(a3) shows the O_2 plasma treatment for 60 sec in which the density of spikes increased on the surface which makes the surface more rough as compared to other plasma treatments. Corresponding SEM images are shown in Figure 5.4(b). The Figure 5.4(b1) shows SEM

image for the treatment for 10 sec which exhibit a rough surface as compared to untreated SU8. The Figure 5.4(b2) shows the plasma treatment for 30 sec and the surface showed moderate change in surface topography as compared to oxygen plasma treated SU8 surface for 10 sec (O10). The oxygen plasma treatment for 60 sec (O60) as shown in Figure 5.4(b3) exhibits significant changes in the surface topography as compared to oxygen plasma treated surfaces for O10 and O30. The treatment with oxygen plasma led to roughing the surface and produced very high wettability.

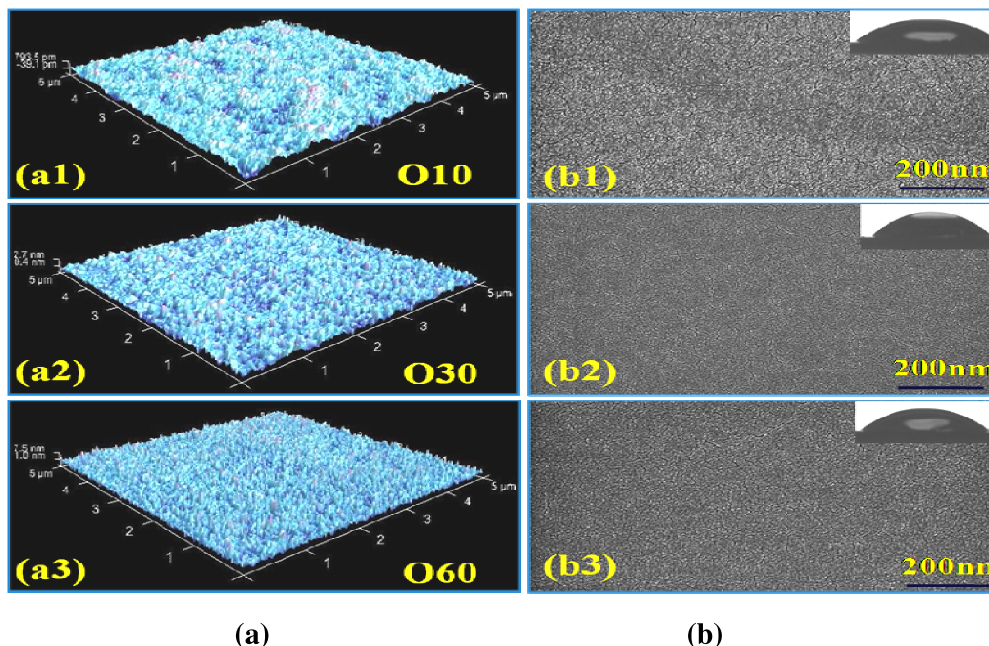

(a) **(b)**

Figure 5.4: Oxygen plasma treated SU8 surface (a) Atomic force morphology (a1) O10 (a2) O30 (a3) O60; (b) Scanning electron microscope images (b1) O10 (b2) O30 (b3) O60

The OTS SAM deposition further increased surface roughness for which the value are given in Figure 5.3(b). It was observed that, the rms roughness value of OTS deposited on O_2 plasma treated SU8 surface increased from 0.26±0.02 nm, 0.60±0.02 nm and 1.77±0.02 nm to 15.7±2 nm, 19.6 ±2 nm and 17.7± 2 nm with different time duration respectively as illustrated in Figure 5.3(b) respectively. The corresponding surface topography by AFM are illustrated in Figure 5.5(a) in sequence of 5.5(a1) for O10, 5.5(a2) for O30, 5.5(a3) for O60 respectively. From Figure 5.5(a1) for the O_2 plasma treatment for 10 sec it is observed that the surface is rougher as compared to OTS SAM modified untreated SU8 surface. The Figure 5.5(a2) for 30 sec plasma treatment exhibits creations of more islands on the surfaces as compared to O10 plasma treatment. Figure 5.5(a3) shows the O_2 plasma treatment for 60 sec in which the density of islands on the surface increased

which makes the surface rougher as compared to oxygen plasma treatment for 10sec (O10) and it is less rough as compared to oxygen plasma treatment for 60 sec (O60).

Corresponding SEM images are shown in Figure 5.5(b). Figure 5.5(b1) shows the treatment for 10 sec which exhibit a rough surface as compared to untextured OTS SAM modified SU8 surface. Figure 5.5(b2) shows the plasma treatment for 30 sec and the surface showed moderate change in surface topography as compared to oxygen plasma treated SU8 surface for 10 sec (O10). The oxygen plasma treatment for 60 sec (O60) as shown in Figure 5.5(b3) exhibits significant changes in the surface topography as compared to oxygen plasma treated surfaces O10 and O30. It is clear from the SEM and AFM images that there is dense formation of monolayer on the SU8 and this trend is seen up to 60 sec. of treatment time.

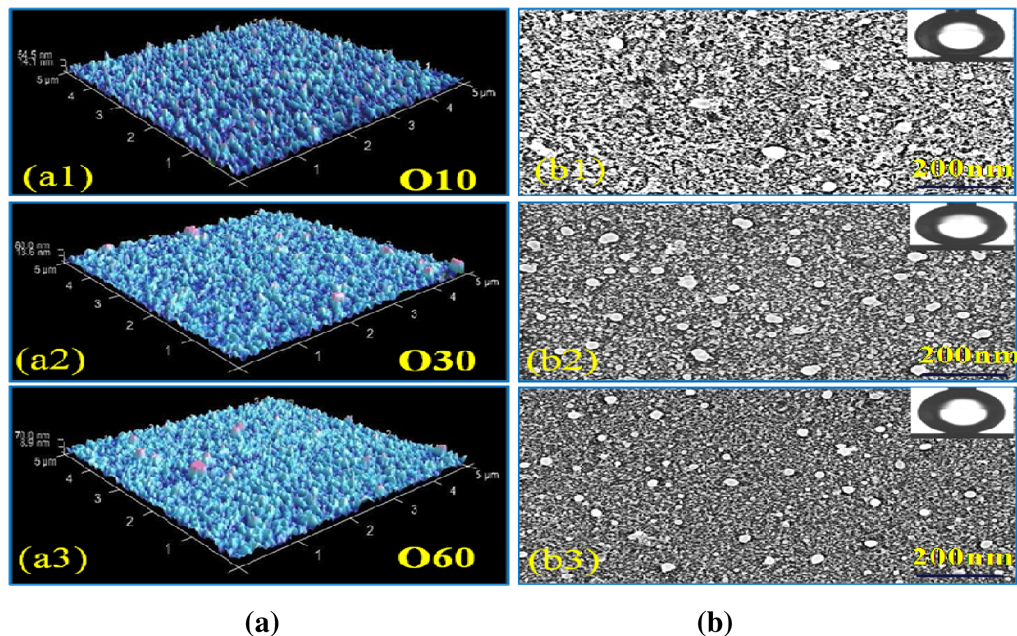

Figure 5.5: Oxygen plasma treated OTS modify SU8 surface (a) Atomic force morphology (a1) O10 (a2) O30 (a3) O60; (b) Scanning electron microscope images (b1) O10 (b2) O30 (b3) O60

5.3.1.3 Fluorine (SF_6) plasma treatment

The fluorine (SF_6) based plasma is widely used and studied for etching of SU8 surface [23]. The fluorine plasma treatment was used by controlling the parameter of RIE etching by number of experiments. The measured rms roughness values with and without OTS SAM are given in bar chart shown in Figure 5.6 for SF_6 plasma treatment with different time durations 10 sec to 60 sec. The SF_6 treatment for 60 sec makes surface

more rough as compared to other treatment time and is illustrated in Figure 5.6 (a). The observed rms roughness changed from 0.23±0.02 nm (untextured SU8) to 0.30±0.02 nm, 0.37±0.02 nm and 0.41±0.02 nm with time duration of 10 sec, 30 sec and 60 sec respectively [Figure 5.6 (a)].

The corresponding surface topography by AFM are illustrated in Figure 5.7(a) in sequence of (a1) for S10 (a2) for S30 (a3) for S60 respectively. Figure 5.7(a1) for the SF_6 plasma treatment for 10 sec shows a rougher surface as compared to untreated SU8. Figure 5.7(a2) for 30 sec plasma treatment exhibits creation of more spikes on the surfaces as compared to S10 plasma treatment. From Figure 5.7(a3) shows the SF_6 plasma treated surface for 60 sec in which the density of spikes on the surface increased which makes the surface rougher as compared to other plasma treatments. Correspondingly SEM images are shown in Figure 5.7(b). The Figure 5.7(b1) shows the treatment for 10 sec which exhibit a rough surface as compared to untreated SU8. The Figure 5.7(b2) shows the plasma treatment for 30 sec and the surface showed moderate change in surface topography as compared to SF_6 plasma treated SU8 surface for 10 sec (S10). The SF_6 plasma treatment for 60 sec (S60) is shown in Figure 5.7(b3) and exhibits significant changes in the surface topography as compared to SF_6 plasma treated surfaces S10 and S30. The treatment with SF_6 plasma led to roughing the surface and assist making the surface hydrophobic.

The OTS SAM deposition further increased surface roughness for which the value are given in Figure 5.6(b). It was observed that, the rms roughness value of OTS deposited on SF_6 plasma treated SU8 surface increased from 0.30±0.02 nm, 0.37±0.02 nm and 0.41±0.02 nm to 12.7±2 nm, 21±2 nm and 21.6± 2 nm with different time duration respectively as illustrated in Figure 5.6(b) respectively. The corresponding surface topography by AFM are illustrated in Figure 5.7(a) in sequence of (a1) for S10 (a2) for S30 (a3) for S60 respectively. From Figure 5.7(a1) for the SF_6 plasma treatment for 10 sec it is observed that the surface is rougher as compared to OTS SAM modified untreated SU8 surface. The Figure 5.7(a2) for 30 sec plasma treatment exhibits creation of more islands on the surfaces as compared to S10 plasma treatment which causes more roughness in S30 sample. Figure 5.5(a3) shows the SF_6 plasma treated surface for 60 sec in which the density of islands on the surface increased which makes the surface rougher as compared to SF_6 treatment for 10 sec (S10) and 60sec (O60). Corresponding SEM images are shown in Figure 5.8(b). Figure 5.8(b1) shows the SEM images of surface treated for 10 sec which exhibit a rough surface as compared to untextured OTS SAM modified SU8 surface and is attributes to formation of more islands on the surface. The Figure 5.8 (b2) shows the

plasma treatment for 30 sec and the surface showed moderate change in surface topography as compared to SF_6 treated SU8 surface for 10 sec (S10). The SF_6 plasma treated surface for 60 sec (S60) is shown in Figure 5.8(b3) which exhibits significant changes in the surface topography as compared to SF_6 plasma treated surfaces S10 and S30 because of formation of more islands on the surface. It is clear from the SEM and AFM images that the formation of monolayer is dense which assists in improvement of hydrophobicity of the SU8.

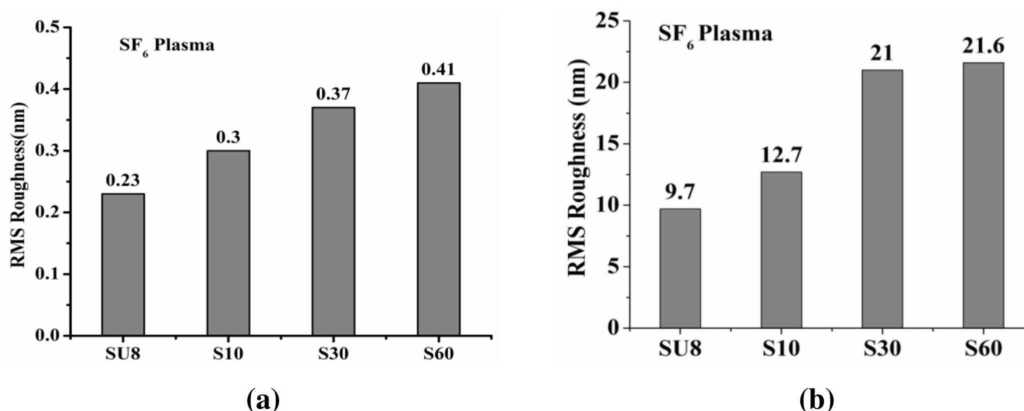

(a) **(b)**

Figure 5.6: Atomic force morphology SF_6 plasma treated SU8 surface (a) without OTS modification (b) with OTS modification

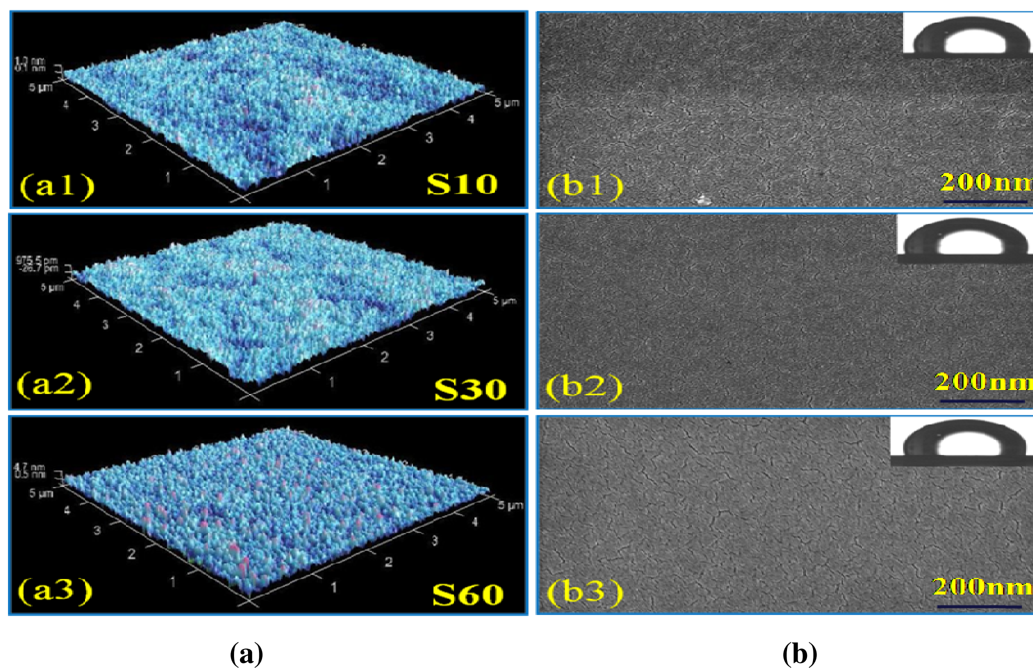

(a) **(b)**

Figure 5.7: Atomic force morphology (a) Untreated SU8 surface (a1) S10 (a2) S30 (a3) S60; Scanning electron microscope images (b) Untreated SU8 surface with contact angle inset (b1) S10 (b2) S30 (b3) S60

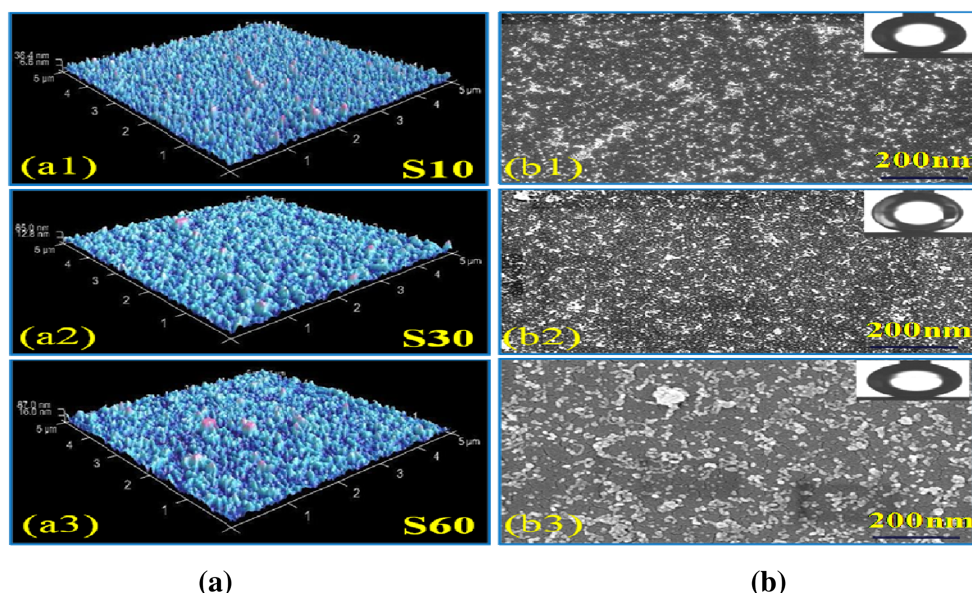

Figure 5.8: Atomic force morphology after OTS SAM modification (a) Untreated SU8 surface (a1) S10 (a2) S30 (a3) S60; Scanning electron microscope images (b) Untreated SU8 surface with contact angle inset (b1) S10 (b2) S30 (b3) S60

5.3.1.4 Fluorine (SF_6) and Oxygen (O_2) plasma treatment

Additions of O_2 (15 sccm) in SF_6 (25 sccm) plasma affect the roughness change response of SU8 because of dilution of the fluorine plasma. The treatment with mixture of fluorine (SF_6) and oxygen (O_2) plasma caused rougher surface as compared to that obtained with O_2, SF_6 and also untreated SU8 surface. The measured rms roughness values with and without OTS SAM are given in bar chart shown in Figure 5.9 for SF_6 plasma treatment with different time durations 10 sec to 60 sec. The rms roughness changed from 0.23±0.02 nm of untreated SU8 to 0.45±0.02 nm, 0.68±0.02 nm and 1.2±0.2 nm with for plasma treatment time duration of 10 sec, 30 sec and 60 sec respectively, as shown in Figure 5.9(a). Obviously, the plasma treatment for 60 sec makes the SU8 surface rougher in comparison to other time durations.

The corresponding surface topography by AFM are illustrated in Figure 5.10(a) in sequence of (a1) for SO10 (a2) for SO30 and (a3) for SO60 respectively. Figure 5.10(a1) for the O_2 + SF_6 plasma treatment for 10 sec shows the rougher surface as compared to untreated SU8. Figure 5.10(a2) for 30 sec plasma treatment creates more spikes on the surfaces as compared to SO10 plasma treatment. From Figure 5.10(a3), it is observed that the O_2 + SF_6 plasma treatment for 60 sec increased the density of spikes on the surface

which makes the surface more rough as compared to other plasma treatments. Corresponding, SEM images are shown in Figure 5.10(b). Figure 5.10(b1) shows the surface treated for 10 sec and exhibit a rough surface as compared to untextured SU8. The Figure 5.10(b2) shows the plasma treatment for 30 sec and the surface showed significant change in surface topography as compared to O_2 and SF_6 plasma treated SU8 surface for 10 sec (SO10). The O_2+SF_6 plasma treatment for 60 sec (SO60) as shown in Figure 5.10(b3) exhibits significant changes in the surface topography as compared to O_2 + SF_6 plasma treated surfaces SO10 and SO30.

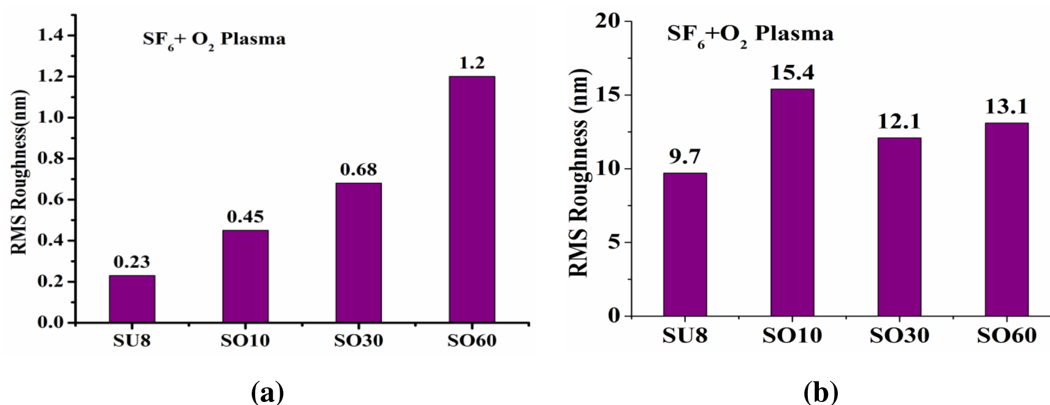

(a) **(b)**

Figure 5.9: Atomic force morphology O_2+SF_6 plasma treated surface (a) without OTS SAM (b) with OTS SAM

The OTS SAM deposition further increased surface roughness for which the value are given in Figure 5.9(b). It was observed that, the rms roughness value of OTS deposited on O_2 plasma treated SU8 surface increased from 0.45±0.02 nm, 0.68±0.02 nm and 1.2±0.02 nm to 15.4±2 nm, 12.1±2 nm and 13.1±2 nm with different time duration respectively as illustrated in Figure 5.9(b) respectively. The corresponding surface topography by AFM are illustrated in Figure 5.11(a) in sequence of (a1) for SO10 (a2) for SO30 (a3) for SO60 respectively. Figure 5.11(a1) for the O_2 + SF_6 plasma treatment for 10 sec shows the rougher surface as compared to OTS SAM modified untreated SU8 surface. Figure 5.11(a2) for 30 sec O_2 + SF_6 plasma treated surface shows which creation of more islands on the surfaces as compared to SO10 plasma treatment. The roughness for SO30 sec is less as compared to SO10 as given in rms roughness values in Figure 5.9(b) and indicates uniform and dense formation of monolayers. Figure 5.11(a3) shows the O_2 + SF_6 plasma treated surface for 60 sec in which the density of islands on the surface increased which though makes the surface less rough as compared to plasma treatment for 10 sec (SO10) but rougher as compared to O_2 + SF_6 plasma treatment for 30 sec (SO30).

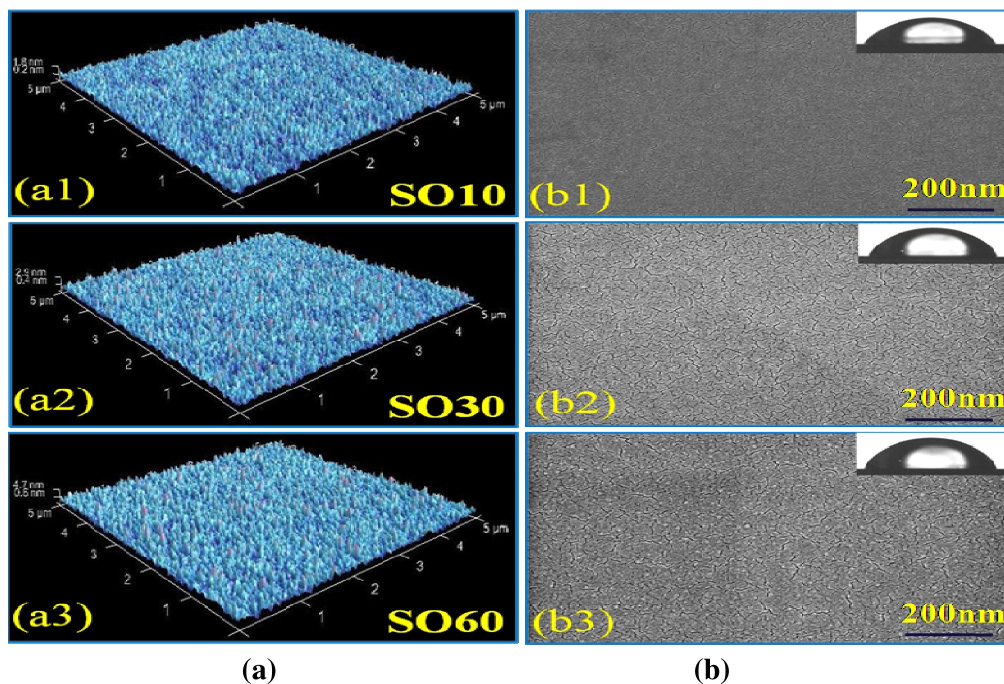

Figure 5.10: Atomic force morphology (a) Untreated SU8 surface (a1) SO10 (a2) SO30 (a3) SO60; Scanning electron microscope images (b) Untreated SU8 surface with contact angle inset (b1) SO10 (b2) SO30 (b3) SO60

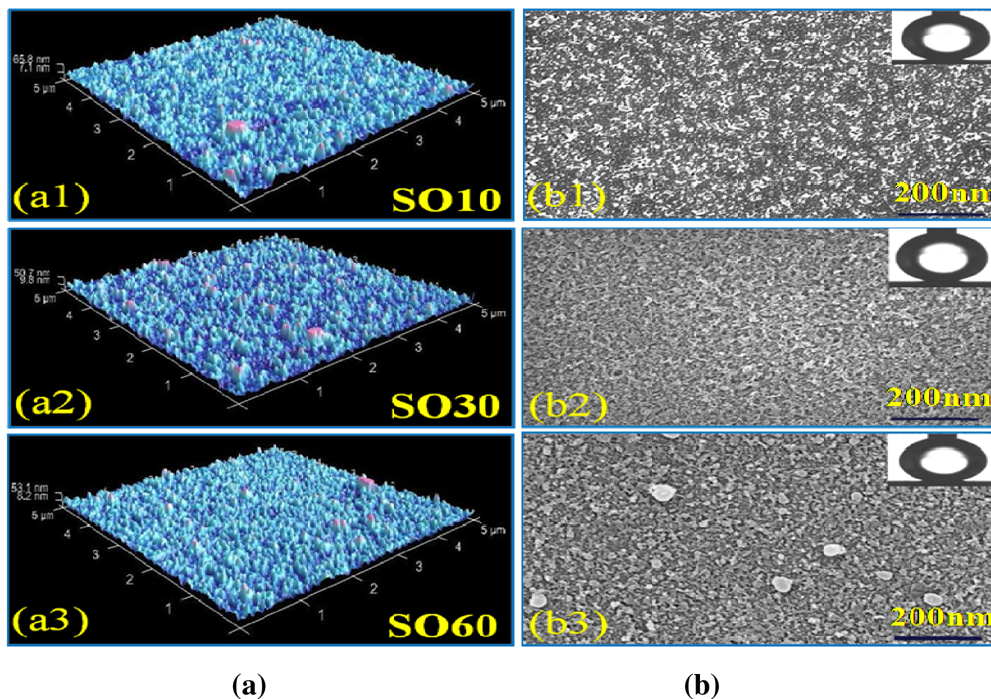

Figure 5.11: Atomic force morphology (a) Untreated SU8 surface (a1) SO10 (a2) SO30 (a3) SO60; Scanning electron microscope images (b) Untreated SU8 surface with contact angle inset (b1) SO10 (b2) SO30 (b3) SO60

Corresponding SEM images are shown in Figure 5.11(b). The Figure 5.11(b1) shows SU8 treated surface for 10 sec which exhibits a rough surface as compared to untextured OTS SAM modified SU8 surface. Figure 5.11(b2) shows the surface plasma treated for 30 sec showing moderate change in surface topography as compared to $O_2 + SF_6$ plasma treated SU8 surface for 10 sec (SO10). The formation of smooth and dense layer formation can be visualized from SEM image 5.11(b2). The $O_2 + SF_6$ plasma treatment for 60 sec (SO60) as shown in Figure 5.11(b3) exhibits significant changes in the surface topography as compared to $O_2 + SF_6$ plasma treated surfaces O10 and O30. It is clear from the SEM and AFM images dense formation of monolayer which assists improvement in hydrophobicity of the SU8.

5.3.2 Contact angle measurements

The change in wetting behaviour was observed by measuring WCA values before and after plasma treatment. We characterized surface modifications with SAM for all plasma treatment and bare SU8 after three and five months and found that not much alteration of the surface wetting behaviour occurred with time elapsed. The measured contact angle value with and without OTS before and after plasma texturing are shown in bar chart in Figure 5.12 for oxygen plasma, Figure 5.13 for SF_6 plasma and Figure 5.14 for SF_6 and O_2 plasma respectively.

5.3.2.1 SU8 surface

The effects of plasma treatment increased the surface rms roughness and completely changed wettability of SU8 surfaces. In published literature, SU8 is reported as hydrophobic with WCA $\approx 90^o \pm 2^o$ [19] and sometimes hydrophilic with WCA $< 90^o$ [25]. From the experiments, as determinant of WCA, untreated SU8 does exhibits hydrophobic property with WCA = $90^o \pm 2^o$ [Figure 5.12(a)]. The WCA angle change significantly after the OTS SAM modification. The WCA for untreated SU8 surface increased from $90^o \pm 2^o$ without OTS SAM to 133 ± 2° with OTS SAM modification and is given in Figure 5.12(b). The effect of oxygen plasma treatment and combination of SF_6 $+O_2$ plasma significantly enhanced the wetting of SU8 surface and became more hydrophilic, whereas SF_6 treatment improved the hydrophobicity of the surface.

5.3.2.2 Oxygen plasma (O_2) with OTS SAM modification

The parameters for the oxygen plasma treatment were chosen to achieve wetting and increased surface roughness for improving the hydrophilicity of SU8. First, the treatment with oxygen led to roughing the surface and induced very high wettability. The water contact angle was measured with and without OTS SAM after oxygen plasma (O_2) texturing shown in Figure 5.12. The Figure 5.12(a) shows the change in water contact angle with plasma treatment of different time durations 10 sec to 60 sec without OTS SAM modification. The Figure 5.12(b) shows the change in water contact angle with plasma treatment of different time durations 10 sec to 60 sec with OTS SAM modifications.

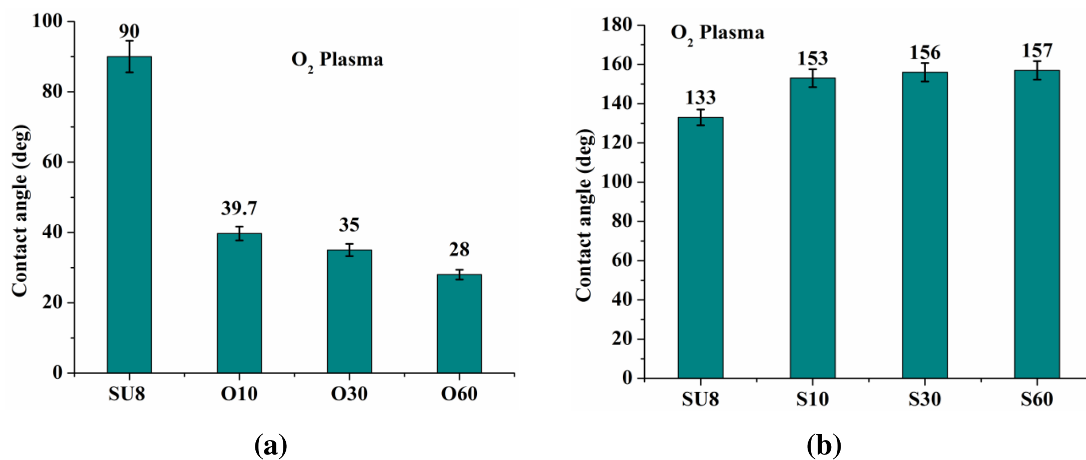

(a) **(b)**

Figure 5.12: WCA of O_2 plasma treated SU8 surface (a) without OTS modification (b) with OTS modification

It can be observed from the Figure 5.12(a) that the SU8 surface becomes more hydrophilic after oxygen plasma texturing. The WCA reduced from 90° for untreated SU8 to 39.7^o±2°, 35° ±2° and 28°±2° with respect to different plasma treatment duration as shown in Figure 5.12(a). It can be concluded that the oxygen plasma treatment for 60 sec make the surface most hydrophilic. Further, plasma texturing can make complete etching of the SU8 surface so we performed the etching for a maximum of 60 sec.

The oxygen plasma treated SU8 surfaces were hydrophilic but after OTS SAM deposition water contact angle increased drastically as shown in Figure 5.12(b). The WCA changed from 39.7^o±2°, 35°±2° and 28°±2° plasma treated SU8 surface without OTS SAM to 153°±2°, 156°±2° and 157°±2° for plasma treatment time duration 10 sec, 30 sec and 60 sec respectively with OTS SAM modifications and are illustrated in Figure 5.12(b). Plasma treatment for 60 sec gives highest WCA but variation was not significant when compared

to other plasma treatment time durations. It can be concluded, that the hydrophobicity can be improved by treating the SU8 even for 10sec plasma treatment duration with OTS deposition.

5.3.2.3 Fluorine plasma (SF_6) with OTS SAM modification

The treatment with SF_6 plasma led to roughing the surface and lowered the wettability of the SU8 surface. The water contact angle was measured with and without OTS SAM after SF_6 plasma treatment shown in Figure 5.13. The Figure 5.13(a) shows the change in water contact angle with plasma treatment of different time durations 10 sec to 60 sec without OTS SAM modification. The Figure 5.13(b) shows the change in water contact angle with plasma treatment of different time durations 10 sec to 60 sec with OTS SAM modifications. It can be observed from the Figure 5.13(a) that the SU8 surface becomes more hydrophobic after SF_6 plasma texturing. The WCA increases from $90^o±2^o$ for untreated SU8 to $100^o±2^o$, $103.5^o±2^o$ and $105.6^o±2^o$ with respect to different plasma treatment duration as shown in Figure 5.12(a). It can be concluded the SF_6 plasma texturing for 60 sec make the surface most hydrophobic.

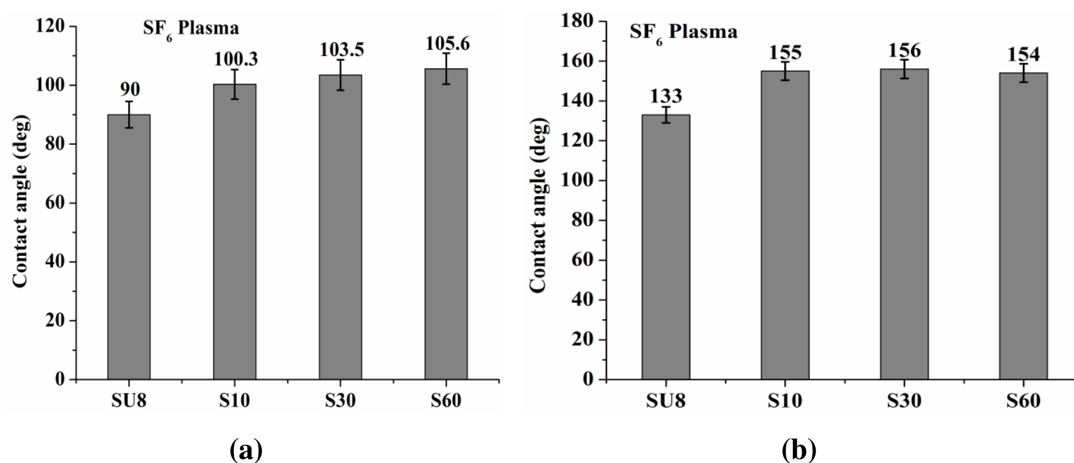

(a) **(b)**

Figure 5.13: WCA of SF_6 plasma treated SU8 surface (a) without OTS modification (b) with OTS modification

5.3.2.4 Fluorine (SF_6) and Oxygen (O_2) plasma with OTS SAM

The plasma treatment with SF_6 plasma does not make much change in the surface roughness but make the surface hydrophobic. The wetting behavior of SU8 surface obtained after SF_6+O_2 treatment are illustrated in Figure 5.14. Figure 5.14(a) shows the change in water contact angle with plasma treatment of different time durations 10 sec to

60 sec without OTS SAM modification. The Figure 5.14(b) shows the change in water contact angle with plasma treatment of different time durations 10 sec to 60 sec with OTS SAM modifications.

It can be observed from Figure 5.14(a) that the SU8 surface becomes hydrophilic after SF_6 $+O_2$ plasma texturing. The WCA reduced from $90^o \pm 2^o$ for untreated SU8 to $62.6^o \pm 2^o$, $65.6^o \pm 2^o$ and $69.6^o \pm 2^o$ with respect to different plasma treatment duration as shown in Figure 5.14(a). It can be concluded the SF_6+O_2 plasma treatment for 10 sec makes the surface most hydrophilic. As compared to O_2 plasma treatment [refer Figure 5.12(a)], the value of WCA increased but remained lower in comparison with SF_6 plasma treated SU8 surface [refer Figure 5.13(a)]. The plasma treatment with SF_6 + O_2 plasma treatment increased the rms roughness as compared to oxygen plasma.

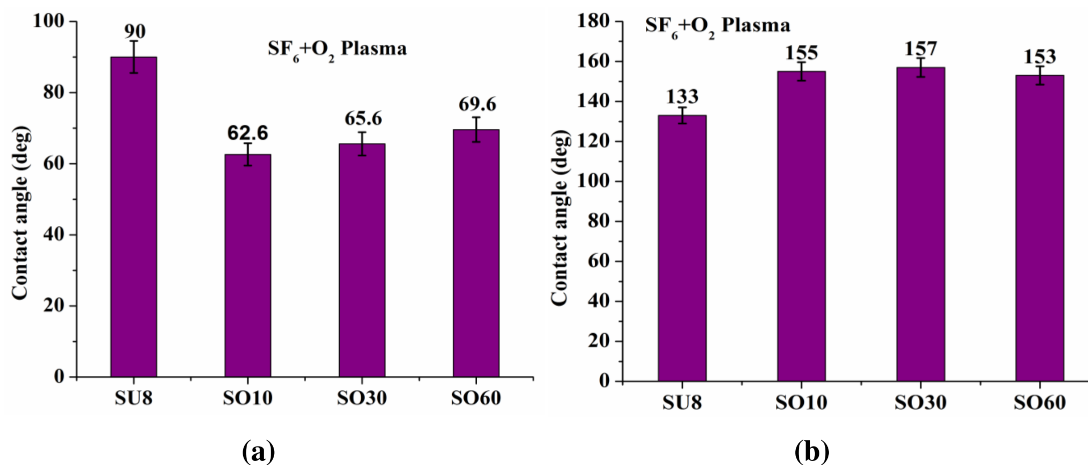

Figure 5.14: WCA of Plasma treated SU8 surface SF_6+O_2 plasma (a) without OTS modification (b) with OTS modification

The measured WCA increased in similar manner to SF_6 treated OTS SAM modified surfaces in superhydrophobic range after deposition of OTS SAM. The SF_6 + O_2 plasma treated SU8 surfaces were hydrophilic but after OTS SAM deposition WCA further increased significantly as shown in Figure 5.14 (b). The WCA $62.6^o \pm 2^o$, $65.6^o \pm 2^o$ and $69.6^o \pm 2^o$ for plasma treatment without OTS SAM modification changed to $155^o \pm 2^o$, $157^o \pm 2^o$ and $153^o \pm 2^o$ for plasma treatment time duration 10 sec, 30 sec and 60 sec respectively with OTS SAM and are illustrated in Figure 5.14(b). Plasma treatment for 30 sec gives higher WCA but variation was not significant when compared to other plasma treatment time durations. We achieved superhydrophobic surface with OTS SAM depositions even with minimum roughness after SF_6 + O_2 plasma treatment.

5.3.3 Chemical behaviour of SU8 surface

To understand the variation in WCA from surface chemistry point of view we analyzed the sample with Raman and XPS to examine the changes in chemical properties of SU8 surface before and after plasma treatment. The few samples with and without OTS SAM were used for studying the chemical behavior of SU8 surface.

5.3.3.1 Raman spectra

Figure 5.15(a) shows the Raman spectra for plasma treated SU8 surfaces and relevant peak details are given in Table 5.1. In Figure 5.15(a) we give the results obtained from Raman spectroscopic measurements of plasma treated SU8 surface without OTS SAM deposition. The Figure 5.15(a) consists of four such spectra pertaining to untreated SU8 surface, oxygen plasma treated SU8 surface (O60), SF_6 plasma treated SU8 surface (S60) and SF_6+O_2 plasma treated SU8 surfaces (SO60). All the spectra shown are for plasma treated surfaces for 60 sec of plasma treatment duration. The relevant peak details for SU8, O60, S60 and SO60 with their bond information are given in Table 5.1. The bond C-S, C-C, C-O-C, CH_2, CH_3, and C=C was observed at different locations as discussed below.

The Figure 5.15(a1) shows the spectra for the untreated SU8. It can be observed from Figure 5.15(a1) that the peak at 690 cm^{-1} and 1300-1680 cm^{-1} were assigned to C-C stretching of respectively cis and trans epoxy group as detailed in Table 5.1. The intensity of C-O and C=O stretching are characteristics of phenol group in SU8. It can be seen from the spectra that a peak exists at 1000-1300 cm^{-1} which is due to formation of C-O-C bond for ether after polymerization and C-S bond is confirming the presence of photo acid generator. Figure 5.15(a2) shows the spectra for the O60. It is easily observed from Figure 5.15(a2) spectra that after oxygen plasma (O60) treatment no major change appeared in the peak values when compared with untreated SU8 [Figure 5.15(a1)]. The C-S bond disappeared after the oxygen plasma as mentioned in Table 5.1. The presence of C-O and C=O bond after oxygen plasma treatment make the surface hydrophilic.

Figure 5.15(a3) shows the spectra for the SF_6 treated plasma. The same peaks were observed for the S60 SU8 surface. The C-S bond disappeared also after the SF_6 plasma as given in Table 5.1 for S60 from 738-762 cm^{-1}. The presence of C-O-C, C-C, and C-S bonds are also observed from the Raman spectra peaks. The C-S bond appeared at location 1250-1300 cm^{-1} as given in Table 5.1 for S60 and other plasma treated sample. The C-S bond which is due to photo acid generator in SU8 is also present. The extra bond of CH_2

and CH_3 are observed at location of 1420-1465 cm^{-1} as illustrated in Table 5.1. The presence of methyl group (CH_3) may be cause of hydrophobicity of the surface. The Figure 5.14(a4) shows the spectra for SF_6 +O_2 plasma treatment. It can be observed that the same peak locations were observed in SO60 as was observed for S60. It can be concluded that, Raman spectra together confirms the peaks of chemical structure (refer Table 5.1) present on SU8 surface before and after plasma treatment.

The chemical properties of SU8 film after OTS SAM on plasma activated were also examined using Raman spectroscopy. The untreated SU8 sample with OTS modification is used as a base sample for Raman measurements. The spectra of after OTS SAM deposited untreated SU8 and plasma treated SU8 surfaces are shown in Figure 5.15(b). Figure 5.15(b) consists of four such spectra for OTS SAM modified surfaces untreated SU8 surface, oxygen plasma treated SU8 surface (O60), SF_6 plasma treated SU8 surface (S60) and SF_6+O_2 plasma treated SU8 surfaces (SO60). All the spectra shows for plasma treated surface for 60 sec of plasma treatment duration. The relevant peak details for SU8, O60, S60 and SO60 with their bond information are given in Table 5.1. The bond C-H, = (CH) was observed at different locations as discussed below.

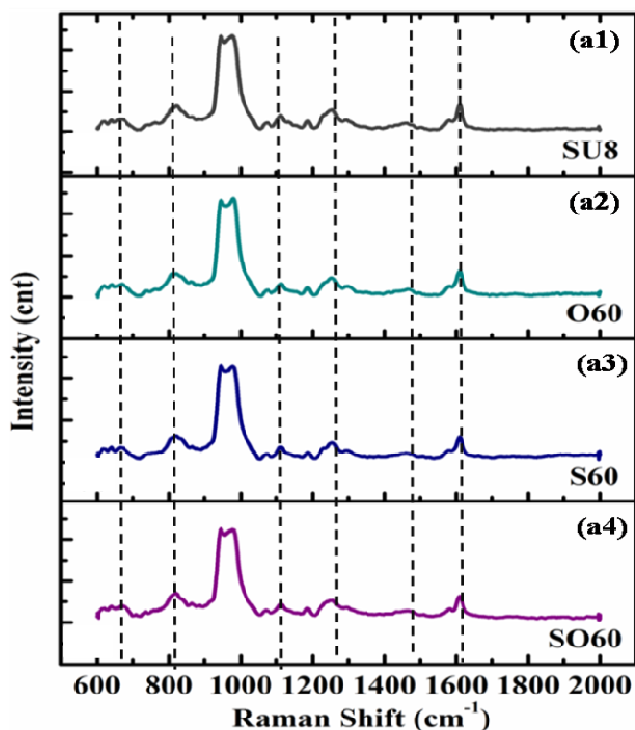

(a)

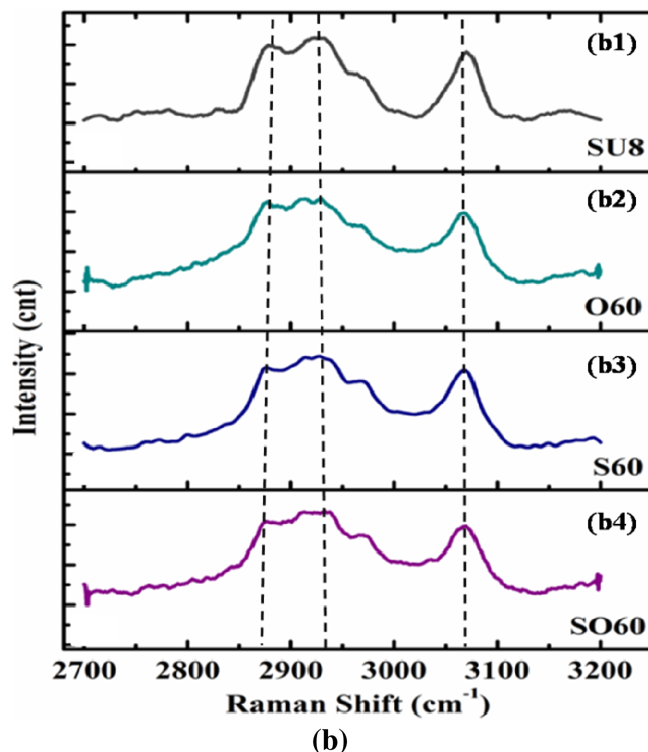

(b)

Figure 5.15: (a) Raman spectra of plasma treated without OTS SU8 surface (b) Raman spectra of plasma treated with OTS SU8 surface (1) bare SU8 (2) O60 (3) SO60 (4) S60

Table 5.1: Raman spectra information of plasma activated SU8 without and with OTS SAM

Peak Values	**SU8- Surface without OTS SAM**			
	SU8	O60	SO60	S60
619-690	C-S, C-C	C-S, C-C	C-S,C-C	C-S aliphatic
738-762	C-S	disappeared	disappeared	disappeared
813-883	C-O-C	C-O-C, O-O	C-O-C, O-O	C-O-C, O-O
943-980	C-O-C	C-O-C	C-O-C	C-O-C
1072	C-O-C	C-O-C	C-O-C	C-O-C
1110-1190	(C-O-C) asym, C-S	(C-O-C) asym , C-S	(C-O-C) asym , C-S	(C-O-C) asym , C-S
1250-1300	C-S, C-C	C-S, C-C	C-S, C-C	C-S, C-C
1420-1465	CH_2, (CH_3)asym	CH_2, (CH_3)asym	CH_2, (CH_3)asym	CH_2, (CH_3)asym
1580	C-C , C=C	C-C , C=C	C-C , C=C	C-C , C=C
1600-1610	C-C	C-C	C-C	C-C
	SU8- Surface with OTS SAM			
2800-3000	C-H	C-H	C-H	C-H
3000-3200	=(CH)	=(CH)	=(CH)	=(CH)

The main spectra of interest at peak location 2844 cm^{-1}, 2948 cm^{-1} are due to stretching of C-H group and are observed in spectra as shown in Figure 5.15(b). The identical peak positions of C-H are observed in all other three plasma treated SU8 as were present in untreated SU8. After oxygen plasma (O60) treatment as in Figure 5.15 (b2), SF_6 (S60) plasma treatment as in [Figure 5.15(b3)) and SF_6 + O_2 (SO60)] plasma treatment as shown in Figure 5.15(b4), no major change appear in the peak values as compared to untreated SU8. Similarly, the observed peak at location 3014 cm^{-1} and 3083 cm^{-1} are due to stretching of peak of =(C-H) in all OTS SAM deposited surface whether plasma untreated or treated SU8 surfaces. There are no changes observed after OTS depositions on untreated and plasma treated SU8 surface on chemical bonding on the surfaces.

5.3.3.2 XPS spectra

Figure 5.16 compares the XPS survey scans of the untreated, chemical and plasma treated oxide surfaces with and without OTS SAM modification. Figure 5.16(a) shows the spectra for untreated SU8 and plasma treated SU8 without OTS SAM deposition. The Figure 5.16(b) shows the spectra for untreated SU8 and plasma treated SU8 with OTS SAM depositions. Figure 5.16(a) consists of four spectra of untreated SU8 surface, oxygen plasma treated SU8 surface, SF_6 plasma treated SU8 surface and SF_6+O_2 plasma treated SU8 surface. All the spectra shown are for plasma treated surface for 60 sec of plasma treatment duration.

Figure 5.16(a1) shows the peaks for untreated SU8. The peaks at location 480 eV and 280 eV were corresponding to O1s and C1s peak. The peak of Sb-3d is also observed at same peak location of O1s at 480 eV. The peak of Si-2p was also observed at l80 eV. Figure 5.16(a2) shows the peaks for oxygen plasma treated SU8 surface (O60) in which also, same peaks C1s, O1s/Sb-3d and Si-2p were observed. The intensity of the Si-2p is higher as compared to untreated SU8 surface. The Figure 5.16(a3) shows the peaks for SF_6 plasma treated SU8 surface (S60). It is observed from the Figure 5.16(a3) the Si-2p peak disappeared and the intensity of the C1s and O1s reduced as compared to O60 and untreated SU8. The fluorine peak was observed at 680eV locations which indicate the presence of fluorine after the SF_6 plasma exposure. The Figure 5.16(a4) shows the spectra for SF_6+O_2 plasma treated SU8 surface. The spectra shows the similar peak C1s and O1s/Sb-3d as observed in SF_6 plasma treated surface. The fluorine peak was also

observed at 680 eV locations for SF_6+O_2 plasma treatment. The intensity of the C1s and O1s also less as compared to O60 and untreated SU8 surface.

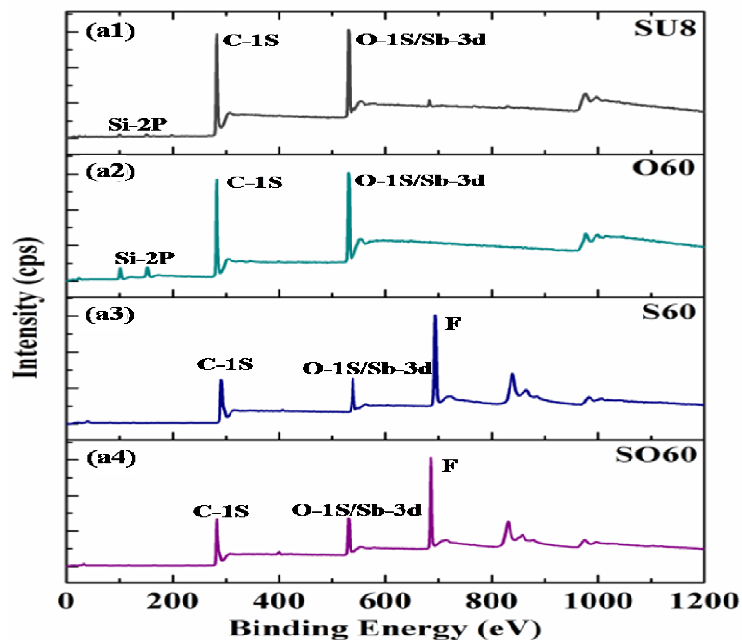

(a)

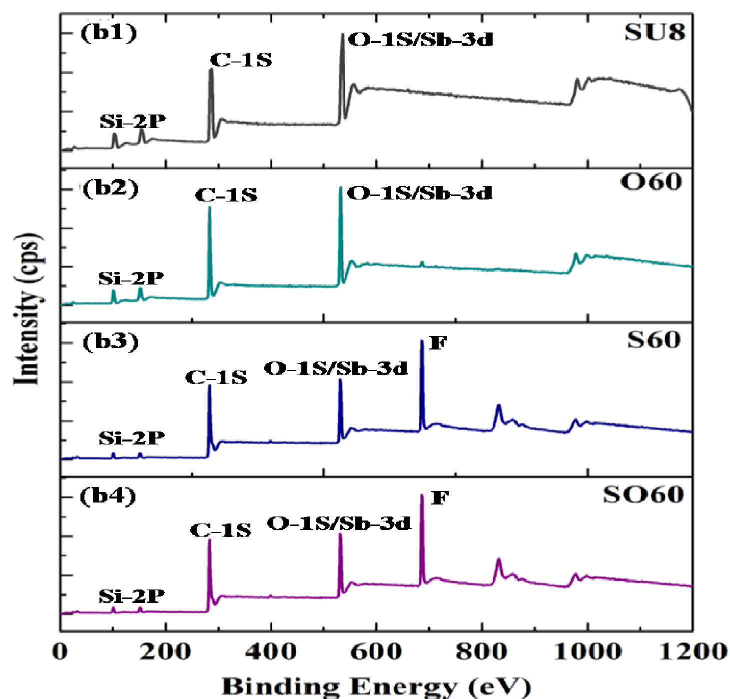

(b)

Figure 5.16: (a) XPS spectra of plasma treated without OTS SU8 surface (b) XPS spectra of plasma activated with OTS SU8 surface (1) bare SU8 (2) O60 (3) SO60 (4) S60

Figure 5.16(b) also consists of four spectra of untreated SU8 surface, oxygen plasma treated SU8 surface, SF_6 plasma treated SU8 surface and SF_6+O_2 plasma treated SU8 surface. The Figure 5.16(b1) shows the spectra for the OTS SAM modified SU8 surface. The peaks at location 480 eV and 280 eV were corresponding to O1s and C1s peak. The peak of Sb-3d was also observed at same peak location of O1s at 480 eV. The peak of Si-2p was also observed at l80 eV. The Figure 5.16(b2) shows the peaks for oxygen plasma treated SU8 surface (O60) in which also same peaks C1s, O1s/Sb-3d and Si-2p were observed. The Figure 5.16(b3) shows the peaks for SF_6 plasma treated SU8 surface (S60). It is observed from the Figure 5.16(a3) that the intensity of Si-2p peak is less and the intensity of the C1s and O1s is also reduced as compared to O60 and untreated SU8 OTS SAM modified.

The fluorine peak was observed at 680 eV locations which indicate the presence of fluorine after the SF_6 plasma exposure. Figure 5.16(b4) shows the spectra for SF_6+O_2 plasma treated SU8 surface. The spectra shows the similar peak C1s and O1s/Sb-3d as observed in SF_6 plasma treated surface. The fluorine peak was also observed at 680eV locations for SF_6+O_2 plasma treatment. The intensity of the C1s and O1s were less as compared to O60 and untreated SU8 surface OTS SAM modified surface. It can be observed from the Figure 5.16(b) that there is no evidence for the Chlorine (Cl) peaks from OTS modified surfaces which indicate complete hydrolysis of the trichlorosilane, hence formation of bond of OH group on SU8 surface and CH_3 chain on OTS SAM.

5.3.4 Stability study of plasma treated OTS SAM deposited SU8 surface

We have studied the stability for the SU8 polymer over half year duration. It is well known that the polymer surface degrades with time. Due to instability problem it is necessary for polymer surfaces to study the stability with time for polymer surfaces. The hydrophobic durability of OTS modified plasma activated surface was monitored by measuring the WCA over several months. Few samples from prepared samples plasma treated with OTS SAM modification were used for investigations of the stability of monolayer on plasma treated SU8 surface. After OTS surface modification the WCA measurements of same set of samples were measured after a period of three months and five months. The monitored contact angle on modified SU8 surface with mentioned period are shown in Figure 5.17.

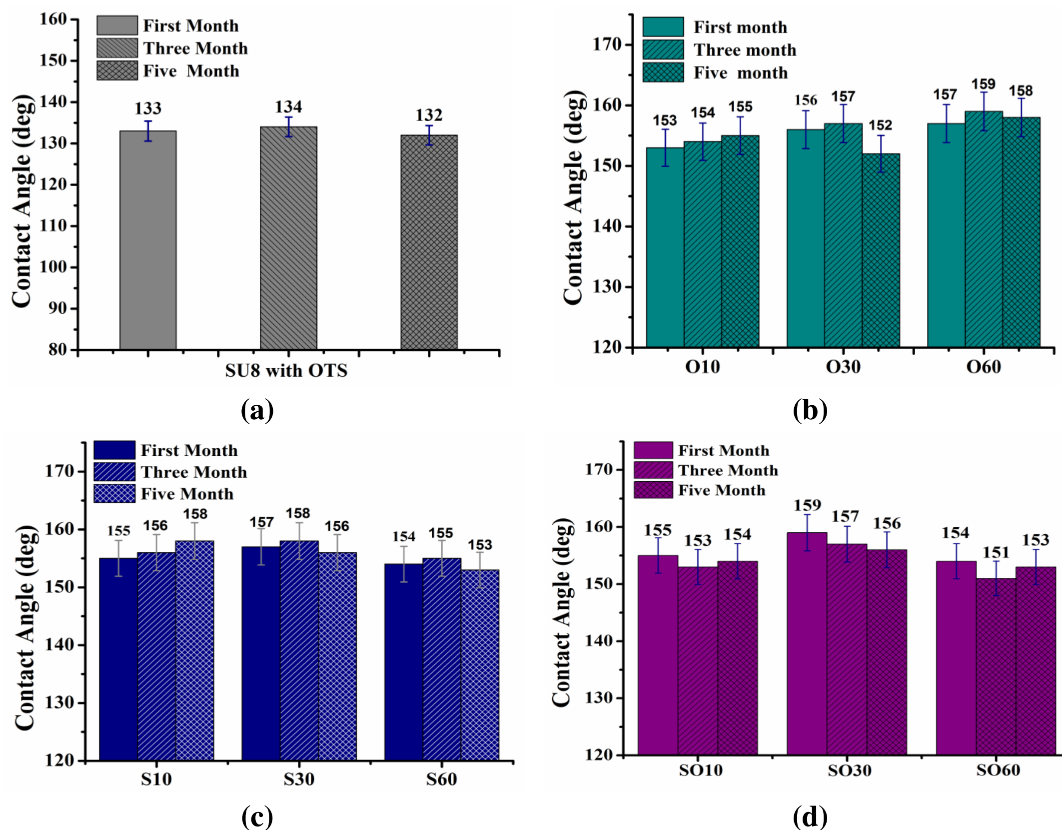

Figure 5.17: Stability behaviour of OTS modified plasma activated SU8 surface with time (a) bare SU8 (b) O_2 plasma (c) SF_6 plasma (d) SF_6+O_2 plasma

The Figure 5.17(a) shows the untreated SU8 surface. It can be observed from the Figure 5.17(a) that not much change was observed for WCA after three and five month. Figure 5.17(b) shows the measured WCA till five months for oxygen plasma (O) OTS treated surface. After three months, WCA decreased from 156 ± 2° measured in first month to 152 ± 2° for O30. There was not much change observed for O10 and O30 with respect to time duration of first and third months. The Figure 5.17(c) shows the WCA till five months duration for SF_6 plasma (S) treated OTS modified surfaces. From Figure 5.17(c), it can be concluded that the slight change was observed in WCA values. In the case of S10, the WCA changed from 155°± 2° for first month to 158°± 2° after five months. The sample S30, the WCA changed from 157°± 2° for first month to 156°± 2° after five months. In the similar way the sample S60, the WCA changed from 154°± 2° for first month to 153°± 2° after five months. It can be concluded there are not much changes in WCA observed with SF_6 plasma treated OTS SAM modified samples.

Figure 5.17(d) shows the change in WCA after five months for SF_6+O_2 (SO) plasma. From Figure 5.17(d), it can be concluded that the slight change was observed in WCA values. In the case of SO10, the WCA changed from $155^o \pm 2^o$ in first month to $154^o \pm 2^o$ after five months. The sample S30, the WCA changed from $159^o \pm 2^o$ in first month to $156^o \pm 2^o$ after five months. In the similar way the sample S60, the WCA changed from $154^o \pm 2^o$ in first month to $153^o \pm 2^o$ after five months. It can be concluded that the WCA for SO30 sample decreased from $159^o \pm 2^o$ in first month to $156^o \pm 2^o$ after five months. The SO10 and SO60 not much change was observed with SF_6 plasma treated OTS SAM modified samples. The OTS modified fluorine base plasma treated SU8 samples gives the stable WCA values with variation of $\pm 2^o$ where as in oxygen plasma treated surface the value of contact angle decreased from 156 ± 2° to 152 ± 2°.

5.4 Conclusion

In this chapter, we explored the utilization of a combination of plasma treatment and OTS SAM mask-less fabrication of SU8 hydrophobic surfaces. The effects of plasma on wetting behaviour of SU8 were investigated seprately and a SAM deposited plasma treated surface were studied for comparison purpose. Three set of samples were prepared namely (i) untreated SU8 surface (ii) the sample were subjected to plasma texturing with different plasma i.e. (i) SF_6 (ii) O_2 (iii) combination of SF_6 and O_2 plasma (iii) OTS SAM modification with and without plasma treated SU8 surface. Each set contains the 4-5 sample of each type of treatment. The plasma treatment was carried out for different time duration i.e. 10 sec, 30 sec and 60 sec. We can conclude the following from the results obtained from this study.

1. The surface roughness increased after the plasma treatment. The plasma treatment for 60 sec provides the maximum roughness as compared to other time durations. For example, the oxygen plasma make the surface more rough 1.77±0.5 nm as compared to SF_6, SF_6 and O_2 plasma. Further surface roughness increase after OTS SAM modification. The large changes were observed for rms roughness after the OTS SAM modification on oxygen plasma treated surface. The largest change was observed in roughness values 21.6±2 nm for S60 whereas smallest change was observed in roughness values 13.1± 2 nm for SO60.

2. After plasma treatment the surface becomes hydrophilic. The oxygen plasma change the WCA from $90^o\pm 2^o$ for untreated SU8 to $28^o\pm 2^o$ for O60 samples. The plasma treatment S60 make the surface hydrophobic and WCA increased from $90^o\pm 2^o$ for untreated SU8 to $105.6^o\pm 2^o$. The combined plasma treatment of SF_6+O_2 makes the surface hydrophilic reducing the WCA from $90^o\pm 2^o$ for untreated SU8 to $69^o\pm 2^o$. It was found that the plasma treatment time for 10 sec is enough to alter the wetting behavior.

3. The wetting behavior of untreated and plasma treated SU8 changes after OTS SAM modification. It was observed that the highest water contact angle of $\theta_c > 150^o$ was achieved by coating OTS SAM on plasma treated SU8 surface. The untreated SU8 surface after OTS SAM makes the surface hydrophobic with WCA $133^o\pm 2^o$.

4. The oxygen plasma (O60) changes the WCA from $28^o\pm 2^o$ plasma treated surface to $157^o\pm 2^o$ after OTS SAM. The plasma treatment S60 make the surface hydrophobic and after OTS SAM WCA increased from $105.6^o\pm2^o$ (plasma treated) to $157^o\pm2^o$.The combined plasma treatment of SF_6+O_2 makes the surface hydrophilic but after OTS SAM modification the WCA change drastically from $69^o\pm2^o$ (plasma treated) to $153^o\pm2^o$. The change in wetting properties after OTS SAM on plasma treated surface gives the importance of surface roughness. The combination of plasma activated SU8 and OTS monolayers give the stable superhydrophobic surfaces which were confirmed by monitoring the WCA for a long period of five months.

5. After OTS SAM the samples surface chemistry were characterized using the RAMAN spectra. The Raman spectra was observed for untreated, plasma treated with and without OTS SAM modification. The spectra for untreated and plasma treated SU8 surface shows the appearance of peak C-S, C-C, C-O-C , CH_2 and CH_3 confirm the charcaterstics of SU8 bonds which contains the phenol group, photoacid genrator.

6. It was observed from the Raman spectra for untreated and plasma treated surface that there is not much change in the peak locations. After OTS modification the peak location were changed as comaprison to those without OTS SAM SU8 samples. The peak C-H and =(CH) were observed after OTS SAM modification. The presence of C-C, C-H and =(CH) makes the surface hydrophobic.

7. The surface chemistry were charcaterized using the XPS spectra. The XPS spectra for untreated, plasma treated with and without OTS SAM modifcation was observed. The C1s, O1s/Sb-3d and Si-2p peaks was observed for all the untreated and plasma treated SU8 surface. The fluorine peak was also observed for S60 and SO60.

8. The same peak was observed after the OTS SAM modification for untreated, plasma treated OTS SAM modified SU8 surface.There was no evidence for the Chlorine (Cl) peaks from OTS modified surfaces confirming the complete hydrolysis of silane in OTS.

References:

1] R. Lipowsky, P. Lenz, S. Swain. Wetting and dewetting of structured and imprinted surfaces. Jl of colloids and surfaces. 2002, 161, 3-22.

2] Gao L, Mc. Carthy. T. Wetting and superhydrophobicity. Langmuir, 2009, 25(24), 14100-04.

3] Liu J., Feng X., Wang G. and Wen Yu S. Mechanism of superhydrophobicity on hydrophilic substrates. Jl of physics: condensed matter. 2007, 19, 356002-14.

4] Xiu Y, Zhu L, W. Hess and C. Wong. Hierarchical Silicon Etched Structures for Controlled Hydrophobicity/Superhydrophobicity. Nanoletters. 2007, 7(11), 3388-3393.

5] Li. X, B. Tay, Miele P, Brioude A., David C .Fabrication of silicon pyramid/nanowire binary structure with superhydrophobicity. Jl of Applied surface Science. 2009, 255, 7147-52.

6] M. Stanton, E. Ducker, C. MacDonald, R. Lambert. Mc Gimpsey. Superhydrophobic, highly adhesive, Polydimethylsiloxane (PDMS) surfaces. Jl of Colloid and Interface science. 2012, 367, 502-508.

7] A. Tropmann, L. Tanguy, P. Koltay, R. Zengerle, and L. Riegge, Completely superhydrophobic PDMS surfaces for microfluidics. Langmuir.2012, 28(22), 8292-8295.

8] Y. Ma, X. Cao, Feng X., Ma.Y, H. Zou, Fabrication of super-hydrophobic film from PMMA with intrinsic water contact angle below 90o. Jl of Polymer.2007 48, 7455-60.

9] E. Chibowski, L. Hołysz, K. Terpilowski, M. Jurak, Investigation of superhydrophobic effect of PMMA layers with different fillers deposited on glass support. Jl of Colloids and surfaces A: Physicochemical. Eng. Aspects. 2006, 291, 181-190.

10] V. Kumar, NN. Sharma, In Micro and Smart Devices and systems; K. Vinoy, R. Pratap, G.K. Ananthsuresh, S. Kurupanidhi.; Springer: 2014; Chapter 16, pp 265-283.

11] P. Abgrall, V. Conedera, H. Camon, A. Gue, N. Nguyen, SU8 as structural materials for lab-on-chips and microelectromechanical system. Jl. of electrophoresis. 2007, 28, 4539-4551.

12] T. Sikanen, S. Tuomikoski, A. Ketola, R. Kostiainen, S. Franssila, T. Kotiaho Characterization of SU8 for electro kinetics microfluidics applications. Lab-on-chip. 2005, 5, 888-896.

13] V. Kumar, NN. Sharma, SU8 as hydrophobic and dielectric thin film in electrowetting-on-dielectric based microfluidics devices. Journal of Nanotechnology.2012, 2012, 312784.

14] H. Sato, H. Matsumura, S. Keino, and S. Shoji , An all SU8 microfluidics chip with built-in 3D fine microstructures. Jl of Micromechanics and Micro engineering. 2006, 16, 2318-2322.

15] S. Keller, G. Blagoi, M. Lillemose, D. Haefliger, and Boisen A. Processing of thin SU8 films. Jl of Micromechanics and Microenigineering. 2008, 18, 125020-30.

16] Campo A. and Greine C. SU8: a photo resist for high-aspect-ratio and 3D submicron lithography. Jl of Micromechanics and Microengineering. 2007, 27, 81-95.

17] J. Zhao, D. Sheadel, W. Xue , Surface treatment of polymers for the fabrications of all-polymer MEMS devices. Sensor and actuators A: Physical. 2012, 187, 43-49.

18] Ferdin and Walther, P. Davydovskaya, S. Zurcher, Michael Kaiser, Helmut Herberg, A. Gigler and R.W Stark. Stability of the hydrophilic behaviour of oxygen plasma activated SU8. Jl of Micromechanics and Microengineering.2007, 17,524-531.

19] K. Rasmussen, S. Keller, F. Jensen, A. Jorgensen, O. Hansen, SU8 etching in inductively coupled oxygen plasma. Jl of Microelectronics engineering. 2013, 112, 35-40.

20] Chung CK. and Hong YZ. Surface modification of SU8 photo resist for shrinkage improvement in a monolithic MEMS microstructure. Jl of Micromechanics and Micro engineering.2007, 17, 207-212.

21] F. Walther, T. Drobek, A Gigler., M. Hennemeyer, M. Kaiser, H. Herberg, T. Shimitsu, E. Morfillc and Stark W. Surface hydrophilization of SU8 by plasma

and wet chemical processes. Jl of Surface and interface analysis, 2010, 42, 1735-1744.

22] J. Velasco, M. Vlachopoulou, A. Tserepi, Gogolides A. Stable superhydrophobic surfaces induced by dual-scale topography on SU8. Jl of Microelectronic Engineering. 2010, 87, 782-785

23] Hong G., Holmes A.S., Heaton M.E.SU8 resist plasma etching and its optimization. Microsystems technologies. 2004, 10, 357-359.

24] N. Shirtcliffe, Aqil. S, Evans. C, McHale C, and M. Newton, C Perry and Roach P. The use of high aspect ratio photo resist (SU8) for superhydrophobic pattern prototyping. Jl of Micromechanics and Microengineering. 2004, 14, 1384-1389.

25] Yoon Y, Lee D, and Lee J. Surface modified nano-patterned SU8 pillar array optically transparent super-hydrophobic thin film. Jl of Micromachining and Microengineering. 2012, 22, 035012-19.

26] Park S.G, Moon J.H, Jeona H.C and Yang S.M. Anisotropic wetting and superhydrophobicity on holographically featured 3D nanostructured surfaces. Jl of Soft matter. 2012, 8, 4567-70.

27] J. Gooding, F. Mearns, and Yang .W, Liu J. Self-Assembled Monolayers into the 21st Century: Recent Advances and applications. Jl of Electroanalysis. 2003, 15 (2), 81-96.

28] Haensch C, Hoeppener S, and Schubert S.U. Chemical modification of self assembled silane based monolayers by surface reactions. Chemical society review. 2010, 39, 2323-2334.

29] Glass N, Tjeung R, Chan P, Yeo L, and. Friend J. Organosilane depositions for microfluidics applications. Biomicrofluidics. 2011, 5, 036201-7.

Chapter 6

Conclusion

6.1 Overall Conclusions

The wetting behaviour of semiconductor materials Si, low-k, high-k dielectric materials and polymers is achieved by synergism of plasma treated surfaces and OTS SAM monolayer deposition. Variations in treatments were carried out using different chemical and physical methods. The hydrophobicity are characterized by measuring the water contact angle before and after OTS SAM modification of surfaces. The wetting behaviour of the surface of different materials are characterized after texturing and OTS SAM modification. The surface roughness of untextured surface, plasma and chemical textured surface, OTS SAM modified untextured surface and OTS SAM modified plasma and chemical textured surface were characterized using the Atomic force microscope and Scanning electron microscope. The chemical composition for the all type of surfaces textured and untextured with OTS SAM wereanalyzed using the RAMAN and XPS results. It was shown that the hydrophobicity of silicon and dielectric materials significantly improved, and increased with WCA>150° in the regime of superhydrophobicity.

In Chapter 3, we have investigatedthe wetting behaviour of the silicon. The hydrophobic silicon surfaces were obtained by combining the texturing and OTS SAM deposition. The texturing was done using chemical and plasma methods. The chemical texturing was performed using different chemical etchants : KOH , TMAH and combination of both KOH and TMAH and the plasma texturing was performed using fluorine plasma chemistry : SF_6, O_2 and the combination of both SF_6 and O_2. The surfaces after cleanser treatment (Piranha and Piranha followed by HF Dip) were also used to study the wetting behaviour of silicon surface.

After texturing, all types of surfaces namely K, T, KT, S, SO, O, PR, HF and BS (refer to nomenclature in Chapter 3, section 3.2) of silicon were subject to OTS SAM deposition. It was observed that the texturing of the silicon make the surface more rough. The chemical texturing will make the surface more rough as compare to plasma texturing. Large size of pyramids were observed after chemical texturing which make the surface

furhter hydrophilic. The use of plasma for texturing also make surface rough and further hydrophilic. The plasma texturing use less silicon as compared to chemical texturing and avoids the contamination like potasium from the chemical ethcant. The surface after the piranha becomes more hydrophilic as compared to other texturing methods. The HF treatment after the pirnaha improve the wetting of silicon but still it is hydrophilic. The back side of the silicon which was treated with Piranah and followed by HF improved hydrophobicity of silicon.

It may observed from the AFM results that the TMAH etching gives the maximum roughness of 838±2 nm in comparison with KOH chemical etchtant. Similarly, the combined plasma of SF_6 and O_2 provide more rough surface as compared to seprately treated SF_6 and O_2 plasma. The surface roughness further increased after the OTS SAM modification because of formation of Islands on the surface. After modification with OTS SAM, the K sample (KOH textured sample) provided a more rough surface with roughness value of 1267±4 nm. The surface modification of combined plasma SF_6 and O_2 also provided maximum roughness value of 23.9±2 nm. The plasma texturing was performed for very less time (Section 3.2.4) in order to have minimum effect on topography of silicon. This enables acheivement of high roughness and also provide higher WCA. The surface roughness also increased in the OTS SAM modified HF and PR treated samples. The hydrophobicity of the silicon were characterized by the water contact angle before and after OTS SAM modification of textured surface. After being modified by OTS, the silicon surfaces shows superhydrophobic surface with high WCA greater than 150°. Both of the texturing i.e. chemical and plasma methods provides the surface hydrophilic nature. In terms of surface roughness and WCA, a significant difference was observed in both methods. The surface treated with piranha and O_2 plasma process offer the most effective way to produce to superhydrophobic surfaces without consumption of much silicon in comparison to chemical and plasma methods.

After OTS SAM the samples surface chemistry were characterized using the RAMAN and XPS. The presence of hydrocarbon group (C-H) confirm the presence of monolayer on the surface.The XPS also confirm the presence of C and O on the OTS SAM modified surface. There was no evidence for the Chlorine (Cl) peaks from OTS modified surfaces confirming the complete hydrolysis of silane in OTS.

In Chapter 4, we have studied the wetting behaviour of dielectric materials. The high-k dielectric materials like HfO_2, Al_2O_3, TiO_2 and Ta_2O_5 and low-k dielectric SiO_2 was used

for this study. It was shown that the hydrophobicity of dielectric materials significantly improved, resulting is a hydrophobic surfaces with WCA >150° in the regime of superhydrophobic surface. The hydrophobicity of the dielectric improved by combined effect of plasma texturing and OTS SAM modification. The fluorine based plasma was used to texture the oxide surfaces. The OTS SAM modification was carried out on the untextured and plasma textured oxide surfaces.

After texturing, all type of surfaces HfO_2, Al_2O_3, TiO_2 and $Ta_2O_5$and SiO_2 were subjected to OTS SAM deposition. It was observed that the texturing of the oxide surfaces make the surface rough. It was observed from the AFM results that surface roughness of plasma treated oxides surface increased. The surface roughness increaed after OTS SAM modifcation on plasma treated and untreated surface. It was observed that plasma untreated oxide surface with OTS SAM makes the surface rougher as compared to plasma treated oxide surface. The WCA was measured on all plasma treated and untreated oxide surface with and without OTS SAM modifcations. The highest WCA θ_c ~160.5^o ±2° was observed for Al_2O_3 dielectric surface.Superhydrophobicity of dielectric surfaces with water contact angle $\theta_c \geq 150.5^o$ was thus far remained unachieved but by methodology presented in this work we have shown to achieve $\theta_c \geq 150.5^o$ invariably on different dielectric surfaces namely, SiO_2, HfO_2, Al_2O_3, Ta_2O_5 and TiO_2. The increase in θ_c is attributed to formation of fluorine trap sites along with -OH traps which contribute to better and denser OTS deposition.

The surface with and without OTS SAM with plasma treated and untreated samples surface chemistry were characterized using the RAMAN and XPS. The presence of hydrocarbon group (C-H) confirm the presence of monolayer on the surface.The XPS also confirm the presence of C and O on the OTS SAM modified surface. There was no evidence for the Chlorine (Cl) peaks from OTS SAM modified surfaces confirming the complete hydrolysis of silane in OTS.

In Chapter 5, we have studied the wetting behaviour of SU8 surface. The SU8 which exhibit the intrinsically hydrophobic nature. The plasma treatment (SF_6 and O_2) can be used to make the surface rougher and which modified with monolayer produces the superhydrophobic surfaces. The effects of plasma on wetting behaviour of SU8 were investigated. The surface roughness was measured using the AFM microscope. It was observed that O_2 plasma treatment increased the surface roughness as compared to other plasma SF_6 and SF_6+O_2 treatment. It was shown that the surface roughness after OTS

SAM also increased as compared to unmodified OTS SAM SU8 surface. Large change was observed in roughness values to 21.6± 2 nm for S60 whereas smallest change was observed in roughness values 13.1± 2 nm for SO60.

The plasma treatment changes the wetting behaviour of SU8. Oxygen plasma makes the surface hydrophilic whereas the SF_6 plasma makes the surface hydrophobic. It was also observed that the wetting behaviour of SU8 after plasma treatment with OTS SAM modification makes the surface superhydrophobic. The untreated SU8 surface after OTS SAM makes the surface hydrophobic with WCA 133°± 2°.The oxygen plasma (O60) changes the WCA from 28°± 2° plasma treated surface to 157°± 2° after OTS SAM. The plasma treatment S60 make the surface hydrophobic and after OTS SAM WCA increased from 105.6^o± 2° (plasma treated) to 157°± 2°. The combined plasma treatment of SF_6+O_2 makes the surface hydrophilic but after OTS SAM modification the WCA change drastically from 69°±2° (plasma treated) to 153°±2°. The change in wetting properties after OTS SAM on plasma treated surface gives the importance of surface roughness. The combination of plasma activated SU8 and OTS monolayers give the stable superhydrophobic surfaces which were confirmed by monitoring the WCA for a period of five months.

The surface chemistry of plasma treated and OTS were charcaterized using the Raman and XPS spectra. It was observed from the Raman spectra for untreated and plasma treated that there was not much change in the peak locations. After OTS modification the peak location were changed when compared with and without OTS SAM SU8 samples. The peak C-H and =(CH) was observed after OTS SAM modification. The presence of C-C, C-H and =(CH) makes the surface hydrophobic. The XPS spectra for untreated, plasma treated with and without OTS SAM modification was observed. The C1s, O1s/Sb-3d and Si-2p peaks was observed for all the untreated and plasma treated SU8 surface. The fluorine peak was also observed for S60 and SO60.The same peak was observed after the OTS SAM modification for untreated, plasma treated OTS SAM modified SU8 surface.There was no evidence for the Chlorine (Cl) peaks from OTS modified surfaces confirming the complete hydrolysis of silane in OTS.

6.2 Future Scope of the Work

No research concludes with an absolute end. There is enough room for innovation in the fabrication of superhydrophobic surfaces. Several materials like low-*k* and high-*k*

dielectric need better understanding so fabrication design strategies can be improved further. The research in this area will find a milestone when the dielectric will be used in the microfluidics application. From the perspective of present work, the following aspects can be studied and investigated further.

1] Silicon metal assisted etching

The improvement in wetting behaviour of silicon with chemical and plasma texturing with OTS SAM modification has been discussed in detail in Chapter 3. Apart from chemical and plasma texturing the metal (Au, Ag, Pt) assisted etching can also be optimized to texture the silicon surface. The textured surface can also be modified using the OTS SAM to achieve the superhydrophobic surfaces. The dielectric and polymers can also be textured with other fluorine plasma (CF_4, C_4F_8) and modification with OTS SAM.

2] Contact angle hysteresis

The superhydrophobicity needs to be characterized by measuring the contact angle hysteresis. The contact angle hysteresis is measured difference in the advancing and receding angles during roll-off of 2μl volume of water. Due to lack of facility, this study was not been able to be conducted during this thesis.

3] Electrowetting-on-dielectric

The focus of research in EWOD is towards reduction of power consumption, use of different dielectric materials, and optimization of devices dimension. Existing EWOD microfluidics flow microchannels normally has Teflon coat as a hydrophobic layer. The uses of Teflon make the process costly and the use of other dielectric materials. A major issue in microfluidics flow-based electrowetting is high voltage which may cause excessive heating and evaporation of fluids in transport. The lowering of the voltage requires reduction of Teflon thickness, but with the thickness reduction of Teflon coat the possibility of breakdown occurs. To avoid such breakdown, Teflon needs to combine with other dielectrics. The use of other dielectric increases the process steps and cost. The use of prepared hydrophobic materials within thesis can be used as dielectric as well as hydrophobic materials. The use of this type of materials will reduced the cost and process time in EWOD based microfluidics applications.

A. Fabrication Equipment

Chemical wet bench:

The chemical wet bench is used for 2-6"silicon wafers priors to processing in diffusion furnaces, LPCVD furnaces or before metal depositions. The clean performed are high quality, final cleans which precede high temperature processing. The wet bench has different acids baths for Piranha, RCA1, RCA2 and HF dip as shown in Figure A-1. The bench includes the controller used to control the time and temperature of the bath during the cleaning. The same type of bench also used for chemical texturing of the silicon.

Figure A-1: Chemical wet bench setup for cleaning and etching purpose

Reactive ion etching system:

Reactive ion etching (RIE) is a kind of dry etching, in which a fundamental part of the process is the ion bombardment of the materials surface. This process combines reactive ion etching with the use of chemical active particles and ions sputtering. Under the action of reactive ion etching substrate matter selectively moves away in the vertical directions due to both chemical reactions and physical bombardment by ions

and radicals produces in the plasma. In the case of reactive ion etching the direction of materials removal is determined only by the directions of the flow of ions. RIE can solve a wide range of technological problems concerning to isotropic and anisotropic dry etching of wide range of materials in microelectronics, MEMS and nanotechnology. The oxford reactive Ion Etching system is used for the plasma texturing as shown in Figure A-2. The system contains the process chamber, Gas lines, loading station and RF generator.

Figure A-2: Reactive ion etching system

Glove box:

The home made glove box was used for all the experimental work. The glove box contained the hot plate and set of gloves as shown in Figure A-3. The continuous argon flow was used to avoid the air during the process. It was observed during the experiments the air reaction with OTS solutions makes the powder on the surface. To avoid such problem used the Ar flow in the glove box.

Figure A-3 Glove box for silanization

B. Characterization Tool

Atomic force microscope (AFM):

The prepared silicon surfaces were characterized by an Atomic force microscope AFM BRUKER. AFM is used to characterize surface topography of given simples and a photograph of AFM is shown in Figure A-4. The AFM has made it possible to obtain 3-dimensional images of surfaces down to the atomic scales as well as to measure forces on a nano-newton scale. Normally, a tapping mode is used for surface topography. Tapping mode imaging is implemented in ambient air by oscillating the cantilever assembly at or near the cantilever's resonant frequency using a piezoelectric crystal. The oscillating tip is then moved towards the surface until it begins to lightly touch, or tap the surface. The reduction in oscillation amplitude is used to identify and measure surface features. The surface roughness measurements for all samples namely cleaned, textured with and without OTS deposition were carried out to obtain corresponding rms roughness with AFM in tapping mode.

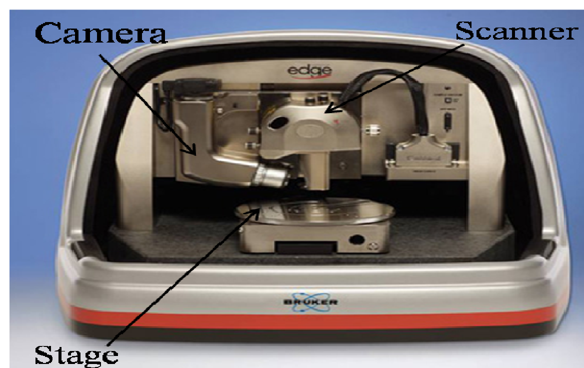

Figure A-4: Photograph of atomic force microscope

Contact angle measurement:

The static water contact angles on all samples were recorded using contact angle goniometer (Data physics) a picture of which is shown in Figure A-5. The all measurements were carried out under ambient condition (21° ± 2°C) and relative humidity 48-50% with deionized water. The WCA of each sample was measured five times across the sample surface using sessile drop method by dispensing 5µl drop of DI water on the sample surface.

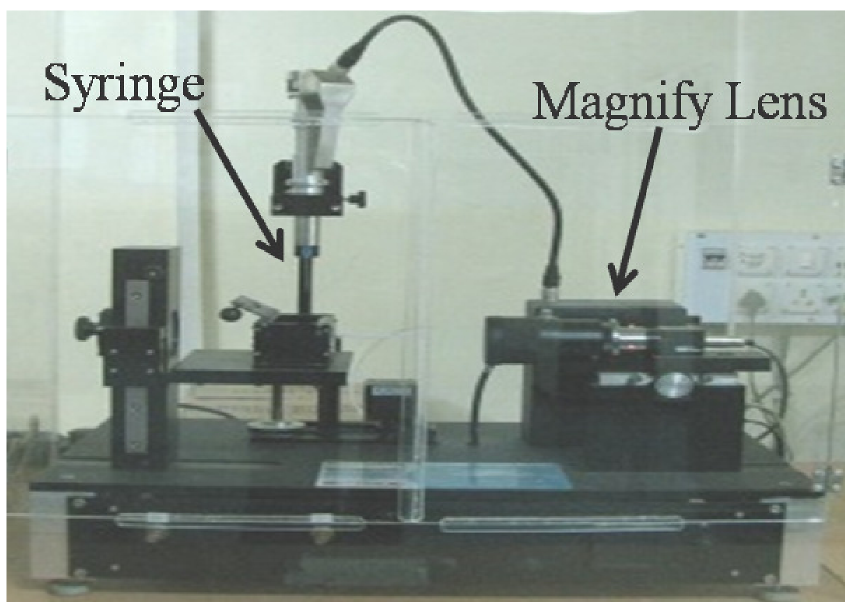

Figure A-5: Goniometer for contact angle measurements

X-Ray photoelectron spectroscopy:

The XPS of OTS modified cleaned and textured surfaces were performed with a Kratos Axis Ultra DLD with monochromatic AlKα excitation (1486.6eV) picture of the instrument shown in Figure A-6. The sample surfaces were etched by argon ion source to eliminate the surface contamination.

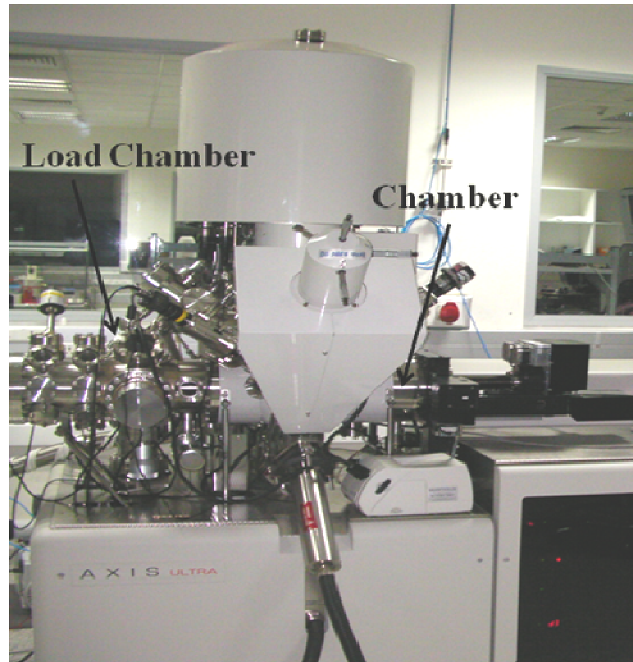

Figure A-6: X-ray photoelectron spectroscopy

RAMAN spectroscopy:

The chemical composition of cleaned and textured samples with OTS was examined by the Raman spectra as shown in Figure A-7. The Raman is a spectroscopic technique used to observe vibration, rotational and other low-frequency mode in the system. The LabRam system was used to characterize the sample after OTS depositions. The 514 nm laser is used for characterization. This presents study investigates wetting behavior of surfaces by combined effect of texturing and OTS SAM modification.

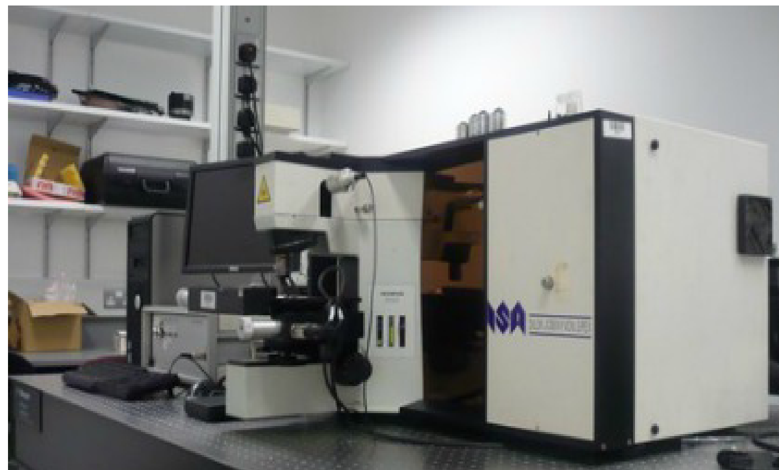

Figure A-7: Raman spectroscopy

PATENT

- "Closed Microchannel for Electrowetting on dielectric based microfluidics using E-beam Lithography" Indian Patent, Application No.: 1950/MUM/2012.
- "Surface modification of Hafnium oxide (HfO_2)" Indian Patent, Application No.: 2453/DEL/2012.

Book Chapter

- **Vijay Kumar**, NN Sharma, "A Study on hydrophobicity of silicon and a few dielectric materials", Micro and Smart devices and systems, Springer, 2014, pp. 265-283.

RESEARCH PUBLICATIONS

A International Journals (*Peer-reviewed*)

1) **Vijay Kumar,** NN Sharma.SU8 as hydrophobic and dielectric thin film in Electrowetting-on-Dielectric based microfluidics device, Journal of Nanotechnology (2012), Volume 2012, Pages 1-6.
2) **Vijay Kumar,** K.N.Bhat, NN Sharma. Surface modification of textured silicon and its wetting behaviour, Journal of Adhesion Science and Technology (2014), DOI: 10.1080/01694243.2014.986835.
3) **Vijay Kumar,** NN Sharma. Synthesis of hydrophilic to superhydrophobic SU8 surfaces, Journal of Applied Polymer Science, Volume 132(8), Pages 41934 (2015).
4) **Vijay Kumar,** NN Sharma. Self Assembled monolayer modified SU8 surface for Electrowetting-on-dielectric application, Journal of Macromolecular Symposia, (accepted with minor revision)
5) **Vijay Kumar,** NN Sharma. Enhancement of wetting behaviour of Dielectric materials with synergetic effect of plasma and Octadecyltrichlorosilane, Journal of Surface and Interface Analysis (under review)

B Conferences

1) **Vijay Kumar,** NN Sharma**.** Self Assembled monolayer modified SU8 surface for Electrowetting-on-dielectric application, International Conference on Soft Matters, October6-10, 2014, MNIT, Jaipur.
2) **Vijay Kumar,** NN Sharma. Self Assembled monolayer for Dielectric materials, International Conference on Soft Matters, October6-10, 2014, MNIT, Jaipur.

Vijay Kumar received the B.Sc degree in Electronic Science from S.D. College, Ambala, Kurukshetra University, Kurukshetra (Haryana), India in 2005, and the M.Sc. degree Electronic Science from Kurukshetra University, Kurukshetra (Haryana), India in 2005. After working for two years in Central Electronic Engineering Research Institute (CEERI), Pilani he joined the Mechanical Engineering Department, BITS-Pilani, Pilani Campus in July 2010, as a research fellow for NPMASS project. During his PhD duration he visited the Indian Institute of Technology (IIT), Bombay. He worked as visiting scholar at Indian institute of Science (IISc), Bangalore. His research interests include design and Fabrication of MEMS and micro fluidics devices.

Prof. (Dr.) Niti Nipun Sharma completed his B.E. (Mechanical) from REC, Srinagar (now NIT, Srinagar) and M.E. (Mechanical) and Ph.D. both from BITS, Pilani. He is a faculty in Mechanical Engineering Department for over 18 years now currently serving as full Professor in Mechanical Engineering Department. Prof. Sharma served as visiting professor in EPFL, Switzerland during May-August 2014. He is first recipient of Kris Ramachandran best faculty award in 2010 at BITS, Pilani.

Prof. Sharma specialized in Robotics and was a part of team which developed 'ACYUT', the humanoid from BITS. He later during his Ph.D. worked on dynamics of nanorobots proposed a simple method to include modelling of Brownian motion attributable to thermal agitation to predict the dynamics of Nanorobots. His methodology of analysing synergism in local and global motion of non-rigid kind of nanoparticles due to thermal agitation from surrounding medium has recently been shown to model radiation of nanoparticle validating with Planck's Radiation Law.

Three patents, over 70 technical papers in high impact factor journals and peer reviewed National and International conferences, around two dozen invited/keynote talks in India and abroad and with ten funded projects from nodal agencies like DBT, UGC, CSIR-CEERI, NPMASS and Industries, currently Prof. Sharma is working in Interdisciplinary areas of MEMS and Nanotechnology.

He is Guest Editor, Journal of Bionanoscience (Springer), Associate Editor of International Journal of Smart Sensors and Intelligent Systems, has reviewed many articles for IEEE Tr. Systems, Man and Cybernetics, IEEE Tr. Education, has been on-board of many Technical Committees of reputed National and International Conference. He was co-chair for International Conference on Emerging Technologies: Micro to Nano 2013 (ETMN-2013) jointly organised by BITS-Pilani and CSIR - Central Electronics Engineering Research Institute, Pilani, International Conference on Emerging Mechanical Technology Macro to Nano (EMTM2N-2007). He also co-organized 2nd ISSS-MEMS-2007 conference with CEERI, Pilani

Prof. Sharma also holds the post of Dean, Academic Registration & Counselling Division at BITS-Pilani, Pilani Campus since 2010.